MENTATION PAGE

Form Approved
OMB No. 0704-0188

1. AGENCY USE ONLY (Leave blank)	2. REPORT DATE	3. REPORT TYPE AND DATES COVERED
	May 14, 1992	THESIS/DISSERTATION

4. TITLE AND SUBTITLE
Structural Simulation Coupling For Transient Analysis

5. FUNDING NUMBERS

6. AUTHOR(S)
Howard Travis Clark, III, 2nd Lt

7. PERFORMING ORGANIZATION NAME(S) AND ADDRESS(ES)
AFIT Student Attending: Massachusetts Institute of Technology

8. PERFORMING ORGANIZATION REPORT NUMBER
AFIT/CI/CIA- 92-101

9. SPONSORING/MONITORING AGENCY NAME(S) AND ADDRESS(ES)
AFIT/CI
Wright-Patterson AFB OH 45433-6583

10. SPONSORING/MONITORING AGENCY REPORT NUMBER

11. SUPPLEMENTARY NOTES

12a. DISTRIBUTION/AVAILABILITY STATEMENT
Approved for Public Release IAW 190-1
Distributed Unlimited
ERNEST A. HAYGOOD, Captain, USAF
Executive Officer

12b. DISTRIBUTION CODE

Accesion For	
NTIS	CRA&I ☒
DTIC	TAB ☐
Unannounced	☐
Justification	
By	
Distribution /	
Availability Codes	
Dist	Avail and / or Special
A-1	

13. ABSTRACT *(Maximum 200 words)*

14. SUBJECT TERMS	15. NUMBER OF PAGES
	163
	16. PRICE CODE

17. SECURITY CLASSIFICATION OF REPORT	18. SECURITY CLASSIFICATION OF THIS PAGE	19. SECURITY CLASSIFICATION OF ABSTRACT	20. LIMITATION OF ABSTRACT

STRUCTURAL SIMULATION COUPLING FOR TRANSIENT ANALYSIS

by

Howard Travis Clark, III

B.S., United States Air Force Academy
Colorado Springs, Colorado (1990)

Submitted to the Department of Aeronautics and Astronautics
in Partial Fulfillment of the Requirements for the Degree of

MASTER OF SCIENCE

at the

MASSACHUSETTS INSTITUTE OF TECHNOLOGY

June 1992

Signature of Author_____
Department of Aeronautics and Astronautics
7 May 1992

Approved by _____
Dr. David S. Kang
Technical Staff, Charles Stark Draper Laboratory
Thesis Supervisor

Certified by _____
Professor John Dugundji
Department of Aeronautics and Astronautics
Thesis Supervisor

Accepted by _____
Professor Harold Y. Wachman
Chairman, Department Graduate Committee
Department of Aeronautics and Astronautics

STRUCTURAL SIMULATION COUPLING FOR TRANSIENT ANALYSIS

by

HOWARD TRAVIS CLARK, III

Submitted to the Department of Aeronautical
and Astronautical Engineering
on May 14, 1992
in partial fulfillment of the requirements for the degree of
Master of Science

ABSTRACT

Analysis of the transient time response of many modern engineering systems requires simulation by means of direct time integration of sets of coupled-field equations. In the past the simulation of such coupled problems has created difficulties which are not seen in analogous single-field problems. Perhaps the most important of these difficulties is the fact that existing engineering analysis packages have been oriented to solving only single-field problems. This suggests one particularly attractive option: the use of existing single-field analysis software while imposing certain modular requirements. If modularity can be maintained, direct integration of the equations can proceed by sequential or parallel operation of the separate analyzers.

This research develops the theory by which the numerical simulations of two or more separate fields may be combined to solve the coupled-field problem. This theory allows simulations to be used with little or no change by considering the constraints that provide for field

coupling. The development takes into account the various numerical methods which may be used by individual simulations to solve their separate problems. Above all this paper does not seek to suggest that simulation coupling is the best or foremost simulation methodology available, merely that it is a viable and cost saving alternative to solving the larger, more involved coupled-field problem.

The specific discipline of focus will be multibody dynamics. The goal will be to show that it is possible to couple multiple single body dynamic analysis packages and come up with solutions comparable to the full multibody dynamic case. The advantages of such a methodology are readily seen here. The single body equations of motion are fairly simple and a great deal of software exists to produce transient analyses of such bodies. This is compared to the multibody analysis where the equations of motion are not readily derived, few reliable analyzers exist, and changes in the model may require a great deal of change to the analysis package.

The paper is organized into three main sections. The first section deals with the tools necessary to evaluate the simulation coupling method. The second part introduces this method as well as dealing with stability and accuracy of the algorithm presented. The final section of the paper involves numerical examples which demonstrate the strengths and weaknesses of this theory.

Thesis Supervisor: Dr. David S. Kang
Technical Staff, Charles Stark Draper Laboratory

Acknowledgements

My sincerest gratitude is extended to my thesis advisor, David S. Kang, for his funding of this thesis and his all his help.

I would like to thank all those who have helped me during my time at MIT and Draper, especially Dr. Dugundji.

I would also like to extend a special thanks to my friends at Draper. Their help and friendship got me through many long days and late nights and made sure the deadlines were met. Joe, Dave, Mike, Ashok, Lou, Bill, and Kevin, thank you all and best of luck. I also want to thank my roommate, Matt, who constantly reminded me how much simpler life would be, if I only had a brain.

It is with all my love and appreciation that I thank my parents for their love and support and without whom I would have never made it this far.

This thesis was researched and written at the Charles Stark Draper Laboratory under Internal Research & Development 332.

Publication of this thesis does not constitute approval by the laboratory of the findings or conclusions herein, but is done for the exchange and stimulation of ideas.

I hereby assign my copyright of this thesis to the Charles Stark Draper Laboratory, Inc., of Cambridge, Massachusetts.

_____

Howard T. Clark, III
2Lt., USAF

Permission is hereby granted by the Charles Stark Draper Laboratory, Inc. to the Massachusetts Institute of Technology to reproduce and to distribute copies of this thesis document in whole or in part.

Table of Contents

List of Illustrations

Figure **Page**

List of Tables

Table **Page**

Nomenclature

In general boldface text indicates vector or matrix quantities with upper case for matrices and lower case for vectors. Also, numbers in parenthesis represent the chapter in which a symbol occurs.

$\dot{(\,)}$	=	$\frac{d}{dt}$ first time derivative
$\ddot{(\,)}$	=	$\frac{d^2}{dt^2}$ second time derivative
δ	=	first variation operator (4)
det	=	determinant operator
0	=	zero matrix (of appropriate dimensions)
I	=	identity matrix (of appropriate dimensions)
x,y	=	physical single field response variables
M	=	general mass matrix
C	=	general damping matrix
K	=	general stiffness matrix
R	=	general nodal forcing functions or nonconservative external factors in Lagrange's equations of motion
Φ	=	physical constraint and interface condition equations
$\mathbf{f}_c$	=	effective constraint forces
u	=	coupled field response variable
s	=	Laplace variable
v	=	auxiliary vector in order reduction
A,B	=	weighting matrices in choice of v
w	=	general vector for integration
h	=	integration stepsize

α_i, β_i = constants for integration approximation

$\mathbf{h}_n^w$ = collection of historical terms associated with $\mathbf{w}$ pertaining to time $t = t_n$

δ = $h\beta_0$, effective stepsize (3)

γ_i, η = constants for second order integration approximation

$\mathbf{A}_n, \mathbf{b}_n$ = complex matrix and forcing function for integration (3)

$\mathbf{z}$ = shift operator

z = discrete variable, $z = e^{sh}$

$\rho(.), \sigma(.), \psi(.)$ = operator notation polynomials

ϕ = operators constants in forcing term $\mathbf{b}_n$

p = operator notation associated with predictors

T = kinetic energy

V = potential energy

$\mathcal{F}$ = Rayleigh's dissipation function

A = action integral

L = Lagrange's function, Lagrangian

λ = Lagrange multiplier

$\mathbf{G}$ = $\frac{\partial \Phi}{\partial u}$, Jacobian of constraints wrt u

κ, α = constants in penalty method

$\mathbf{H}$ = $\frac{\partial \Phi}{\partial \dot{u}}$, Jacobian of constraints wrt $\dot{u}$

μ = complex polynomial for prediction of constraints

C = system characteristic equation/matrix

$\mathbf{R}_0$ = translation from inertial (5)

θ = Euler angle rotations

${}^aC_b$ = rotation matrix from frame b to frame a

ω = angular momentum of a body

$\mathbf{S}$ = transformation from Euler angle rates to angular momentum coordinates

Subscripts

x or y	=	attendant matrix of single field analysis
xx,yy, xy,yx	=	attendant matrix of couple field analysis
h or nh	=	indicates with holonomic or nonholonomic problems
r, p	=	indicates rotor or platform(5)
a, s	=	indicates arm end effector or shuttle(5)
ss	=	indicates steady state quantity
0	=	indicates inertial quantity

Superscripts

T	=	transpose operator
I	=	implicit portion of a partition
E	=	explicit portion of a partition
c	=	attendant matrix connected with constraints
u, v, w	=	denotes quantities associated with integration vectors u, v, or w
P	=	terms are associated with prediction (3,4)
'	=	indicates a normalized quantities (3)
		indicates concurrent or staggered coupling (4)
*	=	fictitious qualifier (ie. V^* = fictitious potential energy)

Acronyms

IE	=	implicit-explicit (partitioning scheme)
DOF	=	degrees-of-freedom
CM	=	center of mass

Chapter One

Introduction

1.1 Background

Flexible multibody problems have become increasingly important in recent years, primarily to support the design and deployment of large space structures. The numerical simulation of these problems becomes especially important in space applications where extensive laboratory research is impractical. Flexible multibody dynamics, however, is only a subset of the larger group of coupled-field problems whose numerical solution has been the subject of a great deal of study over the past decade. Coupled-field systems are readily solved single-field subsystems linked together by constraints or interface boundaries; systems whose solution is made difficult by the size of the combined problems, the widely varying time response characteristics that the combined subsystems may have, and the fact that most analysis software currently available is written for single-field analysis.

Traditional solutions to the coupled-field problem involve solving the system as a whole, either through field elimination or by

simultaneous solution. Recently, partitioned solution methods have received a great deal consideration for their ability to divide the problem into pieces which may be dealt with individually. A more extreme form of partitioning exists in the form of simulation coupling, where the constraint or boundary interface effects are combined with single field analyzers to solve coupled systems.

The major advantage of the simulation coupling method is its maximal use of available software and existing analyses. This is especially true for coupled structural problems. Transient analysis of such problems are of particular interest in the design process when variations of secondary structural systems need to be coupled to a primary structure. Analysis of the loading due to different satellites carried in the space shuttle's main bay and the construction and deployment of laboratory and habitation modules connected to the space station's main structure are two examples where, if certain stability and accuracy needs can be reached, there would be an advantage to coupling existing simulations instead of using the more traditional methods to re-solve the problem for each variation.

1.2 Motivation for Current Work

Analysis of the transient time response of many modern engineering systems requires simulation by means of direct time integration of sets of coupled-field equations. The simulation of such coupled problems has created difficulties which are not normally seen in analogous single-field problems. Perhaps the most important of these difficulties is the fact that existing engineering analysis

packages have been oriented to solving single-field problems. This suggests one particularly attractive answer: the use existing single-field analysis software while imposing certain modular requirements. If modularity can be maintained, direct integration of the equations can proceed by sequential or parallel operation of separate analyzers.

The motivation for this thesis is the development of a theory by which the numerical simulations of two or more separate fields may be combined to solve the coupled-field problem. This theory should allow simulations to be used without change through consideration of the constraints that provide for the field coupling. This theory should account for the various numerical methods which may be used by the individual simulations to solve their separate problems. It should be noted that this thesis is aimed at solving coupled problems where at least one field is structural in nature. Even then the arguments and theory contained within this thesis are aimed at the more physical interaction problems (ie. fluid-structure and structure-structure problems versus control-structure and thermal-mechanical problems).

1.3 Restrictions Considered

In developing the theory described earlier certain restrictions of the general problem are assumed. First, the constraints which couple the separate fields are assumed to exist as two-way interactions between two individual fields. For this reason the coupled problem can be examined by considering only two fields.

Additional fields can be dealt with in a similar fashion. Figure 1.3-1 shows the allowable interactions for a system of three coupled fields.

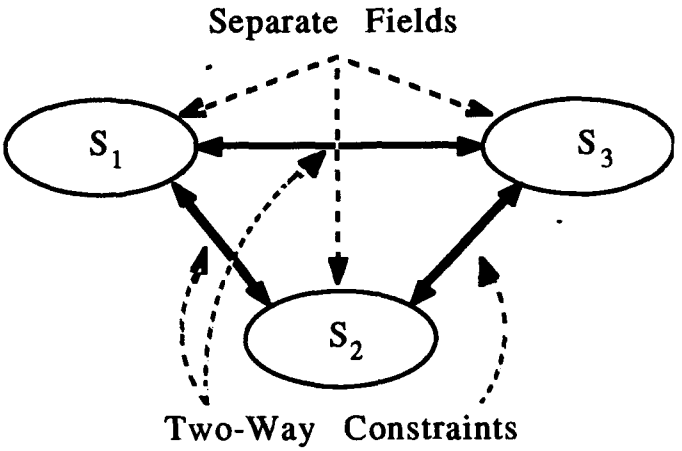

Figure 1.3-1 Coupled System Interaction

It is also assumed that the equations of motion for the separate fields are initially describable in a semi-discrete second order form:

$$\mathbf{M}\ddot{\mathbf{x}} + \mathbf{C}\dot{\mathbf{x}} + \mathbf{K}\mathbf{x} = \mathbf{R}(t)$$

This is not an overly limiting assumption since most fields in coupled problems are easily placed in this form.

1.4 Overview

The remainder of this thesis is organized in the following manner. Chapter two reviews the available methods of solving coupled field problems along with the benefits and shortcomings of each method. Field-elimination and simultaneous solutions are discussed as well as partitioned solution methods, where simulation coupling is introduced as a special case of these methods.

Chapter Three describes some of the tools essential to the development of the theory for coupling simulations, namely integration procedures and stability analysis procedures.

Chapter Four sets forth the simulation coupling procedures in addition to discussing how to deal with the constraints which couple the separate fields. The stability and accuracy of the coupling procedures are also discussed.

Chapters Five and Six set forth numerical examples designed to illuminate points made about the simulation coupling theory developed in chapter five. Chapter Five involves small scale examples designed to highlight specifics on the stability and accuracy of this method. Chapter Six is dedicated to the large scale example, namely, coupling single body simulations to form the assembly complete form of the space station; a problem at the scale to which simulation coupling is specifically directed.

Chapter Seven concludes this thesis by reviewing work done, major findings included within, as well as outlining future work for consideration in this area.

Chapter Two

Solution Methods of Coupled-Field Problems

This chapter presents a basic overview of the primary means by which coupled-field problems are solved. These problems are often sufficiently large and complex that the only feasible solution process is direct integration, which leaves the major question of what form to place the equations of motion in order to carry out the integration. Field elimination and simultaneous solution are standard methods by which these problems are currently handled although both have serious drawbacks which hinder their performance. More recently partitioned solutions have been suggested as a possible alternative [2.1-2.10]. A large number of partitioning schemes have been recommended in literature and some of the more popular methods will be introduced here. At the end of this chapter simulation coupling is shown as a natural extension of partitioned solutions.

2.1 Idealization of the Coupled-Field Problem

Consider an arbitrary domain, S, shown in Figure 2.1-1. Allowing that S is the domain of a two-field coupled problem it may be decomposed into three distinct subdomains: S_x and S_y, the separate single field subdomains; and S_I, the interface subdomain.

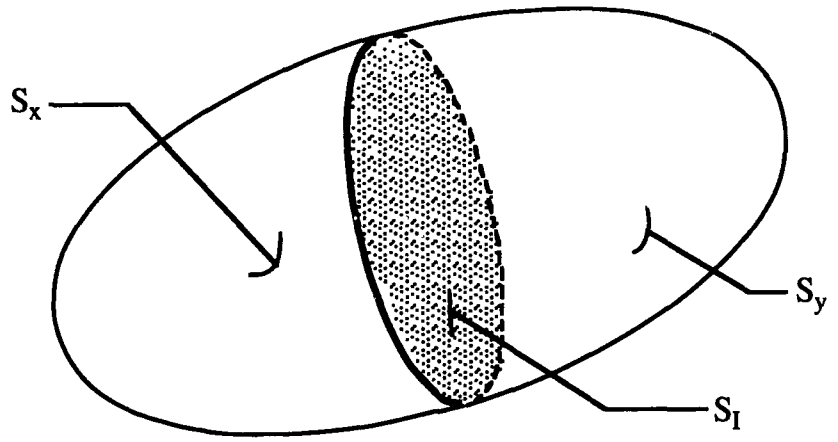

Figure 2.1-1 Arbitrary Two-Field Coupled Domain

If the effects of S_I are ignored then the single fields may be modelled by finite difference or finite element methods as semidiscrete, linear, second order matrix differential equations

$$\begin{aligned} \mathbf{M}_x\ddot{\mathbf{x}} + \mathbf{C}_x\dot{\mathbf{x}} + \mathbf{K}_x\mathbf{x} &= \mathbf{R}_x \\ \mathbf{M}_y\ddot{\mathbf{y}} + \mathbf{C}_y\dot{\mathbf{y}} + \mathbf{K}_y\mathbf{y} &= \mathbf{R}_y \end{aligned} \qquad (2.1\text{-}1)$$

where

$\mathbf{x} = \mathbf{x}(t), \mathbf{y} = \mathbf{y}(t)$: Separate field response vectors

$\mathbf{M}_x, \mathbf{M}_y$: General mass matrix

$\mathbf{C}_x, \mathbf{C}_y$: General damping matrix

$\mathbf{K}_x, \mathbf{K}_y$: General stiffness matrix

$\mathbf{R}_x = \mathbf{R}_x(t), \mathbf{R}_y = \mathbf{R}_y(t)$: Separate field vector forcing functions and $\dot{(\ )}$ denotes time integration

The fields expressed in equation (2.1-1) are coupled by the physical constraints and interface conditions of S_I which are expressed as

$$\Phi(\dot{\mathbf{x}}, \dot{\mathbf{y}}, \mathbf{x}, \mathbf{y}) = 0 \qquad (2.1\text{-}2)$$

Note that the constraints which lead to coupled-field problems are generally not assumed to be time varying functions.

Through appropriate use of Lagrange multipliers, penalty formulations, or other methods equations (2.1-1) and (2.1-2) may be combined as

$$\begin{aligned} \mathbf{M}_x\ddot{\mathbf{x}} + \mathbf{C}_x\dot{\mathbf{x}} + \mathbf{K}_x\mathbf{x} &= \mathbf{R}_x + \mathbf{f}_{cx} \\ \mathbf{M}_y\ddot{\mathbf{y}} + \mathbf{C}_y\dot{\mathbf{y}} + \mathbf{K}_y\mathbf{y} &= \mathbf{R}_y + \mathbf{f}_{cy} \end{aligned} \qquad (2.1\text{-}3)$$

where $\mathbf{f}_{cx}$ and $\mathbf{f}_{cy}$ are effective constraint forces used to correct the separate field response.

In the case where the interactions are linear in nature then (2.1-3) can be rearranged as follows:

$$\begin{aligned} \mathbf{M}_{xx}\ddot{\mathbf{x}} + \mathbf{C}_{xx}\dot{\mathbf{x}} + \mathbf{K}_{xx}\mathbf{x} &= \mathbf{R}_x - \mathbf{C}_{xy}\dot{\mathbf{y}} - \mathbf{K}_{xy}\mathbf{y} \\ \mathbf{M}_{yy}\ddot{\mathbf{y}} + \mathbf{C}_{yy}\dot{\mathbf{y}} + \mathbf{K}_{yy}\mathbf{y} &= \mathbf{R}_y - \mathbf{C}_{yx}\dot{\mathbf{x}} - \mathbf{K}_{yx}\mathbf{x} \end{aligned} \qquad (2.1\text{-}4)$$

or if $\mathbf{u} = [\ \mathbf{x}^T\ \mathbf{y}^T\ ]^T$

$$\mathbf{M}\ddot{\mathbf{u}} + \mathbf{C}\dot{\mathbf{u}} + \mathbf{K}\mathbf{u} = \mathbf{R} \qquad (2.1\text{-}5)$$

where

$$\mathbf{M} = \begin{bmatrix} \mathbf{M}_{xx} & 0 \\ 0 & \mathbf{M}_{yy} \end{bmatrix}, \quad \mathbf{C} = \begin{bmatrix} \mathbf{C}_{xx} & \mathbf{C}_{xy} \\ \mathbf{C}_{yx} & \mathbf{C}_{yy} \end{bmatrix}, \quad \mathbf{K} = \begin{bmatrix} \mathbf{K}_{xx} & \mathbf{K}_{xy} \\ \mathbf{K}_{yx} & \mathbf{K}_{yy} \end{bmatrix},$$

and $\mathbf{R} = \begin{bmatrix} \mathbf{R}_x^T & \mathbf{R}_y^T \end{bmatrix}^T$.

Note: $\mathbf{K}_x$ may be modified by terms from $\mathbf{f}_{cx}$ in (2.1-3) in order to obtain $\mathbf{K}_{xx}$ in (2.1-4). Similar effects may be seen in $\mathbf{K}_{yy}$, $\mathbf{C}_{xx}$, $\mathbf{C}_{yy}$. However, $\mathbf{M}_{xx} = \mathbf{M}_x$ and $\mathbf{M}_{yy} = \mathbf{M}_y$.

2.2 Field Elimination

Field elimination is aimed at the elimination of the interaction terms through substitutions from the other available equations. This method is usually suggested when the response of one field is considered to be more important than the other. This process reduces the number of states associated with each problem to only one field but has several considerable drawbacks which should be highlighted in the following example.

Consider the simpler system of the form of (2.1-4)

$$\begin{aligned} \mathbf{M}_{xx}\ddot{\mathbf{x}} + \mathbf{C}_{xx}\dot{\mathbf{x}} + \mathbf{K}_{xx}\mathbf{x} &= \mathbf{R}_x - \mathbf{K}_{xy}\mathbf{y} \\ \mathbf{M}_{yy}\ddot{\mathbf{y}} + \mathbf{C}_{yy}\dot{\mathbf{y}} + \mathbf{K}_{yy}\mathbf{y} &= \mathbf{R}_y - \mathbf{K}_{yx}\mathbf{x} \end{aligned} \qquad (2.2\text{-}1)$$

Transforming these equations by means of the Laplace variable

$$\begin{aligned} (\mathbf{M}_{xx}s^2 + \mathbf{C}_{xx}s + \mathbf{K}_{xx})\mathbf{X}(s) &= \mathbf{R}_x(s) - \mathbf{K}_{xy}\mathbf{Y}(s) \\ (\mathbf{M}_{yy}s^2 + \mathbf{C}_{yy}s + \mathbf{K}_{yy})\mathbf{Y}(s) &= \mathbf{R}_y(s) - \mathbf{K}_{yx}\mathbf{X}(s) \end{aligned} \qquad (2.2\text{-}2)$$

Eliminating Y(s) from (2.2-2a) using (2.2-2b)

$$\left[\left(\mathbf{M}_{yy}s^2 + \mathbf{C}_{yy}s + \mathbf{K}_{yy}\right)\mathbf{K}_{xy}^{-1}\left(\mathbf{M}_{xx}s^2 + \mathbf{C}_{xx}s + \mathbf{K}_{xx}\right) - \mathbf{K}_{yx}\right]\mathbf{X}(s) = \left(\mathbf{M}_{yy}s^2 + \mathbf{C}_{yy}s + \mathbf{K}_{yy}\right)\mathbf{K}_{xy}^{-1}\mathbf{R}_x(s) - \mathbf{R}_y(s) \quad (2.2\text{-}3)$$

Multiplying through

$$\begin{aligned}\left\{\left(\mathbf{M}_{yy}\mathbf{K}_{xy}^{-1}\mathbf{M}_{xx}\right)s^4 + \left(\mathbf{C}_{yy}\mathbf{K}_{xy}^{-1}\mathbf{M}_{xx} + \mathbf{M}_{yy}\mathbf{K}_{xy}^{-1}\mathbf{C}_{xx}\right)s^3\right.\\ + \left(\mathbf{M}_{yy}\mathbf{K}_{xy}^{-1}\mathbf{K}_{xx} + \mathbf{C}_{yy}\mathbf{K}_{xy}^{-1}\mathbf{C}_{xx} + \mathbf{K}_{yy}\mathbf{K}_{xy}^{-1}\mathbf{M}_{xx}\right)s^2\\ \left. + \left(\mathbf{K}_{yy}\mathbf{K}_{xy}^{-1}\mathbf{C}_{xx} + \mathbf{C}_{yy}\mathbf{K}_{xy}^{-1}\mathbf{K}_{xx}\right)s + \left(\mathbf{K}_{yy}\mathbf{K}_{xy}^{-1}\mathbf{K}_{xx} - \mathbf{K}_{yx}\right)\right\}\mathbf{X}(s)\\ = \left(\mathbf{M}_{yy}s^2 + \mathbf{C}_{yy}s + \mathbf{K}_{yy}\right)\mathbf{K}_{xy}^{-1}\mathbf{R}_x(s) - \mathbf{R}_y(s)\end{aligned} \quad (2.2\text{-}4)$$

Use of the inverse Laplace transform returns a differential expression

$$\begin{aligned}\left(\mathbf{M}_{yy}\mathbf{K}_{xy}^{-1}\mathbf{M}_{xx}\right)\dddot{\mathbf{x}} + \left(\mathbf{C}_{yy}\mathbf{K}_{xy}^{-1}\mathbf{M}_{xx} + \mathbf{M}_{yy}\mathbf{K}_{xy}^{-1}\mathbf{C}_{xx}\right)\ddot{\mathbf{x}}\\ + \left(\mathbf{M}_{yy}\mathbf{K}_{xy}^{-1}\mathbf{K}_{xx} + \mathbf{C}_{yy}\mathbf{K}_{xy}^{-1}\mathbf{C}_{xx} + \mathbf{K}_{yy}\mathbf{K}_{xy}^{-1}\mathbf{M}_{xx}\right)\dot{\mathbf{x}}\\ + \left(\mathbf{K}_{yy}\mathbf{K}_{xy}^{-1}\mathbf{C}_{xx} + \mathbf{C}_{yy}\mathbf{K}_{xy}^{-1}\mathbf{K}_{xx}\right)\mathbf{x} + \left(\mathbf{K}_{yy}\mathbf{K}_{xy}^{-1}\mathbf{K}_{xx} - \mathbf{K}_{yx}\right)\mathbf{x}\\ = \mathbf{M}_{yy}\mathbf{K}_{xy}^{-1}\ddot{\mathbf{R}}_x + \mathbf{C}_{yy}\mathbf{K}_{xy}^{-1}\dot{\mathbf{R}}_x + \mathbf{K}_{yy}\mathbf{K}_{xy}^{-1}\mathbf{R}_x - \mathbf{R}_y\end{aligned} \quad (2.2\text{-}5)$$

An expression similar to (2.2-4) can be found for the variable y(t).

The following disadvantages can be seen in this example:

- Higher-order derivatives are introduced for which there are no readily available integrators.
- Additional initial conditions are required.
- Additional derivatives of the forcing functions are required.
- The sparsity (and possibly symmetry) of the attendant matrices is lost.
- There is little possible use of existing software or single field analyzers

- The above disadvantages become more serious as the complexity of the problem increases.

Although field climination does succeed in reducing the states associated with the problem it does so at the cost of introducing further difficulties not easily solved at this time. Furthermore, every time a secondary field to be coupled with the primary changes the process must be repeated to solve the new problem.

2.3 Simultaneous Solutions

In simultaneous solution methods the coupled equations of motion are integrated as a single large second-order problem in the form of equation (2.1-5). By integrating all the equations in second-order form, as opposed to field elimination procedures, higher order derivatives and additional initial conditions are not required. In addition there are accepted integration methods for use on second-order differential systems. However, to be placed in the form of (2.1-5) the interactions must be linear and there is still no possibility of using existing single field analyzers.

Another shortcoming of this method is the requirement of treatment in fully explicit or fully implicit form. This specification carries with it the following problems. Since coupled problems typically have very diverse time characteristics, the stability limits on the step size tend to be unreasonably restrictive. This is especially true if the problem includes rigid effects or incorporates the constraints by penalty formulations. Also the interaction tends

to produce extremely large bandwidths in the associated coefficient matrices. As a result the solution of realistic three dimensional problems becomes rapidly prohibitive due to the number of calculations necessary to set up and solve equations involving these matrices.

So despite the superiority of simultaneous solutions to field elimination there still exists the problem of setting up and solving large set of coupled equations, along with a continued lack of modularity.

2.4 Partitioned Solutions

Partitioned solution methods are based on dividing the system matrices of equation (2.1-5) into two parts,

$$\mathbf{K} = \mathbf{K}^I + \mathbf{K}^E \text{ and } \mathbf{C} = \mathbf{C}^I + \mathbf{C}^E \qquad (2.4\text{-}1)$$

where $\mathbf{K}^I$ and $\mathbf{C}^I$ are the implicit portions of the partition and $\mathbf{K}^E$ and $\mathbf{C}^E$ are the explicit portions. It should be mentioned that the entire mass matrix must be contained in the implicit portion of the partition (see [2.6]). In a partitioned solution the explicit portion, combined with a predictor, acts like an applied force input to the differential equation. There are two things which define a partition method: the partitioning strategy and the particular partition used to divide the system matrices.

The partitioning strategy is defined by the point at which the partitioning occurs. At some point in order to solve the differential system a numerical integration scheme must be applied. If the

scheme is applied and then the resulting matrix equation is partitioned the strategy is call algebraic partitioning. If the partition is applied before the integration scheme, then a differential partitioning strategy results. The work of Felippa and Park [2.6] shows a strong connection between the stability of the method and the partitioning strategy used.

For a two-field system there are sixteen possible ways to fully partition the system matrices and six of these simply represent field switches. The ten remaining unique partitions for the explicit portion, $\mathbf{K}^E$ are

$$^1\begin{bmatrix} 0 & 0 \\ 0 & 0 \end{bmatrix} \; ^2\begin{bmatrix} 0 & 0 \\ 0 & \mathbf{K}_{yy} \end{bmatrix} \; ^3\begin{bmatrix} 0 & 0 \\ \mathbf{K}_{yx} & 0 \end{bmatrix} \; ^4\begin{bmatrix} 0 & 0 \\ \mathbf{K}_{yx} & \mathbf{K}_{yy} \end{bmatrix} \; ^5\begin{bmatrix} 0 & \mathbf{K}_{xy} \\ 0 & \mathbf{K}_{yy} \end{bmatrix} \quad (2.4\text{-}2)$$

$$^6\begin{bmatrix} \mathbf{K}_{xx} & 0 \\ 0 & \mathbf{K}_{yy} \end{bmatrix} \; ^7\begin{bmatrix} 0 & \mathbf{K}_{xy} \\ \mathbf{K}_{yx} & 0 \end{bmatrix} \; ^8\begin{bmatrix} \mathbf{K}_{xx} & \mathbf{K}_{xy} \\ \mathbf{K}_{yx} & 0 \end{bmatrix} \; ^9\begin{bmatrix} \mathbf{K}_{xx} & 0 \\ \mathbf{K}_{yx} & \mathbf{K}_{yy} \end{bmatrix} \; ^{10}\begin{bmatrix} \mathbf{K}_{xx} & \mathbf{K}_{xy} \\ \mathbf{K}_{yx} & \mathbf{K}_{yy} \end{bmatrix}$$

The first and last cases correspond to the limiting fully implicit and fully explicit simultaneous solutions, respectively. Partitions numbers 2, 4, 5, 8, and 9 are all implicit-explicit partitions with 2 and 4 being more widely used, as will be discussed later. Also number 3 is of particular importance; it is referred to as a staggered partition and warrants further consideration. A more complete analysis of all the available partitions is contained in [2.7].

Implicit-explicit partitions were first suggested for use in structural dynamics by Belytschko and Mullen [2.1,2.2] in problems where the mesh had two distinct set of time characteristics. The specific application in mind were fluid-structure problems where a very large, slow responding mesh (fluid) was coupled with a smaller,

quicker responding mesh (structure). Since the fluid mesh is very large an explicit method was desired for improved computational efficiency, but the large range of response frequencies in the structure called for an implicit method for stability. By introducing a boundary field, thus making it a three-field problem, and a three-field partition equivalent to 4 the fluid was dealt with explicitly and the structure implicitly. This form of partition is known as node-by-node implicit-explicit (IE) partitioning.

Shortly thereafter Hughes and Liu [2.3,2.4] introduced the three-field partition based on 2. This model defined the elements as either implicit or explicit. The element-by-element IE partitioning is easier to implement but may be more computationally intensive for large boundary problems. However both element-by-element and node-by-node IE partitioning still retain little modularity in solving the problem.

Perhaps the most extensively used partition is the staggered partition. It has thus far been effectively applied to fluid-structure interaction problems [2.10], control-structure interaction problems [2.9] and multibody dynamic simulation [2.8]. Staggered solutions predict one field (in this case x) and use the prediction to solve the second field (y). The first field is then solved using the solution of the second in an implicit fashion. This process is depicted below in Figure 2.4-1 where EP is an explicit prediction flow and IS is an implicit solution flow. Although it has been successful in allowing more use of single field analysis software [see 2.6], it still does not come through with the desired modularity.

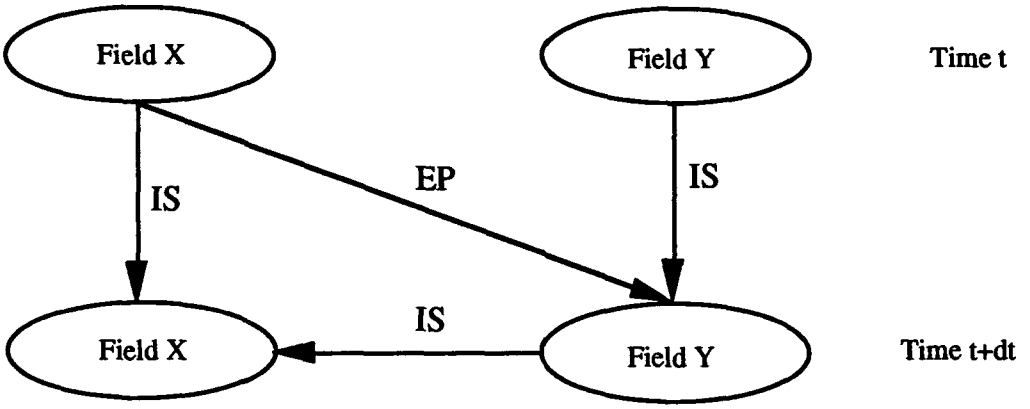

Figure 2.4-1 Flow of Information in a Staggered Solution

2.5 Simulation Coupling

Simulation coupling does not fall under one of the ten partitions already mentioned since it is not a complete partition. Instead of starting from (2.1-5) the partition is formed from the terms in (2.1-3)

$$\mathbf{M}_x\ddot{\mathbf{x}} + \mathbf{C}_x\dot{\mathbf{x}} + \mathbf{K}_x\mathbf{x} = \mathbf{R}_x + \mathbf{f}_{cx}$$
$$\mathbf{M}_y\ddot{\mathbf{y}} + \mathbf{C}_y\dot{\mathbf{y}} + \mathbf{K}_y\mathbf{y} = \mathbf{R}_y + \mathbf{f}_{cy}$$

If these equations are manipulated into the form of (2.1-5) they look like

$$\begin{bmatrix} \mathbf{M}_x & 0 \\ 0 & \mathbf{M}_y \end{bmatrix}\ddot{\mathbf{u}} + \begin{bmatrix} \mathbf{C}_x & 0 \\ 0 & \mathbf{C}_y \end{bmatrix}\dot{\mathbf{u}} + \begin{bmatrix} \mathbf{K}_x & 0 \\ 0 & \mathbf{K}_y \end{bmatrix}\mathbf{u} = \mathbf{R} + \begin{bmatrix} \mathbf{f}_{cx} \\ \mathbf{f}_{cy} \end{bmatrix} \quad (2.5\text{-}1)$$

where all terms are as previously defined.

Again by approximating the interaction terms as linear, the effective constraint terms may be written

$$\begin{bmatrix} \mathbf{f}_{cx} \\ \mathbf{f}_{cy} \end{bmatrix} = \begin{bmatrix} \mathbf{C}^c_{xx} & \mathbf{C}^c_{xy} \\ \mathbf{C}^c_{yx} & \mathbf{C}^c_{yy} \end{bmatrix} \dot{\mathbf{u}} + \begin{bmatrix} \mathbf{K}^c_{xx} & \mathbf{K}^c_{xy} \\ \mathbf{K}^c_{yx} & \mathbf{K}^c_{yy} \end{bmatrix} \mathbf{u} \qquad (2.5\text{-}2)$$

Using these terms the partition for simulation coupling is defined as follows:

$$\mathbf{K}^I = \begin{bmatrix} \mathbf{K}_x & 0 \\ 0 & \mathbf{K}_y \end{bmatrix} \text{ and } \mathbf{K}^E = \begin{bmatrix} \mathbf{K}^c_{xx} & \mathbf{K}^c_{xy} \\ \mathbf{K}^c_{yx} & \mathbf{K}^c_{yy} \end{bmatrix} \qquad (2.5\text{-}3)$$

and the damping terms are similarly partitioned. The advantages to using such a partition are that the implicit portion of the partition is exactly the single field problem with interaction effects neglected. This is readily seen by examining the left-hand side of (2.5-1), where the system matrices are completely uncoupled. The interaction effects are handled exclusively in the explicit portion of the partition. This solution form allows existing single field analysis packages to be applied directly with the inclusion of constraint terms as applied forces being the only modification necessary. As this is a partitioned solution form, the partitioning strategy, the chosen predictors, as well as the details of implementation have great impact on overall stability and performance of simulation coupling. These effects are addressed in the remaining parts of this thesis.

Chapter Three

Methods for the Analysis of Numerical Integration

Since the primary means of solving large sets of differential equations is direct time integration, it is important to review the basic theory and notation involved. This chapter outlines reduced order forms as well as operational notation used to determine the stability of a given procedure. Additionally, details of computer implementation such as computational paths and choice of auxiliary vectors are covered. Much of this information was first introduced by Jensen [3.1] and is covered in detail in a series of papers by Felippa and Park [3.2, 3.3 and 2.6].

3.1 Time Discretization

The equation for a general space-discretized structural system described earlier is

$$\mathbf{M}\ddot{\mathbf{u}} + \mathbf{C}\dot{\mathbf{u}} + \mathbf{K}\mathbf{u} = \mathbf{R} \qquad (3.1\text{-}1)$$

This system may be placed in reduced first order form by introducing an auxiliary vector, v (see [3.1])

$$\mathbf{v} = \mathbf{AM}\dot{\mathbf{u}} + \mathbf{Bu} \qquad (3.1\text{-}2)$$

where **A** and **B** are suitably chosen n x n matrices. By manipulating (3.1-1) $\ddot{\mathbf{u}}$ may be eliminated in favor of $\dot{\mathbf{v}}$

$$\mathbf{AM}\ddot{\mathbf{u}} + \mathbf{AC}\dot{\mathbf{u}} + \mathbf{AKu} = \mathbf{AR} \rightarrow \dot{\mathbf{v}} + (\mathbf{AC} - \mathbf{B})\dot{\mathbf{u}} + \mathbf{AKu} = \mathbf{AR} \qquad (3.1\text{-}3)$$

With the equations of motion cast in first order form [(3.1-2) and (3.1-3)], numerical integration is carried out by introducing a first order, linear multistep integration approximation for the variables $\dot{\mathbf{u}}$ and $\dot{\mathbf{v}}$. Given a constant stepsize, h, the form of such approximations is

$$\sum_{i=0}^{m} \alpha_i \mathbf{w}_{n-i} = h \sum_{i=0}^{m} \beta_i \dot{\mathbf{w}}_{n-i} \qquad (3.1\text{-}4)$$

The α_i's and β_i's are specific to each approximation and frequently normalized so that $\alpha_0 = 1$. Also, $\mathbf{w}_k$ is a generic vector with k denoting the vector $\mathbf{w}(t)$ at time $t = t_k$.

Note 1: A large number of integration methods have been left out due to the restriction to linear multistep methods. Perhaps the most frequently used of these are the Runge-Kutta class. Although popular, this class is not feasible for large scale problems like structural simulation due to their multiple derivative evaluations per time step and the difficulty associated with analyzing the stability of multiple evaluation methods.

Note 2: It is assumed that the same integration approximation is used for both **u** and **v**. This is consistent with the basic principles of simulation coupling; in making maximum use of existing software a single favorite or best available integration package would be applied to all equations within the separate simulations. If this is not the case then (3.1-4) may be replaced by

$$\sum_{i=0}^{m} \alpha_i^u \mathbf{u}_{n-i} = h \sum_{i=0}^{m} \beta_i^u \dot{\mathbf{u}}_{n-i}$$

$$\sum_{i=0}^{m} \alpha_i^v \mathbf{v}_{n-i} = h \sum_{i=0}^{m} \beta_i^v \dot{\mathbf{v}}_{n-i} \qquad (3.1\text{-}5)$$

and the separate terms may be carried throughout the remaining equations.

Removing the current state term ($t = t_n$) from the past terms, (3.1-4) may be recast

$$\mathbf{w}_n = h\beta_0 \dot{\mathbf{w}}_n + \mathbf{h}_n^w \qquad (3.1\text{-}6)$$

where

$$\mathbf{h}_n^w = h\mathbf{b}_n^{\dot{w}} - \mathbf{a}_n^w = h[\dot{\mathbf{w}}_{n-1} \cdots \dot{\mathbf{w}}_{n-m}] \begin{Bmatrix} \beta_1 \\ \vdots \\ \beta_m \end{Bmatrix} - [\mathbf{w}_{n-1} \cdots \mathbf{w}_{n-m}] \begin{Bmatrix} \alpha_1 \\ \vdots \\ \alpha_m \end{Bmatrix} \qquad (3.1\text{-}7)$$

$h\beta_0$ is usually defined as δ, termed the generalized or effective stepsize, and $\mathbf{h}_n^w$ is the historical vector.

Using (3.1-6) to substitute for the $\dot{\mathbf{u}}$ in (3.1-2), $\mathbf{v}_n$ is found in terms of $\mathbf{u}_n$ and the historical vector

$$\delta \mathbf{v}_n = (\delta \mathbf{B} + \mathbf{A}\mathbf{M})\mathbf{u}_n - \mathbf{A}\mathbf{M}\mathbf{h}_n^u \qquad (3.1\text{-}8)$$

This equation can be used along with forms of (3.1-6) for $\dot{\mathbf{u}}$ and $\dot{\mathbf{v}}$ to remove everything except $\mathbf{u}_n$, the historical vectors $\mathbf{h}_n^u$ and $\mathbf{h}_n^v$, and the current forcing term $\mathbf{R}_n$ from (3.1-3). Making the appropriate substitutions leaves

$$[\mathbf{M} + \delta\mathbf{C} + \delta^2\mathbf{K}]\mathbf{u}_n = [\mathbf{M} + \delta(\mathbf{C} - \mathbf{A}^{-1}\mathbf{B})]\mathbf{h}_n^u + \delta\mathbf{A}^{-1}\mathbf{h}_n^v + \delta^2\mathbf{R}_n \qquad (3.1\text{-}9)$$

Note 3: Until now nothing has been said about discretization by means of the popular second order methods, such as Newmark, Houbolt, or Wilson-θ integration. These second order, linear multistep methods have been examined in detail by Geradin [3.4] and are easily cast in forms similar to the first order methods. Two integration approximations are required, one like the first order (3.1-4), the other in terms of accelerations

$$\sum_{i=0}^{m} \alpha_i \mathbf{u}_{n-i} = h \sum_{i=0}^{m} \beta_i \dot{\mathbf{u}}_{n-i}$$

$$\sum_{i=0}^{m} \gamma_i \mathbf{u}_{n-i} = h^2\eta \sum_{i=0}^{m} \beta_i \ddot{\mathbf{u}}_{n-i} \qquad (3.1\text{-}10)$$

or in simpler notation

$$\mathbf{u}_n = \delta_u \dot{\mathbf{u}}_n + \mathbf{h}_n^u$$

$$\mathbf{u}_n = h\eta\delta_u \ddot{\mathbf{u}}_n + \mathbf{h}_n^{\ddot{u}} \qquad (3.1\text{-}11)$$

where δ_u is δ from before, $\mathbf{h}_n^u$ is as defined in (3.1-7) and $\mathbf{h}_n^{\ddot{u}}$ is defined as

$$\mathbf{h}_n^{\ddot{u}} = h^2\eta\mathbf{b}_n^{\ddot{u}} - \mathbf{c}_n^{u} = h^2\eta\left[\ddot{\mathbf{u}}_{n-1} \cdots \ddot{\mathbf{u}}_{n-m}\right]\begin{Bmatrix}\beta_1\\ \vdots \\ \beta_m\end{Bmatrix} - \left[\mathbf{u}_{n-1} \cdots \mathbf{u}_{n-m}\right]\begin{Bmatrix}\gamma_1\\ \vdots \\ \gamma_m\end{Bmatrix} \quad (3.1\text{-}12)$$

Using (3.1-11) to substitute for $\dot{\mathbf{u}}$ and $\ddot{\mathbf{u}}$ in (3.1-1) and defining $\delta_{\dot{u}} = h\eta$ results in a final form similar to (3.1-9)

$$\left[\mathbf{M} + \delta_{\dot{u}}\mathbf{C} + \delta_{\dot{u}}\delta_u\mathbf{K}\right]\mathbf{u}_n = \mathbf{C}\mathbf{h}_n^{u} + \mathbf{M}\mathbf{h}_n^{\ddot{u}} + \delta_{\dot{u}}\delta_u\mathbf{R}_n \qquad (3.1\text{-}13)$$

Since this result is merely an extension of the first order form (by choosing $\mathbf{v} = \dot{\mathbf{u}}$ and using separate integration formulas for each), it may be treated in the same fashion and is not be dealt with independently.

3.2 Effects of Computer Implementation

There are two primary decisions to be made when implementing a numerical integration scheme. The first involves choosing one of the equations already presented to compute the necessary terms for $\mathbf{h}_n^{v}$, while the second deals with the choice of weighting matrices **A** and **B** to determine the auxiliary vector **v**. Both decisions affect the solution's stability, error propagation, and efficiency.

3.2.1 Computing the Historical Vector

The calculation of the historical vector $\mathbf{h}_n^{v}$ is referred to as the computational path. The three steps in finding $\mathbf{h}_n^{v}$, for each of the three paths (0,1,2), are shown in Table 3.2-1. The remaining steps which find $\mathbf{h}_n^{u}$, form the right hand side of (3.1-9), and then solve for

$\mathbf{u}_n$ are the same for all paths and are listed in Table 3.2-2. It should be mentioned that there are other possible ways in which $\mathbf{h}_n^v$ may be calculated, but these are the most frequently encountered. However, one common variation is to update $\dot{\mathbf{u}}_n$ within the 0 path, creating a 0' path.

3.2.2 Choice of Auxiliary Vector

There are two widely accepted choices for $\mathbf{v}$. The physically intuitive choice is to let $\mathbf{v} = \dot{\mathbf{u}}$. This is called the conventional form of $\mathbf{v}$. The other major form was introduced in [3.1] by Jensen. This form is determined by

$$\mathbf{v} = \mathbf{M}\dot{\mathbf{u}} + \mathbf{C}\mathbf{u} \qquad (3.2\text{-}1)$$

so that $\dot{\mathbf{v}} = \mathbf{R} - \mathbf{K}\mathbf{u}$. The conventional form and Jensen's form are numerically equivalent, however, the effort and efficiency of each is significantly different.

The conventional form has the benefit of reducing four state vectors to three ([$\mathbf{u},\dot{\mathbf{u}},\mathbf{v},\dot{\mathbf{v}}$] to [$\mathbf{u},\dot{\mathbf{u}},\ddot{\mathbf{u}}$]) as well as the physical significance of $\mathbf{v}$. Unfortunately, this form sometimes requires a non-singular mass matrix. Jensen's form does not have this difficulty and is more computationally efficient than the conventional form (see [3.2]). It should be noted, however, that in a simulation coupling context the auxiliary vector and the computational path are determined by the choice of integration package and not selected for efficiency or effectiveness of implementation of the overall coupled problem.

Table 3.2-1 Steps in Finding $\mathbf{h}_n^v$

Variable	Equation Used	Form of Equation
	0 Path	
$\dot{\mathbf{v}}_{n-1}$	(3.1-3)	$\dot{\mathbf{v}}_{n-1} + (\mathbf{AC} - \mathbf{B})\dot{\mathbf{u}}_{n-1} + \mathbf{AKu}_{n-1} = \mathbf{AR}_{n-1}$
$\mathbf{v}_{n-1}$	(3.1-6)	$\mathbf{v}_{n-1} = h\beta_0\dot{\mathbf{v}}_{n-1} + \mathbf{h}_{n-1}^v$
$\mathbf{h}_n^v$	(3.1-7)	$\mathbf{h}_n^v = h\mathbf{b}_n^{\dot{v}} - \mathbf{a}_n^v$
	1 Path	
$\dot{\mathbf{v}}_{n-1}$	(3.1-3)	$\dot{\mathbf{v}}_{n-1} + (\mathbf{AC} - \mathbf{B})\dot{\mathbf{u}}_{n-1} + \mathbf{AKu}_{n-1} = \mathbf{AR}_{n-1}$
$\mathbf{v}_{n-1}$	(3.1-2)	$\mathbf{v}_{n-1} = \mathbf{A}\,\mathbf{M}\dot{\mathbf{u}}_{n-1} + \mathbf{Bu}_{n-1}$
$\mathbf{h}_n^v$	(3.1-7)	$\mathbf{h}_n^v = h\mathbf{b}_n^{\dot{v}} - \mathbf{a}_n^v$
	2 Path	
$\mathbf{v}_{n-1}$	(3.1-2)	$\mathbf{v}_{n-1} = \mathbf{A}\,\mathbf{M}\dot{\mathbf{u}}_{n-1} + \mathbf{Bu}_{n-1}$
$\dot{\mathbf{v}}_{n-1}$	(3.1-6)	$\dot{\mathbf{v}}_{n-1} = (\mathbf{v}_{n-1} - \mathbf{h}_{n-1}^v)/h\beta_0$
$\mathbf{h}_n^v$	(3.1-7)	$\mathbf{h}_n^v = h\mathbf{b}_n^{\dot{v}} - \mathbf{a}_n^v$

Table 3.2-2 Remaining Steps in Finding $\mathbf{u}_n$

Variable	Equation Used	Form of Equation
$\mathbf{h}_n^u$	(3.1-7)	$\mathbf{h}_n^u = h\mathbf{b}_n^{\dot{u}} - \mathbf{a}_n^u$
$\mathbf{b}_n$	(3.1-9)	$[\mathbf{M} + \delta(\mathbf{C} - \mathbf{A}^{-1}\mathbf{B})]\mathbf{h}_n^u + \delta\mathbf{A}^{-1}\mathbf{h}_n^v + \delta^2\mathbf{R}_n$
$\mathbf{A}_n$	(3.1-9)	$[\mathbf{M} + \delta\mathbf{C} + \delta^2\mathbf{K}]$
$\mathbf{u}_n$	Solve	$\mathbf{A}_n\mathbf{u}_n = \mathbf{b}_n$
$\dot{\mathbf{u}}_n$	(3.1-6)	$\dot{\mathbf{u}}_n = (\mathbf{u}_n - \mathbf{h}_n^u)/h\beta_0$

3.3 Operational Notation

Operational notation is presented to produce a concise presentable notation form and to facilitate stability and accuracy analysis. The discrete Laplace transform and the z-transform are introduced to the integration approximation and the historical terms to produce an operational expression for $\mathbf{b}_n$, the right hand side of (3.1-9). All of these expressions are necessary for the evaluation of the simulation coupling algorithm.

3.3.1 The Shift Operator and the Z Transform

In any series a single term may be related to the previous or following term by means of the shift operator

$$w_k = \mathbb{Z}\, w_{k-1}\,, \quad w_k = \mathbb{Z}^{-1}\, w_{k+1} \tag{3.3-1}$$

Repeated application will relate any term w_k to the initial or final term

$$w_k = \mathbb{Z}^k\, w_0\,, \quad w_k = \mathbb{Z}^{k-n}\, w_n \tag{3.3-2}$$

Since the integration methods discussed so far require only the $w_{n-m},\ldots,w_n$ terms, we can focus on the second of each of the forms above. Applying the discrete Laplace transform to the shift operator produces

$$w_k = e^{(k-n)sh}\, w_n \tag{3.3-3}$$

Substituting the standard z-transform definition, $z = e^{sh}$, into the

above expression

$$w_k = z^{k-n} w_n \qquad (3.3\text{-}4)$$

With these definitions a function f

$$f(k) = w_n + \alpha_1 w_{n-1} + \alpha_2 w_{n-2} + \alpha_3 w_{n-3} \qquad (3.3\text{-}5)$$

is transformed into the Laplace domain

$$f(s) = (1 + \alpha_1 e^{-sh} + \alpha_2 e^{-2sh} + \alpha_3 e^{-3sh}) w_n \qquad (3.3\text{-}6)$$

and into the z domain

$$f(z) = (1 + \alpha_1 z^{-1} + \alpha_2 z^{-2} + \alpha_3 z^{-3}) w_n \qquad (3.3\text{-}7)$$

or sometimes

$$f(z) = z^{-3}(z^3 + \alpha_1 z^2 + \alpha_2 z^1 + \alpha_3) w_n \qquad (3.3\text{-}8)$$

Although for the function listed above the Laplace and z variables are exact, the substitutions which following are only approximately true. Since the time series is obtained from numerical integration the properties of the shift operator in (3.3-1) and (3.3-2) are not met exactly as they would be if the true solution series was used.

3.3.2 Notation for Approximations and Historical Vectors

Since numerical integration produces a time series of vectors the terms may be readily carried into the Laplace or z domains. Given an integration approximation of the form previously introduced (where α_0 is normalized to 1 and now factoring β_0 out, leaving $\beta'_i = \beta_i/\beta_0$)

$$\mathbf{w}_n + \sum_{i=1}^{m} \alpha_i \mathbf{w}_{n-i} = \delta\left(\dot{\mathbf{w}}_n + \sum_{i=1}^{m} \beta'_i \dot{\mathbf{w}}_{n-i}\right) \qquad (3.3\text{-}9)$$

Applying the shift operator and taking the discrete Laplace transform of the approximation gives

$$\left(1 + \sum_{i=1}^{m} \alpha_i e^{-ish}\right)\mathbf{w}_n = \delta\left(1 + \sum_{i=1}^{m} \beta'_i e^{-ish}\right)\dot{\mathbf{w}}_n \qquad (3.3\text{-}10)$$

or in the z domain

$$\left(1 + \sum_{i=1}^{m} \alpha_i z^{-i}\right)\mathbf{w}_n = \delta\left(1 + \sum_{i=1}^{m} \beta'_i z^{-i}\right)\dot{\mathbf{w}}_n \qquad (3.3\text{-}11)$$

By rearranging (3.1-6) the historical vector may be written as

$$\mathbf{h}_n^w = \mathbf{w}_n - \delta\dot{\mathbf{w}}_n \qquad (3.3\text{-}12)$$

Using this definition for $\mathbf{h}_n^w$, (3.3-10) and (3.3-11) may be manipulated to form the following expressions:

$$\mathbf{h}_n^w(s) = \delta\left(\sum_{i=1}^{m} \beta'_i e^{-ish}\right)\dot{\mathbf{w}}_n - \left(\sum_{i=1}^{m} \alpha_i e^{-ish}\right)\mathbf{w}_n$$

$$\mathbf{h}_n^w(z) = \delta\left(\sum_{i=1}^{m} \beta'_i z^{-i}\right)\dot{\mathbf{w}}_n - \left(\sum_{i=1}^{m} \alpha_i z^{-i}\right)\mathbf{w}_n \qquad (3.3\text{-}13)$$

It is useful to define commonly occurring polynomials in z and e^{sh}

$$\rho(.) = 1 + \sum_{i=1}^{m} \alpha_i (.)^{-i}$$

$$\sigma(.) = 1 + \sum_{i=1}^{m} \beta'_i (.)^{-i} \qquad (3.3\text{-}14)$$

Then in either domain

$$\rho(.)\mathbf{w}_n = \delta\sigma(.)\dot{\mathbf{w}}_n \tag{3.3-15}$$

This also allows the historical vector to be written as

$$\mathbf{h}_n^w(.) = \delta\big(\sigma(.)\text{-}1\big)\dot{\mathbf{w}}_n + \big(1\text{-}\rho(.)\big)\mathbf{w}_n \tag{3.3-16}$$

Another useful operator definition which is needed is

$$\dot{\mathbf{w}}_n = \big[\rho(.)/\delta\sigma(.)\big]\mathbf{w}_n = \psi(.)\,\mathbf{w}_n \tag{3.3-17}$$

3.3.3 Notation for Forcing Term $\mathbf{b}_n$

The presence of $\mathbf{h}_n^v$ in the forcing term requires that computational path be dealt with in order to come up with the correct notation. Although each path has a distinct operational form, the choice of auxiliary vector has no effect. Recalling the basic form of $\mathbf{b}_n$

$$\mathbf{b}_n = \big[\mathbf{M} + \delta(\mathbf{C} - \mathbf{A}^{-1}\mathbf{B})\big]\mathbf{h}_n^u + \delta\mathbf{A}^{-1}\mathbf{h}_n^v + \delta^2\mathbf{R}_n \tag{3.3-18}$$

Using the definitions of the previous section $\mathbf{h}_n^u$ can be written

$$\mathbf{h}_n^u(.) = \big(1\text{-}\delta\psi(.)\big)\mathbf{u}_n \tag{3.3-18}$$

which is also independent of path. The form of $\mathbf{h}_n^v$ for each path comes from the equations in Table 3.2-1 and when combined with the above equations the following general form results:

$$\mathbf{b}_n = \big[\phi_M\mathbf{M} + \phi_C\mathbf{C} + \phi_K\mathbf{K}\big]\mathbf{u}_n + \phi_R\mathbf{R}_n \tag{3.3-19}$$

These constants are detailed in Table 3.3-1.

Table 3.3-1 Operational Constants in $\mathbf{b}_n$

Path	ϕ_M	ϕ_C	ϕ_K	ϕ_R
0	$1-\delta\psi$	0	$\delta^2-\delta\psi^{-1}$	$\delta\psi^{-1}$
1	$1-(\rho^2/\sigma)$	$\delta(1-\rho)$	$\delta^2(1-\sigma)$	$\delta^2\sigma$
2	$1-(\delta\psi)^2$	$\delta(1-\delta\psi)$	0	1

3.4 Use Of Predictors

Simulation coupling is made possible by the ability to accurately predict $\mathbf{w}_n$ from earlier knowledge of $\mathbf{w}$. A general linear multistep predictor is suggested in [2.6] for use in large coupled problems. The form of this predictor is

$$\mathbf{w}_n^P = \sum_{i=1}^{m} \alpha_i^P \mathbf{w}_{n-i} + h\beta_0 \sum_{i=1}^{m} \beta_i^P \dot{\mathbf{w}}_{n-i} + (h\beta_0)^2 \sum_{i=1}^{m} \gamma_i^P \ddot{\mathbf{w}}_{n-i} \qquad (3.4\text{-}1)$$

As with the integration methods it is also beneficial to place the predictor in operational form by defining polynomials in e^{sh} and z as follows:

$$p_w(.) = \sum_{i=1}^{m} \alpha_i^P (.)^{-i}$$

$$p_{\dot{w}}(.) = \delta \sum_{i=1}^{m} \beta_i^P (.)^{-i} \qquad (3.4\text{-}2)$$

$$p_{\ddot{w}}(.) = \delta^2 \sum_{i=1}^{m} \gamma_i^P (.)^{-i}$$

Using these definitions as well as (3.3-16) gives the final form of the predictor as:

$$w_n^P(.) = p(.)w_n = \left[p_w(.) + \delta\psi p_{\dot{w}}(.) + (\delta\psi)^2 p_{\ddot{w}}(.)\right]w_n \quad (3.4\text{-}3)$$

3.5 Examples

3.5.1 Trapezoidal Rule

The trapezoidal rule is a one step (m=1) implicit method commonly used in many integration applications. Its constants are

$$\alpha_0 = 1,\ \alpha_1 = -1,\ \beta_0 = \beta_1 = 0.5$$

Then the operational forms are

$$\rho(e^{sh}) = 1 - e^{-sh},\ \rho(z) = 1 - z^{-1}$$

$$\sigma(e^{sh}) = 1 + e^{-sh},\ \sigma(z) = 1 + z^{-1}$$

$$\psi(e^{sh}) = \frac{2}{h}\frac{1 - e^{-sh}}{1 + e^{-sh}} = \frac{2}{h}\tanh(sh/2),\ \psi(z) = \frac{2}{h}\frac{1 - z^{-1}}{1 + z^{-1}} = \frac{2}{h}\frac{z - 1}{z + 1}$$

and the historical forms are

$$h_n^w(s) = (0.5\,h\,\dot{w}_n + w_n)e^{-sh}$$

$$h_n^w(z) = (0.5\,h\,\dot{w}_n + w_n)z^{-1}$$

3.5.2 Gear's Two Step Method

Another implicit method introduced by Gear in [3.5] is a two step A-stable form. Its constants are

$$\alpha_0 = 1,\ \alpha_1 = -4/3,\ \alpha_2 = 1/3$$
$$\beta_0 = 2/3,\ \beta_1 = \beta_2 = 0$$

The operational forms are

$$\rho(e^{sh}) = 1 - \frac{4}{3}e^{-sh} + \frac{1}{3}e^{-2sh}, \quad \rho(z) = 1 - \frac{4}{3}z^{-1} + \frac{1}{3}z^{-2}$$

$$\sigma(e^{sh}) = 1 = \sigma(z)$$

$$\psi(e^{sh}) = \left(\frac{3}{2h}\right)\left(1 - \frac{4}{3}e^{-sh} + \frac{1}{3}e^{-2sh}\right) = \frac{3 - 4e^{-sh} + e^{-2sh}}{2h}$$

$$\psi(z) = \left(\frac{3}{2h}\right)\left(1 - \frac{4}{3}z^{-1} + \frac{1}{3}z^{-2}\right) = \frac{3z^2 - 4z + 1}{2hz^2}$$

and the historical forms are

$$\mathbf{h}_n^w(s) = \frac{1}{3}\left(4e^{-sh} - e^{-2sh}\right)\mathbf{w}_n$$

$$\mathbf{h}_n^w(z) = \frac{1}{3}\left(4z^{-1} - z^{-2}\right)\mathbf{w}_n$$

Chapter Four

Constraint Equations and Numerical Simulation Coupling

Before the simulation coupling process may be fully developed and analyzed, the incorporation of constraints into equations of motion must be covered. The remaining portion of this chapter provides the details of simulation coupling. Finally, the analysis of the stability and accuracy of the coupling process is addressed.

4.1 Methods of Handling Constraints

In an attempt to develop an accurate and reliable method of dealing with constraints, many different procedures have been suggested [4.1-4.6]. Two methods of primary interest for use in coupled-field problem are penalty formulations and more traditional Lagrange multiplier forms. Besides the basic implementations of the methods there are additional stabilization procedures to improve performance which are covered. Both methods detailed here are developed from using traditional variational principles and specifically the Euler-Lagrange equations.

4.1.1 The Lagrange Multiplier Method

A typical n-DOF mechanical system is defined by the following energy products:

$$\text{Kinetic: } T = \frac{1}{2}\dot{\mathbf{u}}^T \mathbf{M}\,\dot{\mathbf{u}} \quad \text{and} \quad \text{Potential: } V = \frac{1}{2}\mathbf{u}^T \mathbf{K}\,\mathbf{u} \qquad (4.1\text{-}1)$$

as well as

$$\mathcal{F} = \mathbf{C}\,\dot{\mathbf{u}} \qquad (4.1\text{-}2)$$

where $\mathcal{F}$ are Rayleigh's dissipative forces, representing damping proportional to velocity. Additionally, the response of the system is restricted by

$$\Phi(\dot{\mathbf{u}},\mathbf{u},t) = 0 \qquad (4.1\text{-}3)$$

where Φ is a vector of p individual constraints.

When no derivative terms are present, these functions may be used to eliminate p DOFs in the vector $\mathbf{u}$. Unfortunately, this is can be difficult and it is not always clear which individual degrees should be removed. Instead, Lagrange's "method of the undetermined multiplier" may be used to form a term which represents the forces which ensure the constraint is satisfied. This term, along with the nonconservative externally applied forces, $\delta W = \mathbf{R}\delta\mathbf{u}$, and energy products, may be combined to form the action integral for a constrained system

$$A = \int_{t1}^{t2} \left(L + W + \Phi^T\lambda + \mathcal{F}^T\,\mathbf{u}\right) dt \qquad (4.1\text{-}4)$$

where λ is the vector of Lagrange multipliers and L is the Lagrangian T - V. By applying the principle of least action, $\delta A = 0$, the Lagrange equation of motion is

$$\left(\frac{d}{dt}\left(\frac{\partial L}{\partial \dot{\mathbf{u}}}\right) - \frac{\partial L}{\partial \mathbf{u}}\right) - \mathcal{F} - \frac{\partial \Phi}{\partial \mathbf{u}}^{T} \lambda = \mathbf{R} \qquad (4.1\text{-}5)$$

By using (4.1-1,2) in (4.1-5) the matrix equation of motion for a constrained system is obtained

$$\mathbf{M}\ddot{\mathbf{u}} + \mathbf{C}\dot{\mathbf{u}} + \mathbf{K}\mathbf{u} = \mathbf{R} + \mathbf{G}^{T}\lambda \qquad (4.1\text{-}6)$$

where $\mathbf{G}$ is the Jacobian of (4.1-3) with respect to $\mathbf{u}$.

By taking the derivative of Φ twice forms the following equation:

$$\mathbf{G}\ddot{\mathbf{u}} + \dot{\mathbf{G}}\dot{\mathbf{u}} = 0 \qquad (4.1\text{-}7)$$

Using (4.1-6) to substitute for the second derivative in the above equation leaves a form which is solvable for λ.

$$\mathbf{G}\mathbf{M}^{-1}\mathbf{G}^{T}\lambda = \mathbf{G}\mathbf{M}^{-1}[\mathbf{C}\dot{\mathbf{u}} + \mathbf{K}\mathbf{u} - \mathbf{R}] - \dot{\mathbf{G}}\dot{\mathbf{u}} \qquad (4.1\text{-}8)$$

Since $\mathbf{M}$ is large, taking the inverse is a costly operation. To correct this the state vector is partitioned into the degrees of freedom which contribute to the constraints and those which do not, $\mathbf{u} = [\mathbf{u}_f^T \mathbf{u}_c^T]^T$. Generally $\mathbf{u}_c$ is small compared to $\mathbf{u}_f$. If a lumped mass model is used then the following substitutions may be made in (4.1-8):

$$\mathbf{G}^{T} = \mathbf{G}_{cc}^{T} \quad \mathbf{M}^{-1} = \mathbf{M}_{cc}^{-1} \quad \dot{\mathbf{G}} = \dot{\mathbf{G}}_{cc}^{T} \qquad (4.1\text{-}9)$$

where

$$\mathbf{G}^T = \begin{bmatrix} 0 & \mathbf{G}_{cc}^T \end{bmatrix} \quad \mathbf{M}^{-1} = \begin{bmatrix} \mathbf{M}_{ff}^{-1} & 0 \\ 0 & \mathbf{M}_{cc}^{-1} \end{bmatrix} \quad \dot{\mathbf{G}} = \begin{bmatrix} 0 & \dot{\mathbf{G}}_{cc}^T \end{bmatrix}$$

With these definitions the Lagrange multipliers are

$$\lambda_{nh} = \left[\mathbf{G}_{cc}\mathbf{M}_{cc}^{-1}\mathbf{G}_{cc}^T\right]^{-1}\mathbf{G}_{cc}\mathbf{M}_{cc}^{-1}[\mathbf{C}\dot{\mathbf{u}} + \mathbf{K}\mathbf{u} - \mathbf{R}] - \left[\mathbf{G}_{cc}\mathbf{M}_{cc}^{-1}\mathbf{G}_{cc}^T\right]^{-1}\dot{\mathbf{G}}_{cc}\dot{\mathbf{u}} \quad (4.1\text{-}10)$$

where the inverses are now taken of matrices with the dimension of $\mathbf{u}_{cc}$ and dimension p.

Holonomically constrained problems may be treated in much the same way. Taking the first derivative of Φ when derivative terms are present leaves

$$\mathbf{H}\ddot{\mathbf{u}} + \mathbf{G}\dot{\mathbf{u}} = 0 \quad (4.1\text{-}11)$$

where

$$\mathbf{H} = \frac{\partial \Phi}{\partial \dot{\mathbf{u}}}$$

This equation is the same in structure as (4.1-7) with $\mathbf{H}$ and $\dot{\mathbf{u}}$ substituted for $\mathbf{G}$ and $\dot{\mathbf{G}}$. Making the same assumptions as the nonholonomically constrained problem, the Lagrange multipliers for the holonomic problem are

$$\lambda_{nh} = \left[\mathbf{H}_{cc}\mathbf{M}_{cc}^{-1}\mathbf{H}_{cc}^T\right]^{-1}\mathbf{H}_{cc}\mathbf{M}_{cc}^{-1}[\mathbf{C}\dot{\mathbf{u}} + \mathbf{K}\mathbf{u} - \mathbf{R}] - \left[\mathbf{H}_{cc}\mathbf{M}_{cc}^{-1}\mathbf{H}_{cc}^T\right]^{-1}\mathbf{G}_{cc}\dot{\mathbf{u}} \quad (4.1\text{-}12)$$

There is one problem with this formulation. Using (4.1-7) and (4.1-11) forces the second and first derivatives of Φ to be zero and not Φ itself. Because of this fact the values of λ need to be corrected

by some form of stabilization technique. At this time a single best way to do this does not exist (see [4.5]).

4.1.2 The Penalty Method

As derived in the previous section, the matrix equation of motion for a holonomically constrained system is

$$\mathbf{M}\ddot{\mathbf{u}} + \mathbf{C}\dot{\mathbf{u}} + \mathbf{K}\mathbf{u} = \mathbf{R} + \mathbf{G}^T\lambda$$

The above equations have n+p unknowns in $\mathbf{u}$ and λ. The penalty method provides the additional p equations by defining λ in the following manner:

$$\lambda = -\kappa\Phi, \quad \text{as } \frac{1}{\kappa} \rightarrow 0 \qquad (4.1\text{-}13)$$

In general the penalty constant κ does not need to be the same in each of the p constraints, in which case κ becomes a p x p diagonal matrix. Substitution into (4.1-6) leaves

$$\mathbf{M}\ddot{\mathbf{u}} + \mathbf{C}\dot{\mathbf{u}} + \mathbf{K}\mathbf{u} = \mathbf{R} - \mathbf{G}^T\kappa\Phi \qquad (4.1\text{-}14)$$

The penalty method format implicitly assumes that the constraints of (4.1-3) are violated.

One difficulty in this type of formulation should be noted. Although this method converges to the correct solution, once an error occurs there is no way in which the energy associated with the penalty correction may be dissipated. To correct for this excess energy, stabilization procedures can be introduced. For the penalty method one such stabilization routine is detailed here (see also [4.5]).

It is useful to note that the penalty formulation of (4.1-14) can be achieved by augmenting the Lagrangian with a fictitious potential representing the compromised constraints

$$V^* = \frac{1}{2}\Phi^T \alpha \kappa \Phi \qquad (4.1\text{-}15)$$

To dissipate energy, fictitious Rayleigh's forces are included

$$\mathcal{F}^* = -\alpha \frac{d\Phi}{dt} \qquad (4.1\text{-}16)$$

Replacing the term $\Phi^T\lambda$ with $\mathcal{F}^* - V^*$ in the action integral and again applying the principle of least action

$$\left(\frac{d}{dt}\left(\frac{\partial L}{\partial \dot{u}}\right) - \frac{\partial L}{\partial u}\right) - \mathcal{F} = \mathbf{R} - \frac{\partial \Phi^T}{\partial u}\alpha\left(\frac{d\Phi}{dt} + \kappa\Phi\right) \qquad (4.1\text{-}17)$$

and making the appropriate substitutions

$$\mathbf{M}\ddot{u} + \mathbf{C}\dot{u} + \mathbf{K}u = \mathbf{R} - \mathbf{G}^T\alpha\left(\frac{d\Phi}{dt} + \kappa\Phi\right) \qquad (4.1\text{-}18)$$

where both α and κ may be p x p diagonal matrices. In this form α acts as the penalty and κ becomes the decay constant for the error in the constraints.

Although the terms introduced above apply to the holonomic case, it is possible to derive the system equations of motion for the nonholonomic case in a similar manner. When derivatives are present in the constraints a fictitious kinetic energy and a fictitious set of Rayleigh's dissipative forces similar to (4.1-15) and (4.1-16) augment the Lagrangian as follows:

$$T^* = \frac{1}{2}\Phi^T \alpha \kappa \Phi \tag{4.1-19}$$

and

$$\mathcal{F}^* = -\alpha \Phi \tag{4.1-20}$$

Placing these terms within the action integral yields:

$$\left(\frac{d}{dt}\left(\frac{\partial L}{\partial \dot{u}}\right) - \frac{\partial L}{\partial u}\right) - \mathcal{F} = \mathbf{R} - \frac{\partial \Phi^T}{\partial \dot{u}} \alpha \left(\frac{d\Phi}{dt}\right) \tag{4.1-21}$$

Making the appropriate substitutions to obtain this equation in matrix form results in

$$\mathbf{M}\ddot{u} + \mathbf{C}\dot{u} + \mathbf{K}u = \mathbf{R} - \mathbf{H}^T \alpha \left(\frac{d\Phi}{dt}\right) \tag{4.1-22}$$

4.2 The Simulation Coupling Process

The solution of dynamic problems by means of simulation coupling requires three distinct elements. The first of these elements is, obviously, the individual simulations for the separate fields. Additionally, elements to evaluate and correct for any violation of the constraints which couple the fields and to handle data management tasks and control the execution of the separate simulations are necessary.

There are two different ways in which the execution of the coupling process may take place. The simplest form starts with a

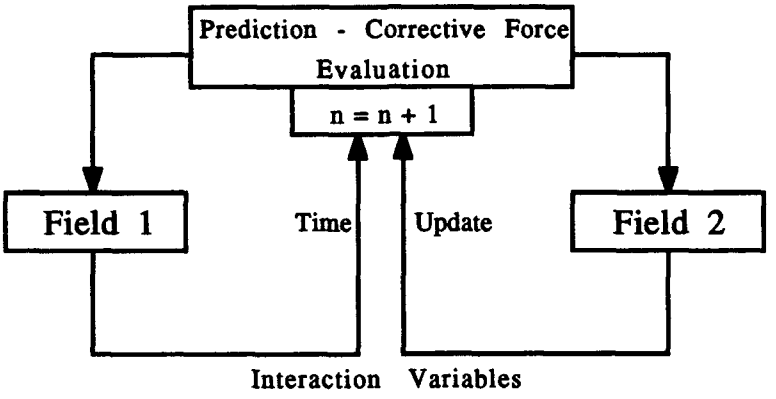

Figure 4.2-1 Information Flow in Concurrent Evaluation

prediction of the field states (x and y) in order to produce a set of corrective forces based on the incorporation of constraints. Then the individual simulations calculate the field responses at the given time. Finally, time is incremented and any necessary updates to the data structure are handled. This sequence is illustrated in Figure 4.2-1. In this case the evaluations made by the simulations may be carried out in series or in parallel. This execution order is called concurrent evaluation.

The second execution process is slightly more involved than the concurrent evaluation. It also starts with a prediction of the state variables and a corrective force prediction. However, only one field evaluation is carried out. This execution is used to update the force evaluation before analyzing the second field. Again, the process ends with time update and data management functions. This is called a staggered evaluation and is shown as Figure 4.2-2. In staggered evaluation one field may be consistently analyzed first or the order may be switched as seems fit.

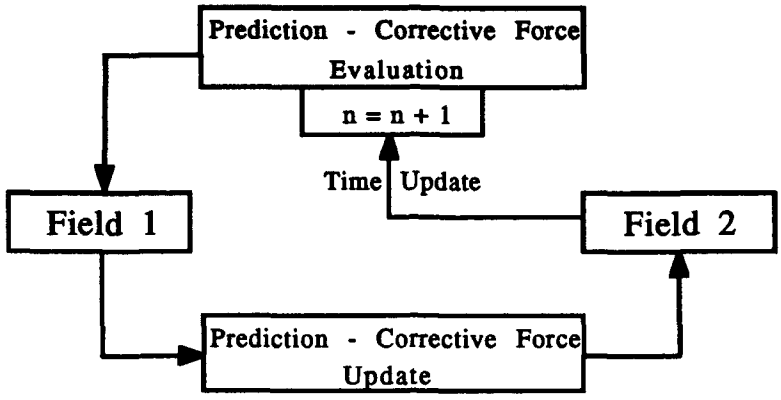

Figure 4.2-2 Information Flow in Staggered Evaluation

As introduced in Chapter Two, the dynamics of a two field coupled system can be expressed as

$$\begin{aligned} \mathbf{M}_x\ddot{\mathbf{x}} + \mathbf{C}_x\dot{\mathbf{x}} + \mathbf{K}_x\mathbf{x} &= \mathbf{R}_x + \mathbf{f}_{cx}(\dot{\mathbf{x}},\mathbf{x},\dot{\mathbf{y}},\mathbf{y}) \\ \mathbf{M}_y\ddot{\mathbf{y}} + \mathbf{C}_y\dot{\mathbf{y}} + \mathbf{K}_y\mathbf{y} &= \mathbf{R}_y + \mathbf{f}_{cy}(\dot{\mathbf{x}},\mathbf{x},\dot{\mathbf{y}},\mathbf{y}) \end{aligned} \qquad (4.2\text{-}1)$$

where the corrective forces due to the constraints, $\mathbf{f}_{cx}$ and $\mathbf{f}_{cy}$, are found using the methods already discussed and other similar methods. For the following discussion the forces are assumed to be calculated using a stabilized penalty formulation. It is useful to note that these equations are uncoupled if $\mathbf{f}_{cx}$ and $\mathbf{f}_{cy}$ are considered to be unresolved externally applied forces.

Solving these equations by means of the numerical integration was discussed in Chapter Three, the system equations become

$$\begin{aligned} \left[\mathbf{M}_x + \delta_x\mathbf{C}_x + \delta_x^2\mathbf{K}_x\right]\mathbf{x}_n &= \left[\phi_{Mx}\mathbf{M}_x + \phi_{Cx}\mathbf{C}_x + \phi_{Kx}\mathbf{K}_x\right]\mathbf{x}_n + \phi_{Rx}\left(\mathbf{R}_{x,n} + \mathbf{f}_{cx,n}\right) \\ \left[\mathbf{M}_y + \delta_y\mathbf{C}_y + \delta_y^2\mathbf{K}_y\right]\mathbf{y}_n &= \left[\phi_{My}\mathbf{M}_y + \phi_{Cy}\mathbf{C}_y + \phi_{Ky}\mathbf{K}_y\right]\mathbf{y}_n + \phi_{Ry}\left(\mathbf{R}_{y,n} + \mathbf{f}_{cy,n}\right) \end{aligned} \qquad (4.2\text{-}2)$$

or in simpler notation

$$\left[(1-\phi_M)\mathbf{M}_u + (\delta-\phi_C)\mathbf{C}_u + (\delta^2-\phi_K)\mathbf{K}_u\right]\mathbf{u}_n = \phi_R\left(\mathbf{R}_n + \mathbf{f}_{c,n}\right) \qquad (4.2\text{-}3)$$

where

$$\mathbf{M}_u = \begin{bmatrix} \mathbf{M}_x & 0 \\ 0 & \mathbf{M}_y \end{bmatrix}, \quad \mathbf{C}_u = \begin{bmatrix} \mathbf{C}_x & 0 \\ 0 & \mathbf{C}_y \end{bmatrix}, \quad \mathbf{K}_u = \begin{bmatrix} \mathbf{K}_x & 0 \\ 0 & \mathbf{K}_y \end{bmatrix}, \quad \mathbf{R}_n = \begin{bmatrix} \mathbf{R}_{x,n} \\ \mathbf{R}_{y,n} \end{bmatrix}$$

$$\delta = [\delta_x \; \delta_y]^T, \quad \phi_\cdot = [\; \phi_{\cdot x} \quad \phi_{\cdot y} \;]^T, \quad \mathbf{f}_{c,n} = [\mathbf{f}_{cx,n} \mathbf{f}_{cy,n}]^T, \quad \mathbf{1} = [1 \; 1]^T$$

Although the forms of the constraining force developed in Section 4.1 do not require linear constraints be used, analysis of the simulation coupling process is greatly aided by a linear approximation as follows:

$$\Phi = \mathbf{C}_c\dot{\mathbf{u}} + \mathbf{K}_c\mathbf{u} \tag{4.2-4}$$

With such an approximation the forces of constraint are

$$\begin{aligned} &\text{Holonomic} && \mathbf{f}_{c,n} = -\mathbf{K}_c^T \alpha \mathbf{K}_c(\dot{\mathbf{u}}_n + \kappa \mathbf{u}_n) \\ &\text{Nonholonomic} && \mathbf{f}_{c,n} = -\mathbf{C}_c^T \alpha(\mathbf{C}_c\ddot{\mathbf{u}}_n + \mathbf{K}_c \dot{\mathbf{u}}_n) \end{aligned} \tag{4.2-5}$$

The manner in which these forces are evaluated is based entirely on the particular execution process used.

4.2.1 Concurrent Evaluation Coupling

As has already been mentioned concurrent evaluation applies the same correction term to each field. For this term to be treated as an applied force (allowing the simulations to remain uncoupled), it cannot be a function of the current time step. Through use of the predictors introduced in Chapter Three, any dependence on the current states is removed.

First the integration approximation is applied to remove derivative terms

$$\text{Holonomic} \quad \mathbf{f}_{c,n} = -\mathbf{K}_c^T \alpha \mathbf{K}_c \left[\frac{1}{\delta}\left(\mathbf{u}_n - \mathbf{h}_n^u\right) + \kappa \mathbf{u}_n \right] \tag{4.2-6}$$

$$\text{Nonholonomic} \quad \mathbf{f}_{c,n} = -\mathbf{C}_c^T \alpha \left[\mathbf{C}_c \frac{1}{\delta}\left(\frac{1}{\delta}\left(\mathbf{u}_n - \mathbf{h}_n^u\right) - \mathbf{h}_n^{\dot{u}} \right) + \mathbf{K}_c \frac{1}{\delta}\left(\mathbf{u}_n - \mathbf{h}_n^u\right) \right]$$

or in operational form

$$\text{Holonomic} \quad \mathbf{f}_{c,n} = -\mathbf{K}_c^T \alpha \mathbf{K}_c \left(\psi(.)\mathbf{I} + \kappa\right)\mathbf{u}_n \tag{4.2-7}$$

$$\text{Nonholonomic} \quad \mathbf{f}_{c,n} = -\mathbf{C}_c^T \alpha \left(\mathbf{C}_c \psi(.)^2 + \mathbf{K}_c \psi(.)\right)\mathbf{u}_n$$

In this form the base states, $\mathbf{u}_n$, are estimated using a predictor of the form of (3.4-1). The predicted correction terms, after substituting $p(.)\mathbf{u}_n$ for $\mathbf{u}_n^P$, are

$$\text{Holonomic} \quad \mathbf{f}_{c,n}^P = -\mathbf{K}_c^T \alpha \mathbf{K}_c \left(\psi(.)\mathbf{I} + \kappa\right) p(.)\mathbf{u}_n \tag{4.2-8}$$

$$\text{Nonholonomic} \quad \mathbf{f}_{c,n}^P = -\mathbf{C}_c^T \alpha \left(\mathbf{C}_c \psi(.)^2 + \mathbf{K}_c \psi(.)\right) p(.)\mathbf{u}_n$$

Making the following definitions to simplify the notation

$$\mu_h = \left(\psi(.)\mathbf{I} + \kappa\right) p(.) \tag{4.2-9}$$

$$\mu_{nh} = \left(\mathbf{I}\psi(.)^2 + \mathbf{C}_c^{-1}\mathbf{K}_c \psi(.)\right) p(.)$$

Then the system equation for the concurrent evaluation is

$$\left[(1-\phi_M)\mathbf{M}_u + (\delta-\phi_C)\mathbf{C}_u + (\delta^2-\phi_K)\mathbf{K}_u + \phi_R \mathbf{K}_c^T \alpha \mathbf{K}_c \mu_h\right]\mathbf{u}_n = \phi_R \mathbf{R}_n \tag{4.2-10}$$

or for the nonholonomic case

$$\left[(1-\phi_M)\mathbf{M}_u + (\delta-\phi_C)\mathbf{C}_u + (\delta^2-\phi_K)\mathbf{K}_u + \phi_R \mathbf{C}_c^T \alpha \mathbf{C}_c \mu_{nh}\right]\mathbf{u}_n = \phi_R \mathbf{R}_n \tag{4.2-11}$$

The implementation of the concurrent evaluation is given as Table 4.2-1.

Table 4.2-1 Implementation of Concurrent Simulation Coupling

Step in Coupling Process	Associated Equation Number
1. Use states n-1 to n-m to find $\mathbf{u}_n^P$	(3.4-1)
2. Use states n-1 to n-m to find $\mathbf{h}_n^u$ and $\mathbf{h}_n^{\dot{u}}$ (if needed)	(3.1-7)
3. Use $\mathbf{u}_n^P$, $\mathbf{h}_n^u$, and $\mathbf{h}_n^{\dot{u}}$ to find $\mathbf{f}_{c,n}^P$	(4.2-6)
4. Send $\mathbf{f}_{c,n}^P$ to separate simulations	
5. Separate simulations solve for $\mathbf{u}_n$	(4.2-3)
6. Calculate $\dot{\mathbf{u}}_n$ and $\ddot{\mathbf{u}}_n$ if simulations do not provide them	(3.1-6)
7. Update time and increment n = n+1	

4.2.2 Staggered Evaluation Coupling

The staggered evaluation follows directly from the concurrent evaluation. However, since the fields must be handled in series, the response from the first field is used instead of a prediction when calculating the correction force for the second. The operational form also comes from the concurrent evaluation in the following manner.

Consider first the form of the correction force, $\mathbf{f}_{c,n}^P$.

$$\mathbf{f}_{c,n}^P = -\begin{bmatrix} (\mathbf{K}_c^T\alpha\mathbf{K}_c)_{xx} & (\mathbf{K}_c^T\alpha\mathbf{K}_c)_{xy} \\ (\mathbf{K}_c^T\alpha\mathbf{K}_c)_{yx} & (\mathbf{K}_c^T\alpha\mathbf{K}_c)_{yx} \end{bmatrix}[\mu_h]\begin{bmatrix} x_n \\ y_n \end{bmatrix} \quad (4.2\text{-}12)$$

or

$$\mathbf{f}_{c,n}^P = -\begin{bmatrix} (\mathbf{K}_c^T\alpha\mathbf{K}_c)_{xx} & (\mathbf{K}_c^T\alpha\mathbf{K}_c)_{xy} & 0 \\ 0 & (\mathbf{K}_c^T\alpha\mathbf{K}_c)_{yx} & (\mathbf{K}_c^T\alpha\mathbf{K}_c)_{yx} \end{bmatrix}[\mu_h]\begin{bmatrix} \mathbf{I} \\ \mathbf{I} \end{bmatrix}\begin{bmatrix} x_n \\ y_n \end{bmatrix} \quad (4.2\text{-}13)$$

The predictor term is expanded as follows:

$$[\mu_h]\begin{bmatrix} \mathbf{I} \\ \mathbf{I} \end{bmatrix} = \begin{bmatrix} \mu_h & 0 \\ 0 & \mu_h \\ \mu_h & 0 \\ 0 & \mu_h \end{bmatrix} \qquad (4.2\text{-}14)$$

The upper half of this matrix deals with the prediction of each field for evaluating the constraint forces acting on the first field; the lower half does the same for the second field. By eliminating the term in the lower half which corresponds to the prediction of the first field, the actual values are used instead of predicted ones. This results in the following matrix:

$$\dot{\mu}_h = \begin{bmatrix} \mu_h & 0 \\ 0 & \mu_h \\ (\psi(.)\mathbf{I} + \kappa) & 0 \\ 0 & \mu_h \end{bmatrix} \qquad (4.2\text{-}15)$$

This makes the notation for the correction force of the staggered case

$$\mathbf{f}^P_{c,n} = -\begin{bmatrix} (\mathbf{K}_c^T \alpha \mathbf{K}_c)_{xx} & (\mathbf{K}_c^T \alpha \mathbf{K}_c)_{xy} & 0 \\ 0 & (\mathbf{K}_c^T \alpha \mathbf{K}_c|_{yx} & (\mathbf{K}_c^T \alpha \mathbf{K}_c)_{yx} \end{bmatrix} \dot{\mu}_h \begin{bmatrix} \mathbf{x}_n \\ \mathbf{y}_n \end{bmatrix} \qquad (4.2\text{-}16)$$

The appropriate term for nonholonomic constraints is

$$\mathbf{f}^P_{c,n} = -\begin{bmatrix} (\mathbf{C}_c^T \alpha \mathbf{C}_c)_{xx} & (\mathbf{C}_c^T \alpha \mathbf{C}_c)_{xy} & 0 \\ 0 & (\mathbf{C}_c^T \alpha \mathbf{C}_c)_{yx} & (\mathbf{C}_c^T \alpha \mathbf{C}_c|_{yx} \end{bmatrix} \dot{\mu}_{nh} \begin{bmatrix} \mathbf{x}_n \\ \mathbf{y}_n \end{bmatrix} \qquad (4.2\text{-}15)$$

where

$$\dot{\mu}_{nh} = \begin{bmatrix} \mu_{nh} & 0 \\ 0 & \mu_{nh} \\ (\mathbf{I}\psi(.)^2 + \mathbf{C}_c^{-1}\mathbf{K}_c\psi(.)) & 0 \\ 0 & \mu_{nh} \end{bmatrix} \qquad (4.2\text{-}16)$$

The implementation of the staggered evaluation is given in Table 4.2-2.

Table 4.2-2 Implementation of Staggered Simulation Coupling

Step in Coupling Process	Associated Equation Number
1. Use states n-1 to n-m to find $\mathbf{u}_n^P$	(3.4-1)
2. Use states n-1 to n-m to find $\mathbf{h}_n^u$ and $\mathbf{h}_n^{\dot{u}}$ (if needed)	(3.1-7)
3. Use $\mathbf{u}_n^P$, $\mathbf{h}_n^u$, and $\mathbf{h}_n^{\dot{u}}$ to find $\mathbf{f}_{c,n}^P$ for x field	(4.2-6)
4. Send $\mathbf{f}_{c,n}^P$ to x field simulation	
5. Simulation solves for $\mathbf{x}_n$	(4.2-3)
6. Use $\mathbf{y}_n^P$, $\mathbf{h}_n^y$, $\mathbf{h}_n^{\dot{y}}$, and $\mathbf{x}_n$ to find $\mathbf{f}_{c,n}^P$ for y field	(4.2-6)
7. Send $\mathbf{f}_{c,n}^P$ to y field simulation	
8. Simulation solves for $\mathbf{y}_n$	(4.2-3)
9. Calculate $\dot{\mathbf{u}}_n$ and $\ddot{\mathbf{u}}_n$ if simulations do not provide them	(3.1-6)
10. Update time and increment n = n+1	

4.3 Analysis of the Simulation Coupling Process

4.3.1 Stability Analysis of Simulation Coupling

Having developed operational expressions for the system equation of motion, the stability analysis is fairly straight-forward. There are two possible methods to accomplish the analysis. Both consider the unforced response ($\mathbf{R}_n = 0$ for (4.2-11)) and develop a system characteristic matrix. Since the response is unforced the eigenvalues of the matrix must be less than or equal to unity, to keep the response from growing with time. Although both methods will

be shown in detail in the examples of Chapter Five, they will be briefly introduced here.

The first method uses the matrix, $\mathbf{C}(z)$, which is the matrix multiplying $\mathbf{u}_n$ in (4.2-11). For instance, the characteristic matrix for the concurrent evaluation and nonholonomic constraints is

$$\mathbf{C}(z) = (1-\phi_M)\mathbf{M}_u + (\delta-\phi_C)\mathbf{C}_u + (\delta^2-\phi_K)\mathbf{K}_u + \phi_R \mathbf{K}_c^T \alpha \mathbf{K}_c \mu_{nh} \quad (4.3\text{-}1)$$

Taking the determinant of this matrix produces the characteristic polynomial, C(z). The simulation coupling process is stable if the roots of C(z) lie within the unit circle. Optimally, it is desired that these roots reflect the same stability as the fully coupled system. An example of this would the trapezoidal rule; an optimally stable coupling process would keep this method's A-stable characteristics.

The second method relies on a time domain analysis and is a common numerical analysis procedure (see [4.7]). The state variable $\mathbf{u}_n$ can be written as a function past state variables and derivatives using a form of (3.1-9)

$$\left[\mathbf{M}+\delta\mathbf{C}+\delta^2\mathbf{K}\right]\mathbf{u}_n = \left[\mathbf{M} + \delta(\mathbf{C} - \mathbf{A}^{-1}\mathbf{B})\right]\mathbf{h}_n^u + \delta\mathbf{A}^{-1}\mathbf{h}_n^v + \delta^2\mathbf{f}_{c,n} \quad (4.3\text{-}2)$$

Using the integration approximation for $\mathbf{u}$ and (4.3-2) to substitute for $\mathbf{u}_n$, the derivative $\dot{\mathbf{u}}_n$ can also be written as function of past states. The definition of the auxiliary vector and integration approximation for $\mathbf{v}$ provide $\mathbf{v}_n$ and $\dot{\mathbf{v}}$ in terms of the past states. These equations make it possible to write a matrix which when multiplied by the vector $[\ \mathbf{u}_{n-1}\ \mathbf{v}_{n-1}\ \mathbf{u}_{n-2}\ \mathbf{v}_{n-2}\ \cdots\ \mathbf{u}_{n-m}\ \mathbf{v}_{n-m}\ ]$ will give the vector $[\ \mathbf{u}_n\ \mathbf{v}_n\ \mathbf{u}_{n-1}\ \mathbf{v}_{n-1}\ \cdots\ \mathbf{u}_{n-m+1}\ \mathbf{v}_{n-m+1}\ ]$. The roots of this

vector must also be less or equal to one for the coupled simulation to be stable. Although developing this matrix is more difficult than finding C(z), then eigenvalues may be calculated directly from this point without first taking the determinant to find the characteristic polynomial.

Unfortunately using these methods is not nearly as easy as it would seem. Large coupled problems tend to have thousands of degrees of freedom, and the number of roots to the characteristic equation can be several times that number. This makes calculation of these roots difficult even with computer methods. Additionally, the only parameters the dynamicist has available to ensure stability are the integration time step, the choice of the predictor, and the penalty used to find the corrective force. The choice of overall penalty is generally governed by requirements to keep the constraints violations very small and the time step must be small enough to stabilize the high frequency poles associated with the application of a penalty. This leaves only the predictor and at this time there are no guaranteed choices for optimally stable predictors.

4.3.2 Accuracy Analysis of Simulation Coupling

The accuracy analysis also involves manipulating the characteristic equation, but this time the s domain form is desired. By expanding the exponential terms in the operational expressions, $e^{-sh} = 1 - sh + 0.5(sh)^2 - \ldots$, the characteristic equation may be written in powers of s. This allows the characteristic equation in s to be transferred back to a differential expression and from there to a standard eigenvalue problem. As an example consider an undamped

system integrated using the trapezoidal rule and computational path 2. The characteristic equation is

$$\left[(\delta\psi)^2\mathbf{M} + \delta^2\mathbf{K}\right]\mathbf{u}_n = 0 \qquad (4.3\text{-}3)$$

Substituting for the operational expressions from Chapter Three

$$\left[\left(\frac{1 - e^{-sh}}{1 + e^{-sh}}\right)^2\mathbf{M} + \mathbf{K}\right]\mathbf{u}_n = 0 \qquad (4.3\text{-}4)$$

Expanding e^{-sh}

$$\left[\left(1 - \frac{1}{6}(sh)^2 + O(sh)^4\right)\mathbf{M}\,s^2 + \mathbf{K}\right]\mathbf{u}_n = 0 \qquad (4.3\text{-}5)$$

This will give the differential equation

$$\mathbf{M}\ddot{\mathbf{u}} - \frac{1}{6}h^2\mathbf{M}\ddot{\mathbf{u}}'' + O(\mathbf{u}^{(4)}) + \mathbf{K}\mathbf{u} = 0 \qquad (4.3\text{-}6)$$

or an eigenvalue problem

$$\left(\mathbf{M} + \frac{1}{6}h^2\mathbf{K} + \ldots\right)(\omega h)^2 - O(\omega h)^4 + \mathbf{K} = 0 \qquad (4.3\text{-}7)$$

These equations show that, as expected, the trapezoidal rule introduces no artificial damping but does produce a certain amount of frequency distortion. The same sort of analysis may be carried out on the simulation coupling characteristic equation. The numerical values can then be compared to similar values obtained for the fully coupled system.

Chapter Five

Illustrative Numerical Examples

Although the simulation coupling theory is aimed at the solution of large scale problems, it is not possible to show all the details of analysis of such problems. For this reason the following chapter is organized to present a series of smaller dimensioned problems in which the all of the aspects of the theory presented are shown. The first example is the one dimensional motion of a single rigid body. The response is considered subject to different forcing conditions. The second example is a more complicated model representing a satellite held at the end of the shuttle's manipulator arm. This example shows some of the effects of imposing constraints on a flexible domain. Finally, the single rigid body is again considered. All six degrees of freedom are allowed to show the interaction between translational and rotational motion in the presence of constraints. All examples use the concurrent evaluation along with a stabilized penalty format to find the constraint forces.

5.1 One Dimensional, Single Body Example

As a single body example consider the structure illustrated in Figure 5.1-1. This body is representative of a dual spin stabilized satellite (see [5.1]). The mass properties for each section are

Rotor = 700 kg Platform = 300 kg

Each center of mass (CM) is located on the spin axis. The platform CM is 0.5 m up from the joint between the bodies and the rotor CM is 0.75 m down from the joint. The complete center of mass is 0.375 m down from the joint.

The inertia properties of the satellite about their CMs are:

	Spin	Transverse
Rotor	350.0 kg-m^2	306.25 kg-m^2
Platform	150.0 kg-m^2	100.0 kg-m^2
Complete	500.0 kg-m^2	734.375 kg-m^2

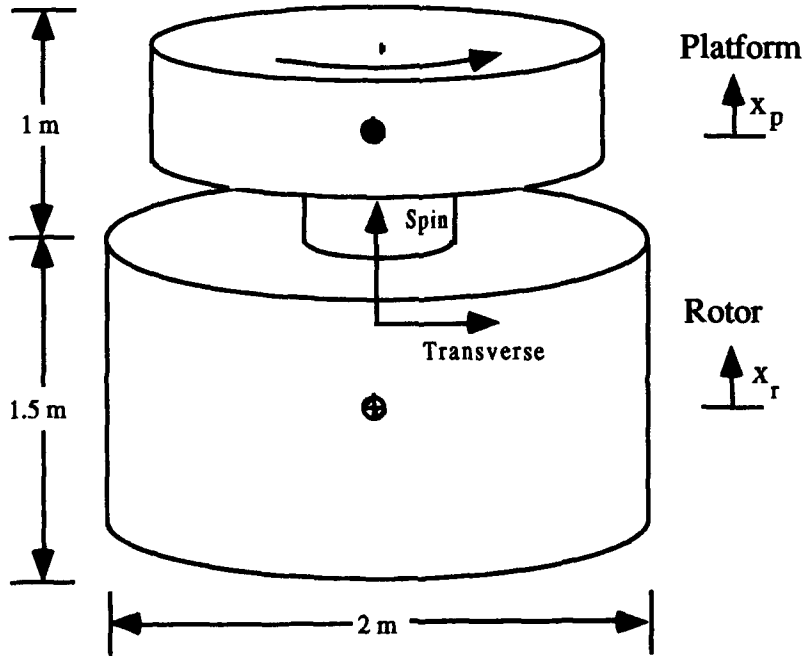

Figure 5.1-1 Satellite Rigid Body Model

The satellite is subject to the following forcing conditions resulting from attitude control type maneuvers:

Forces = 1 N any axis Torques = 10 N-m about spin

The forces and torques are applied on the rotor section. For the purpose of simulation coupling the single body is divided into two separate rigid bodies where the platform joins the rotor.

5.1.1 Analysis of 1-D Example

Considering the response of each body in the direction of the spin axis, the equations of motion are

$$M_r\ddot{x}_r = R_r \text{ and } M_p\ddot{x}_p = R_p \qquad (5.1\text{-}1)$$

Additionally, the bodies are rigidly connected along the spin axis, or $x_r - x_p = 0$. By applying the stabilized penalty method discussed in Chapter Four, the following constraint forces are found:

$$f_c = -[1\ -1]^T \alpha [(\dot{x}_r-\dot{x}_p) + \kappa(x_r-x_p)] \qquad (5.1\text{-}2)$$

Adding these forces to the system leaves

$$\begin{bmatrix} M_r & 0 \\ 0 & M_p \end{bmatrix}\begin{Bmatrix} \ddot{x}_r \\ \ddot{x}_p \end{Bmatrix} = \begin{Bmatrix} R_r \\ R_p \end{Bmatrix} + f_c \qquad (5.1\text{-}3)$$

Subtracting the second equation from the first and rearranging terms produces the constraint error equation

$$(\ddot{x}_r-\ddot{x}_p) - \alpha\frac{M_{tot}}{M_rM_p}(\dot{x}_r-\dot{x}_p) + \alpha\kappa\frac{M_{tot}}{M_rM_p}(x_r-x_p) = \frac{R_r}{M_r} - \frac{R_p}{M_p} \qquad (5.1\text{-}4)$$

The penalty κ controls the steady state error

$$\alpha\kappa\frac{M_{tot}}{M_rM_p}\left|(x_r-x_p)_{ss}\right| \approx \left|\frac{R_rM_p - R_pM_r}{M_rM_p}\right| \qquad (5.1\text{-}5)$$

With the given mass properties and a requirement that the steady state error be less than 1.0×10^{-7} meters

$$\kappa = \frac{1}{\alpha}\cdot 3.0\times10^{5} \tag{5.1-6}$$

The other penalty, α, determines the damping ratio of the error. For a ratio of 0.3, α = 2400.0 which leaves κ = 125.0.

The equations of motion may be integrated following the (0) computational path and using the trapezoidal rule

$$w_n - w_{n-1} = 0.5\,h(\dot{w}_n + \dot{w}_{n-1}) \tag{5.1-7}$$

Using this equation to substitute for the accelerations in (5.1-3) gives

$$\begin{Bmatrix} x_r \\ x_p \end{Bmatrix}_n = \begin{Bmatrix} x_r \\ x_p \end{Bmatrix}_{n-1} + h\begin{Bmatrix} \dot{x}_r \\ \dot{x}_p \end{Bmatrix}_{n-1} + \frac{h^2}{4}\begin{Bmatrix} \ddot{x}_r \\ \ddot{x}_p \end{Bmatrix}_{n-1} + \frac{h^2}{4}\begin{bmatrix} M_r & 0 \\ 0 & M_p \end{bmatrix}^{-1}\left[\begin{Bmatrix} R_r \\ R_p \end{Bmatrix}_n + (\mathbf{f}_c)_n\right] \tag{5.1-8}$$

The constraint force is found using a last value predictor, $x^P_n = x_{n-1}$, leaving

$$\mathbf{f}_{c,n} = -\alpha\begin{bmatrix} 1 & -1 \\ -1 & 1 \end{bmatrix}\left[\begin{Bmatrix} \dot{x}_r \\ \dot{x}_p \end{Bmatrix}_{n-1} + \kappa\begin{Bmatrix} x_r \\ x_p \end{Bmatrix}_{n-1}\right] \tag{5.1-9}$$

These two equations are used to carry out the simulation.

To perform the analysis of the simulation coupling the notation introduced in Chapter Three is used. Defining $\mathbf{u} = [\, x_r\ x_p \,]^T$, $R_r = 0$, $R_p = 0$, and $\mathbf{M} = \begin{bmatrix} M_r & 0 \\ 0 & M_p \end{bmatrix}$ leaves

$$\mathbf{u}_n = \mathbf{u}_{n-1} + h\dot{\mathbf{u}}_{n-1} + \frac{h^2}{4}\ddot{\mathbf{u}}_{n-1} - \alpha\frac{h^2}{4}\mathbf{M}^{-1}\left[\begin{bmatrix} 1 & -1 \\ -1 & 1 \end{bmatrix}\left[\dot{\mathbf{u}}_{n-1} + \kappa\mathbf{u}_{n-1}\right]\right] \tag{5.1-10}$$

Using the characteristic equation for holonomically constrained coupled problems listed in (4.2-10)

$$\left[(1-\phi_M)\mathbf{M} + \alpha\phi_R\mathbf{K}_c^T\mathbf{K}_c(\psi + \kappa)p(z)\right]\mathbf{u}_n = 0 \qquad (5.1\text{-}11)$$

For this example the last value predictor is characterized by the shift operator, z^{-1}, and the polynomials ϕ_M and ϕ_R are listed in Table 3.3-1. Making the appropriate substitutions results in the following form:

$$\left[(\delta\psi)\mathbf{M} + \alpha(\delta\psi^{-1})\mathbf{K}_c^T\mathbf{K}_c(\psi + \kappa)z^{-1}\right]\mathbf{u}_n = 0 \qquad (5.1\text{-}12)$$

The operational notation for the trapezoidal rule is found in Section 3.5. Using the given polynomials and clearing most fractions leaves

$$\left[z(z-1)^2\mathbf{M} + \frac{\alpha h}{2}\mathbf{K}_c^T\mathbf{K}_c\left[(z-1)(z+1) + \frac{\kappa h}{2}(z+1)^2\right]\right]\mathbf{u}_n = 0 \qquad (5.1\text{-}13)$$

From the form of the constraint, $\Phi = x_r - x_p$, the matrix $\mathbf{K}_c$ is found to be $[1\ -1]^T$. Expanding the polynomials and matrices gives the characteristic matrix equation, $\mathbf{C}(z)$

$$\mathbf{C}(z) = \left[(z^3-2z^2+z)\begin{bmatrix} M_r & 0 \\ 0 & M_p \end{bmatrix} + \frac{\alpha h}{2}\begin{bmatrix} 1 & -1 \\ -1 & 1 \end{bmatrix}\left[\left(1+\frac{\kappa h}{2}\right)z^2 + (\kappa h)z + \left(\frac{\kappa h}{2} - 1\right)\right]\right] \qquad (5.1\text{-}14)$$

Defining a temporary variable, $a(z) = \left(1+\frac{\kappa h}{2}\right)z^2 + (\kappa h)z + \left(\frac{\kappa h}{2} - 1\right)$

$$\mathbf{C}(z) = \begin{bmatrix} M_r(z^3-2z^2+z) + \frac{\alpha h}{2}a(z) & -\frac{\alpha h}{2}a(z) \\ -\frac{\alpha h}{2}a(z) & M_p(z^3-2z^2+z) + \frac{\alpha h}{2}a(z) \end{bmatrix} \qquad (5.1\text{-}15)$$

For stability, the roots of the determinant, det(C), must be within the unit circle. Taking the determinant

$$z(z-1)^2\left[z^3+\left\{\left(\frac{M_{Tot}}{M_rM_p}\right)\left(\frac{\alpha h}{2}+\frac{\alpha\kappa h^2}{4}\right)-2\right\}z^2+\left\{\left(\frac{M_{Tot}}{M_rM_p}\right)\left(\frac{\alpha\kappa h^2}{2}\right)+1\right\}z+\left\{\left(\frac{M_{Tot}}{M_rM_p}\right)\left(\frac{\alpha\kappa h^2}{4}-\frac{\alpha h}{2}\right)\right\}\right] \quad (5.1\text{-}16)$$

Since the first three roots (z = 0,1,1) do not vary with α, κ, or h, they are not as important as the remaining three. For the penalties given, Figure 5.1-2 shows two of the remaining three roots moving away from z=1 as the step size is varied from 0 to 0.008, where 0.008 is at the point of instability. The third pole moves from the origin toward a value of z = 0.02. The desired time step should be as large as possible while still being stable. For this reason h is chosen to be 0.005.

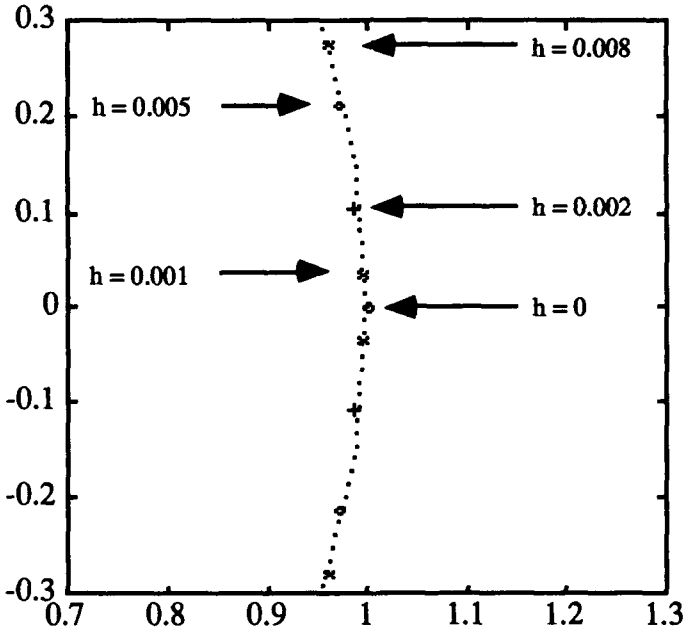

Figure 5.1-2 Pole Locations of Rigid Body Model

The choice of α does not seem to have a great effect on the overall stability. If α is doubled the limiting time step increases by less than 5%. Therefore, since α is proportional to the damping ratio and large damping ratios mean small overshoot, it is often feasible to increase α by as much as a factor of five. Additionally, changing the

mass ratio of platform to rotor does not have any effect on the coupled simulation stability. On the other hand κ has a great effect on stability. Doubling the value of κ will almost double the stable time step.

5.1.2 Response of 1-D Example

The response is considered subject to three separate forcing conditions; a constant force input, a ramp input, and a pulse sequence input. In each case the responses of the rotor and platform are compared to the response of the complete rigid case for a two second run. The time step used is h = 0.005 and the penalties are those suggested in the previous section. The position, velocity, and acceleration for the constant forcing case are illustrated in Figure 5.1-3.

The error between the coupled and complete response is noticeable only in the acceleration plot and then only during the first two seconds. The steady state error settles out to exactly 1.0×10^{-7} as desired. To check the calculated stability boundary, a coupled simulation was made with h = 0.008. The constraint error and the constraint error rate are shown in Figure 5.1-4.

The second forcing condition is a ramp thrust from 0 to 1 N over a two second period. The position, velocity, and acceleration for this case are presented in Figure 5.1-5. In this case the constraint error also increases with time reaching a final value of 1.0×10^{-7}.

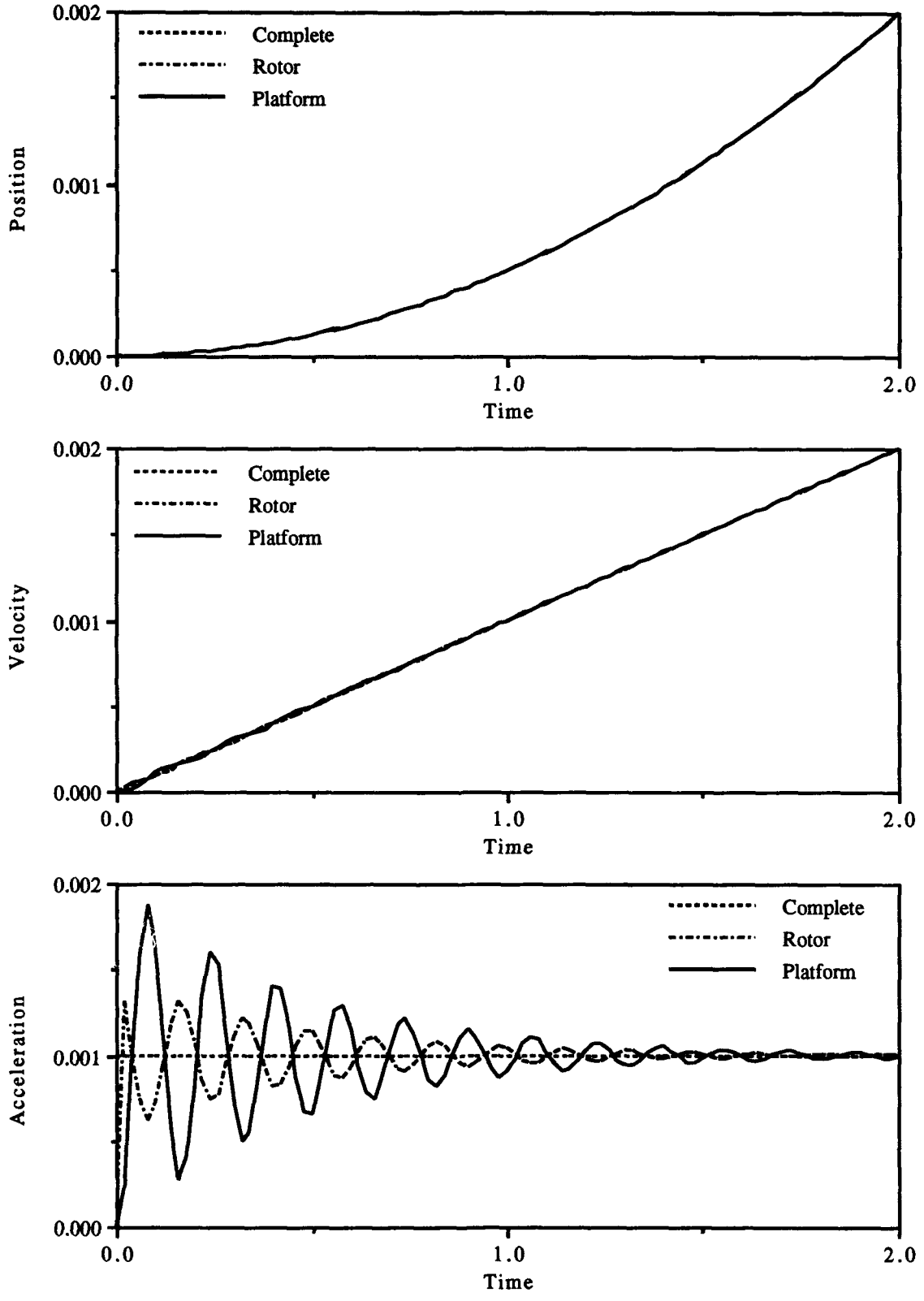

Figure 5.1-3 1-D Example Response to Constant Forcing

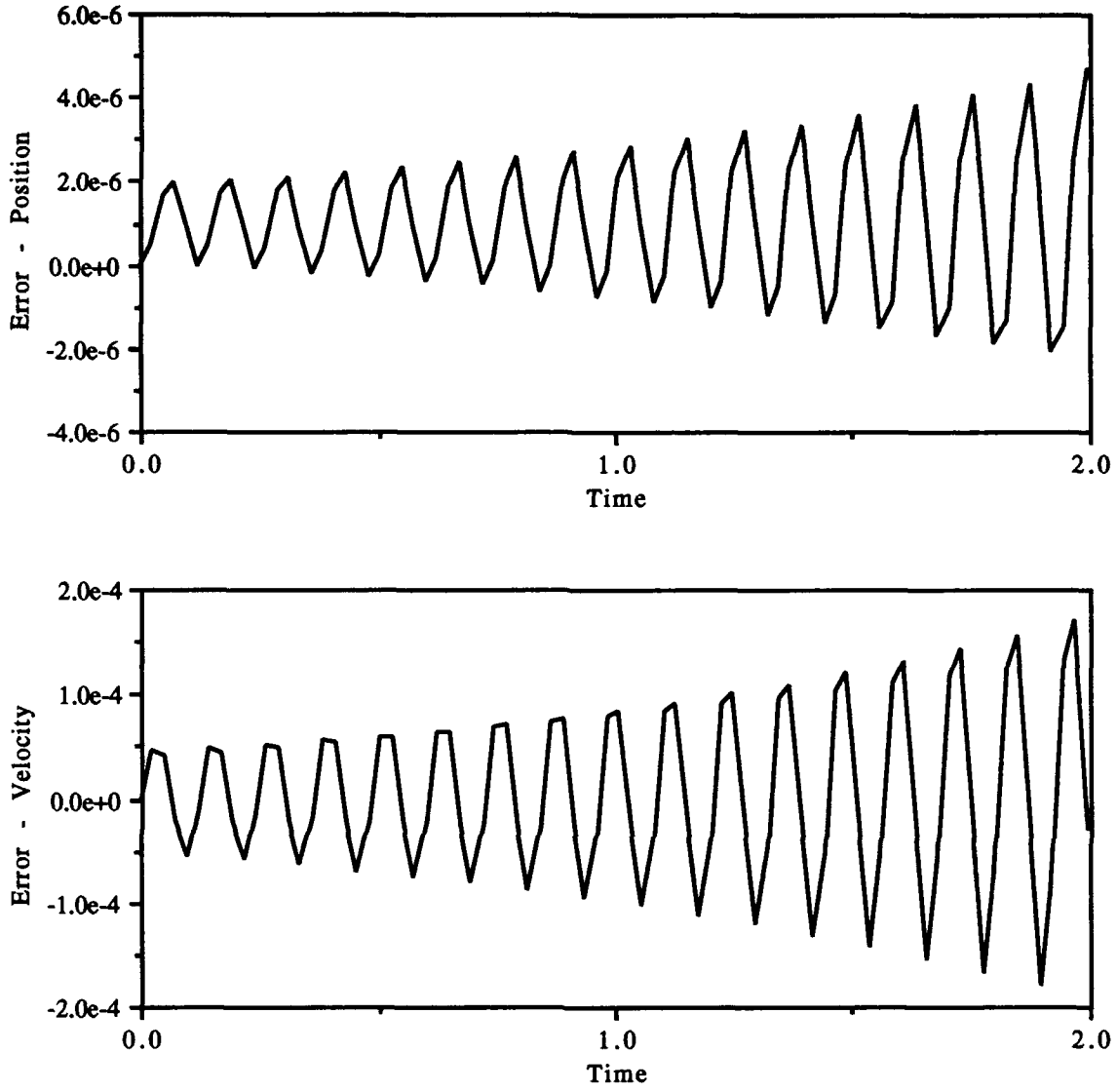

Figure 5.1-4 1-D Example Constraint Error, h = 0.008

The third forcing condition is a series of 1 N thrust pulses. Each pulse lasts a quarter second and separated from the next pulse by the same interval. The position, velocity, and acceleration for this case are illustrated in Figure 5.1-6. Some noticeable differences occur in this case due to the rapidly changing input. However, the coupled position and velocity still track the actual solution fairly well.

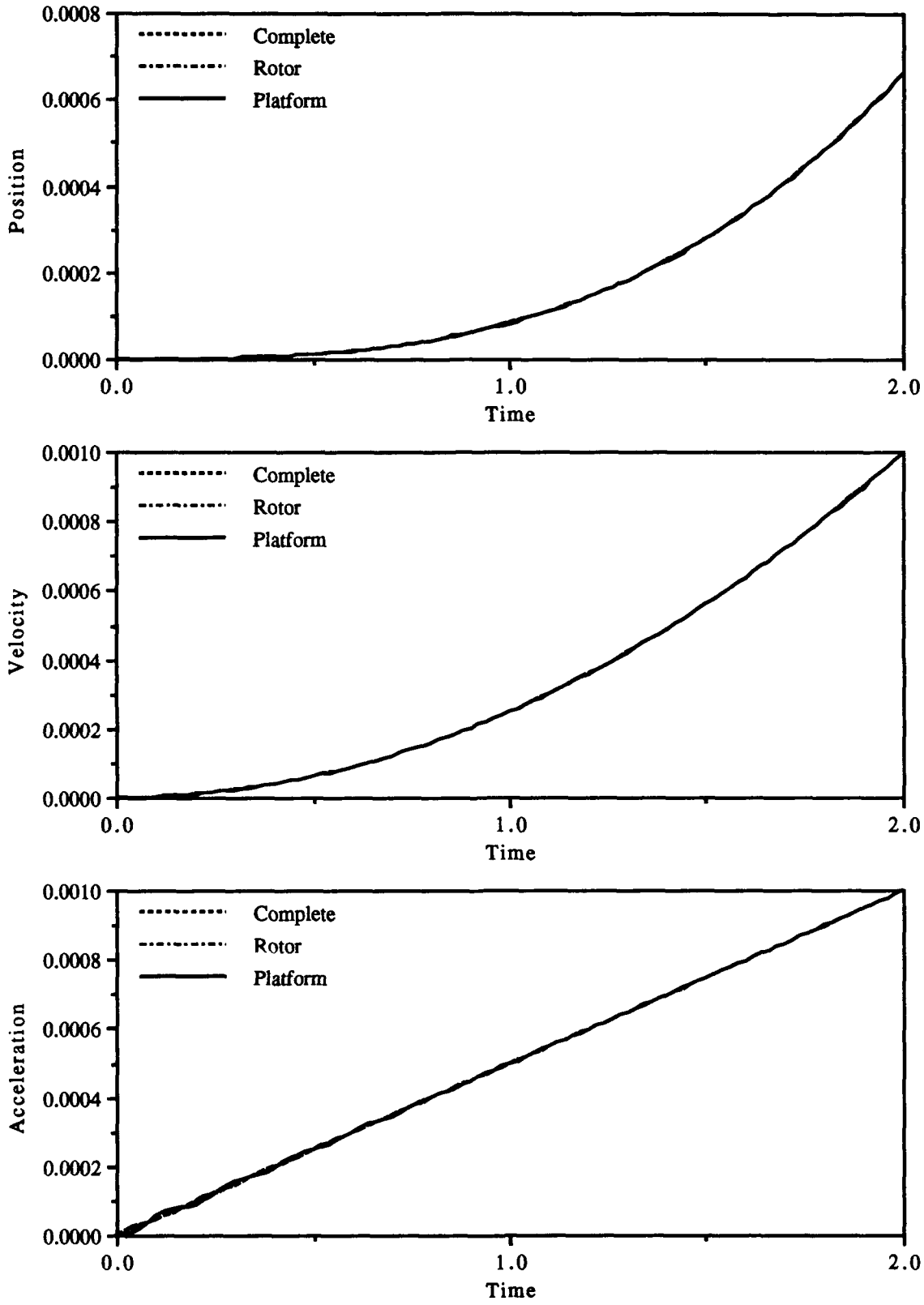

Figure 5.1-5 1-D Example Response to Ramped Forcing

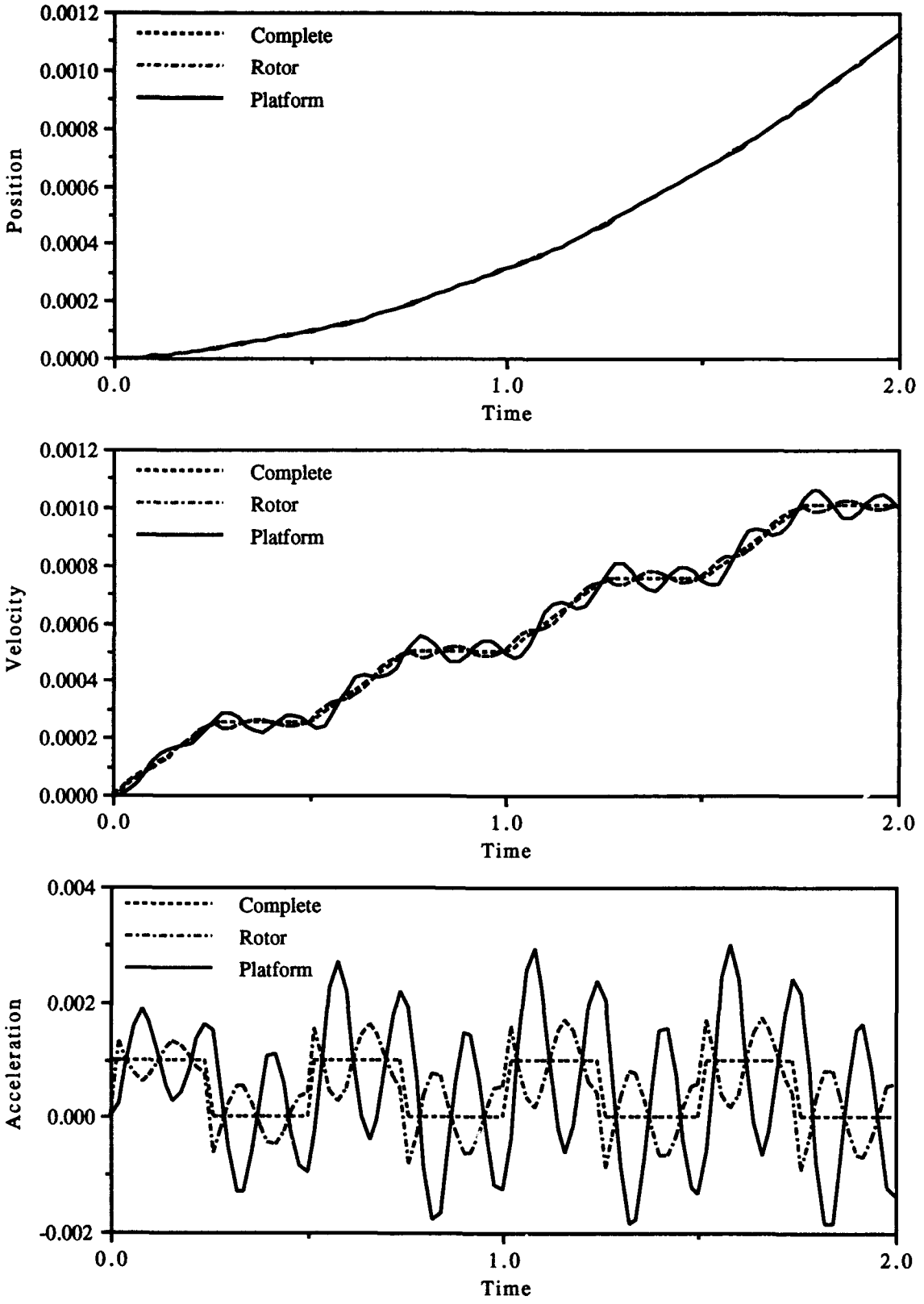

Figure 5.1-6 1-D Example Response to Pulsed Forcing

5.2 One Dimensional Shuttle-Satellite Example

The next example is the one dimensional, four mass model of a satellite held in the space shuttle manipulator arm illustrated in Figure 5.2-1. In actuality the connection between the end effector of the arm and the satellite platform is assumed rigid, and this will provide the coupling between the separate fields of the shuttle dynamics and the satellite dynamics. The shuttle partition is made up of the shuttle and the manipulator arm. The one dimensional idealization of the flexibility in the arm is a spring connecting the two masses. The satellite partition is similar to the satellite in the previous rigid example with the addition of a small amount of flexibility between the rotor and the platform. The masses involved are

Shuttle Body (M_s)	85,000 kg
Manipulator Arm (M_a)	140 kg
Satellite Platform (M_p)	300 kg
Satellite Rotor (M_r)	700 kg

The flexibilities involved are

Manipulator Flexibility (K_a)	300 N/m
Satellite Flexibility (K_{rp})	1800 N/m

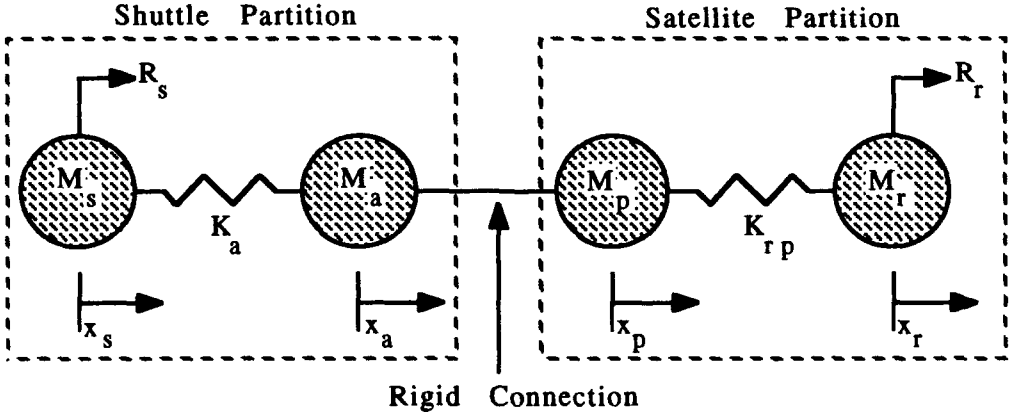

Figure 5.2-1 1-D Shuttle-Satellite Model

Forces are allowed to the system from the control jets on the shuttle and the satellite. The satellite jets are capable of the same 1 N thrust while the shuttles jets can deliver up to 2 kN (see [5.2] and [5.3]).

5.2.1 Stability Analysis of Shuttle-Satellite Example

The equation of motion for each partition is

$$\begin{bmatrix} M_s & 0 \\ 0 & M_a \end{bmatrix}\begin{Bmatrix} \ddot{x}_s \\ \ddot{x}_a \end{Bmatrix}+\begin{bmatrix} K_a & -K_a \\ -K_a & K_a \end{bmatrix}\begin{Bmatrix} x_s \\ x_a \end{Bmatrix}=\begin{Bmatrix} R_s \\ 0 \end{Bmatrix}$$

$$\text{and} \quad \begin{bmatrix} M_p & 0 \\ 0 & M_r \end{bmatrix}\begin{Bmatrix} \ddot{x}_p \\ \ddot{x}_r \end{Bmatrix}+\begin{bmatrix} K_{rp} & -K_{rp} \\ -K_{rp} & K_{rp} \end{bmatrix}\begin{Bmatrix} x_p \\ x_r \end{Bmatrix}=\begin{Bmatrix} 0 \\ R_r \end{Bmatrix} \qquad (5.2\text{-}1)$$

The complete system equation of motion found by eliminating a degree of freedom due to the rigid connection, $x_a - x_p = 0$

$$\begin{bmatrix} M_s & 0 & 0 \\ 0 & M_a+M_p & 0 \\ 0 & 0 & M_r \end{bmatrix}\begin{Bmatrix} \ddot{x}_s \\ \ddot{x}_p \\ \ddot{x}_r \end{Bmatrix}+\begin{bmatrix} K_a & -K_a & 0 \\ -K_a & K_a+K_{rp} & -K_{rp} \\ 0 & -K_{rp} & K_{rp} \end{bmatrix}\begin{Bmatrix} x_s \\ x_p \\ x_r \end{Bmatrix}=\begin{Bmatrix} R_s \\ 0 \\ R_r \end{Bmatrix} \qquad (5.2\text{-}2)$$

The equivalent simulation coupled system with corrective constraint forces is

$$\begin{bmatrix} M_s & 0 & 0 & 0 \\ 0 & M_a & 0 & 0 \\ 0 & 0 & M_p & 0 \\ 0 & 0 & 0 & M_r \end{bmatrix}\begin{Bmatrix} \ddot{x}_s \\ \ddot{x}_a \\ \ddot{x}_p \\ \ddot{x}_r \end{Bmatrix}+\begin{bmatrix} K_a & -K_a & 0 & 0 \\ -K_a & K_a & 0 & 0 \\ 0 & 0 & K_{rp} & -K_{rp} \\ 0 & 0 & -K_{rp} & K_{rp} \end{bmatrix}\begin{Bmatrix} x_s \\ x_a \\ x_p \\ x_r \end{Bmatrix}=\begin{Bmatrix} R_s \\ f_c \\ -f_c \\ R_r \end{Bmatrix} \qquad (5.2\text{-}3)$$

where the constraint force is

$$f_c = -\alpha\left[(\dot{x}_a-\dot{x}_p)+\kappa(x_a-x_p)\right] \qquad (5.2\text{-}4)$$

To determine the penalty constants, α and κ, an error analysis similar to the one used in the first example is done. Subtracting the third line of (5.2-3) from the second

$$(\ddot{x}_a - \ddot{x}_p) + \frac{K_a}{M_a}(x_a - x_s) - \frac{K_{rp}}{M_p}(x_r - x_p) = \frac{M_a + M_p}{M_a M_p} f_c \qquad (5.2\text{-}5)$$

Rearranging terms, defining $e = x_a - x_p$, and substituting for f_c

$$\ddot{e} + \alpha\frac{M_a + M_p}{M_a M_p}\dot{e} + \alpha\kappa\frac{M_a + M_p}{M_a M_p}e = \frac{K_{rp}}{M_p}(x_r - x_p) - \frac{K_a}{M_a}(x_a - x_s) \qquad (5.2\text{-}6)$$

Replacing the terms on the right hand side with terms from the first and fourth lines of (5.2-3) leaves

$$\ddot{e} + \alpha\frac{M_a + M_p}{M_a M_p}\dot{e} + \alpha\kappa\frac{M_a + M_p}{M_a M_p}e = \frac{(R_r - M_r\ddot{x}_r)}{M_p} - \frac{(R_s - M_s\ddot{x}_s)}{M_a} \qquad (5.2\text{-}7)$$

Using (5.2-7) to require the steady state error be less than 10^{-6} meters

$$\kappa = \frac{1}{\alpha} \cdot 1.5 \cdot 10^8 \qquad (5.2\text{-}8)$$

The other penalty, α, determines the damping ratio of the error. For a ratio of 0.1, α = 24,000.0 which leaves κ = 6,250.0.

Since using $\mathbf{C}(z)$ to do the stability analysis would require taking the determinant of a 4x4 matrix of third order polynomials, the second method of determining stability is used instead. Applying the trapezoidal rule and a last value predictor, (3.1-9) becomes

$$\left[\mathbf{M} + \delta^2\mathbf{K}\right]\mathbf{u}_n = \delta^2\mathbf{M}\ddot{\mathbf{u}}_{n-1} + 2\delta\mathbf{M}\dot{\mathbf{u}}_{n-1} + \mathbf{M}\mathbf{u}_{n-1} + \delta^2\mathbf{f}_{c,n} \qquad (5.2\text{-}9)$$

where M and K are the defined in the coupled equation (5.2-3). After substituting for $\mathbf{f}_{c,n}$

$$\left[\mathbf{M}+\delta^2\mathbf{K}\right]\mathbf{u}_n = \delta^2\mathbf{M}\ddot{\mathbf{u}}_{n-1} + \left[2\delta\mathbf{M} - \alpha\delta^2\mathbf{G}\right]\dot{\mathbf{u}}_{n-1} + \left[\mathbf{M} - \alpha\delta^2\mathbf{G}\kappa\right]\mathbf{u}_{n-1} \quad (5.2\text{-}10)$$

where $\mathbf{G} = \mathbf{K}_c^T\mathbf{K}_c = [\ 0\ 1\ -1\ 0]^T[\ 0\ 1\ -1\ 0]$. Using the the trapezoidal rule $\dot{\mathbf{u}}_n$ may be written

$$\dot{\mathbf{u}}_n = \delta^{-1}(\mathbf{u}_n - \mathbf{u}_{n-1}) - \dot{\mathbf{u}}_{n-1} \quad (5.2\text{-}11)$$

or using (5.2-10) for $\mathbf{u}_n$

$$\left[\mathbf{M}+\delta^2\mathbf{K}\right]\dot{\mathbf{u}}_n = \delta\mathbf{M}\ddot{\mathbf{u}}_{n-1} + \left[\mathbf{M} - \delta^2\mathbf{K} - \alpha\delta\mathbf{G}\right]\dot{\mathbf{u}}_{n-1} + \left[-\delta\mathbf{K} - \alpha\delta\mathbf{G}\kappa\right]\mathbf{u}_{n-1} \quad (5.2\text{-}12)$$

Doing the same thing for $\ddot{\mathbf{u}}_n$

$$\left[\mathbf{M}+\delta^2\mathbf{K}\right]\ddot{\mathbf{u}}_n = \left[-\delta^2\mathbf{K}\right]\ddot{\mathbf{u}}_{n-1} + \left[-2\delta\mathbf{K} - \alpha\mathbf{G}\right]\dot{\mathbf{u}}_{n-1} + \left[-\mathbf{K} - \alpha\mathbf{G}\kappa\right]\mathbf{u}_{n-1} \quad (5.2\text{-}13)$$

Defining $\mathbf{K}_{Eff} = \left[\mathbf{M}+\delta^2\mathbf{K}\right]$ and using (5.2-10,-12,-13) leaves the following amplification matrix relating states at t_{n-1} to states at t_n:

$$\begin{bmatrix} \mathbf{K}_{Eff}^{-1}\left[-\delta^2\mathbf{K}\right] & \mathbf{K}_{Eff}^{-1}\left[-2\delta\mathbf{K} - \alpha\mathbf{G}\right] & \mathbf{K}_{Eff}^{-1}\left[-\mathbf{K} - \alpha\mathbf{G}\kappa\right] \\ \mathbf{K}_{Eff}^{-1}\delta\mathbf{M} & \mathbf{K}_{Eff}^{-1}\left[\mathbf{M} - \delta^2\mathbf{K} - \alpha\delta\mathbf{G}\right] & \mathbf{K}_{Eff}^{-1}\left[-\delta\mathbf{K} - \alpha\delta\mathbf{G}\kappa\right] \\ \mathbf{K}_{Eff}^{-1}\delta^2\mathbf{M} & \mathbf{K}_{Eff}^{-1}\left[2\delta\mathbf{M} - \alpha\delta^2\mathbf{G}\right] & \mathbf{K}_{Eff}^{-1}\left[\mathbf{M} - \alpha\delta^2\mathbf{G}\kappa\right] \end{bmatrix} \quad (5.2\text{-}14)$$

All of the eigenvalues of this matrix must be within the unit circle to ensure the coupling process is stable. Performing this analysis, the maximum time step that maintains stability is h = $1.50\text{x}10^{-4}$.

5.2.2 Accuracy Analysis of Shuttle-Satellite Example

The characteristic equation for an undamped structural system with holonomic constraints is

$$\left[(1-\phi_M)\mathbf{M} + (\delta^2-\phi_K)\mathbf{K} + \alpha\phi_R\mathbf{G}(\psi+\kappa)p(sh)\right]\mathbf{u}_n = 0 \qquad (5.2\text{-}15)$$

For the 0 computational path using the trapezoidal rule and a last value predictor the following constants are defined:

$$\phi_M = 1-\delta\psi,\ \phi_K = \delta^2-\delta\psi^{-1},\ \phi_R = \delta\psi^{-1},\ p(sh) = e^{sh},\ \psi = \tanh\left(\frac{sh}{2}\right)$$

With these constants (5.2-15) becomes

$$\left[\delta\tanh\left(\frac{sh}{2}\right)\mathbf{M} + \delta\tanh^{-1}\left(\frac{sh}{2}\right)\mathbf{K} + \alpha\delta\tanh^{-1}\left(\frac{sh}{2}\right)\mathbf{G}(\tanh\left(\frac{sh}{2}\right)+\kappa)e^{sh}\right]\mathbf{u}_n = 0 \qquad (5.2\text{-}16)$$

or after clearing fractions

$$\left[\tanh^2\left(\frac{sh}{2}\right)\mathbf{M} + \mathbf{K} + \alpha\mathbf{G}(\tanh\left(\frac{sh}{2}\right)+\kappa)e^{sh}\right]\mathbf{u}_n = 0 \qquad (5.2\text{-}17)$$

Using the series expansion for tanh and e

$$\tanh\left(\frac{sh}{2}\right) = s\left(1-\frac{1}{12}s^2h^2+\frac{1}{240}s^4h^4-\cdots\right) \quad \text{and} \quad e^{sh} = \left(1+sh+\frac{1}{2}s^2h^2+\frac{1}{6}s^3h^3+\frac{1}{24}s^4h^4+\cdots\right)$$

which makes the complex terms

$$\tanh^2\left(\frac{sh}{2}\right) = s^2\left(1-\frac{1}{6}s^2h^2+\frac{11}{720}s^4h^4-\cdots\right)$$

$$\tanh\left(\frac{sh}{2}\right)e^{sh} = s\left(1+sh+\frac{5}{12}s^2h^2+\frac{1}{12}s^3h^3+\frac{1}{240}s^4h^4+\cdots\right)$$

Inserting these terms into (5.2-17) leaves

$$\left[\begin{array}{l}\mathbf{M}s^2\left(1-\frac{1}{6}s^2h^2+\frac{11}{720}s^4h^4-\cdots\right)+\mathbf{K}\\ \quad+\alpha\mathbf{G}s\left(1+sh+\frac{5}{12}s^2h^2+\frac{1}{12}s^3h^3+\frac{1}{240}s^4h^4+\cdots\right)\\ \quad\quad+\alpha\mathbf{G}\kappa\left(1+sh+\frac{1}{2}s^2h^2+\frac{1}{6}s^3h^3+\frac{1}{24}s^4h^4+\cdots\right)\end{array}\right]\mathbf{u}_n = 0 \qquad (5.2\text{-}18)$$

or rearranging terms

$$\left[\begin{array}{l}\left(\mathbf{M}-\frac{h^2}{6}\mathbf{M}s^2+\alpha Gh+\alpha G\frac{h^3}{12}s^2+O(h^4)\right)s^2 \\ +\left(\alpha G(1+\kappa h)+\alpha G(\frac{5h^2}{12}h^2+\frac{\kappa h^3}{6})s^2+O(h^4)\right)s \\ +\left(\mathbf{K}+\alpha G\kappa+\frac{h^2}{2}\alpha G\kappa s^2+O(h^4)\right)\end{array}\right]\mathbf{u}_n = 0 \qquad (5.2\text{-}19)$$

Dropping higher order terms and using the fact that $[\mathbf{M}s^2 + \mathbf{K}]\mathbf{u}_n = 0$

$$\left[\begin{array}{l}\left(\mathbf{M}-\frac{h^2}{6}\mathbf{K}+\alpha Gh+\alpha G\frac{h^3}{12}\mathbf{M}^{-1}\mathbf{K}\right)s^2 \\ +\left(\alpha G(1+\kappa h)+\alpha G(\frac{5h^2}{12}h^2+\frac{\kappa h^3}{6})\mathbf{M}^{-1}\mathbf{K}\right)s \\ +\left(\mathbf{K}+\alpha G\kappa+\frac{h^2}{2}\alpha G\kappa\mathbf{M}^{-1}\mathbf{K}\right)\end{array}\right]\mathbf{u}_n = 0 \qquad (5.2\text{-}20)$$

This equation can be used to find the coupled system frequencies. Table 5.2-1 compares the continuous system frequencies to the frequencies shifted by integration alone (discrete frequencies) and the frequencies shifted by integration and coupling. As (5.2-20) shows some artificial damping occurs as a result of the simulation coupling process. However, the damping ratios of the coupled frequencies is less than 10^{-7}. The is also a coupled frequency corresponding to the constraint penalties at approximately 1200 rad/sec.

Table 5.2-1 Comparison of Frequency Shifting Effects (rad/sec)

Continuous	Discrete	Coupled
0.00000000	0.00000000	0.00000000
0.50034156	0.50034155	0.50034119
2.66408400	2.66408398	2.66408308

5.2.3 Response of Shuttle-Satellite Example

Two different responses were considered for this example. Both cases involved forcing the system using the shuttles control jet thrusters. Each run is compared to the identical conditions using the complete system shown in (5.2-2). For both, the complete and the coupled systems, a time step of 0.0001 seconds was used. The penalties suggested in Section 5.2.1 were used for the coupled case.

The first case is a 20 second run where the force of 2 kN has been applied for the first second. Figure 5.2-2 shows the position of the shuttle, the satellite rotor, and the joint between the arm and the platform. Additionally, Figure 5.2-3 shows the constraint error and constraint error rate for this case.

Since this is an undamped example the system energy should be constant. However, due to the stabilization of the constraints, energy will be bled off from the system. This process will continues as long as there is any potential energy stored due to flexibility. This artificial damping is a very slow process and has little noticeable effect, but care should still be taken to make the damping ratio for constraints less than or equal to the damping present in the structure, if possible.

The second case should show that no significant energy is lost even over a period of many time constants. It is a two minute run where the 2 kN force is applied for ten seconds. The figures for this run shows a twenty second period at the end of the two minutes. Figure 5.2-4 shows the translations of the major system parts. Figure 5.2-5 illustrates the error between the coupled response and the complete response for the shuttle, the rotor and the end effector.

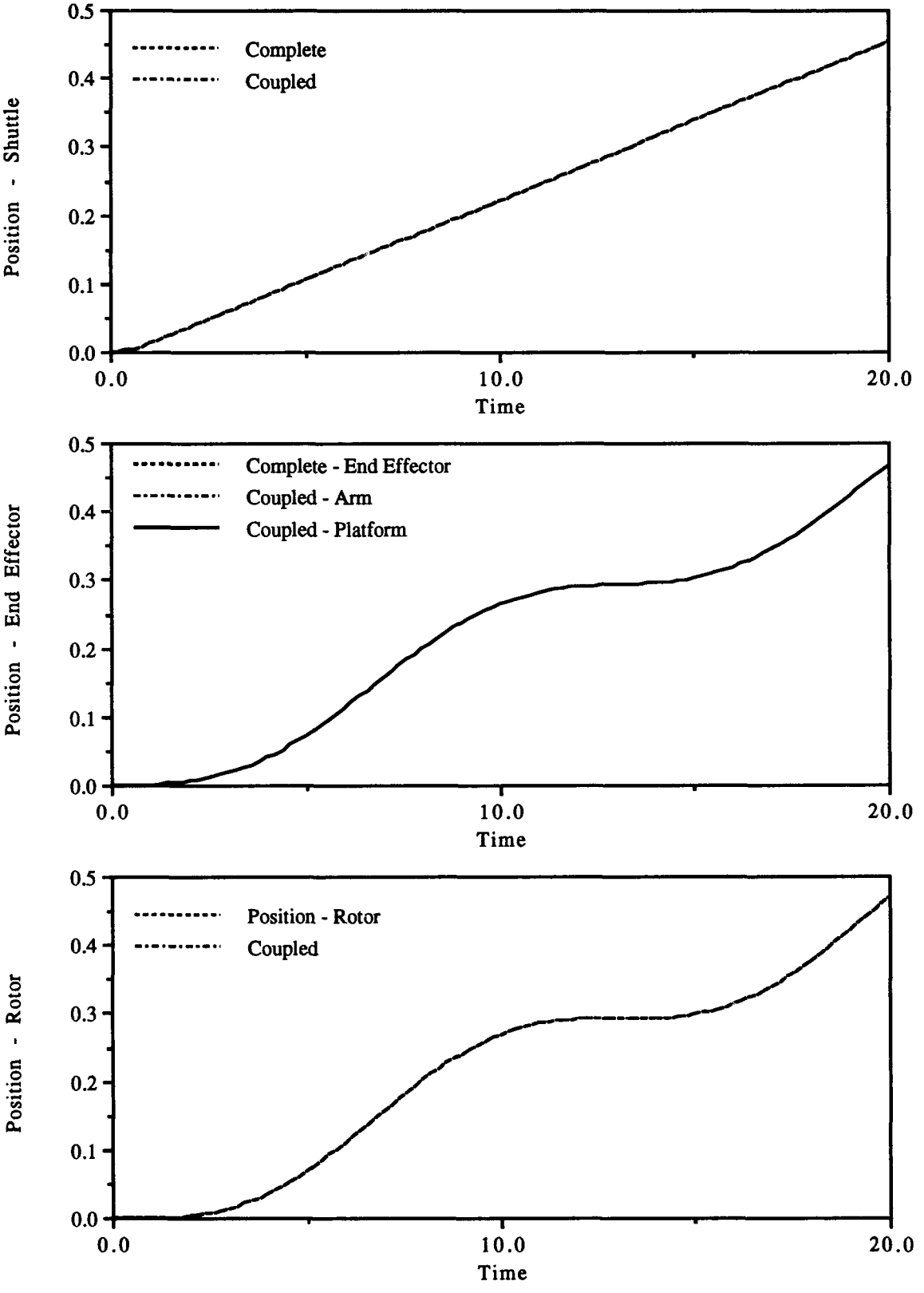

Figure 5.2-2 Shuttle-Satellite Example Short Term Response

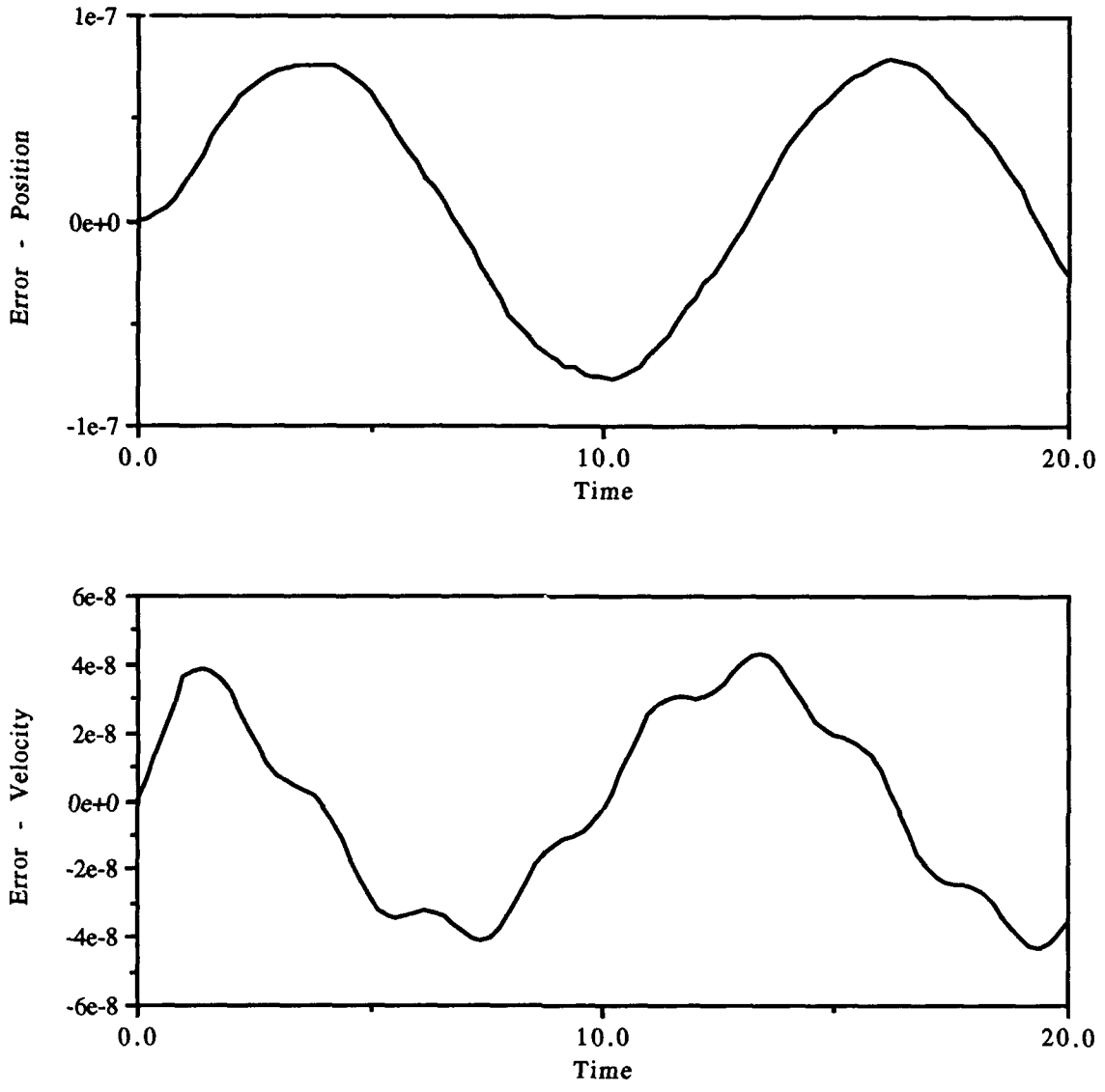

Figure 5.2-3 Shuttle-Satellite Example Constraint Error

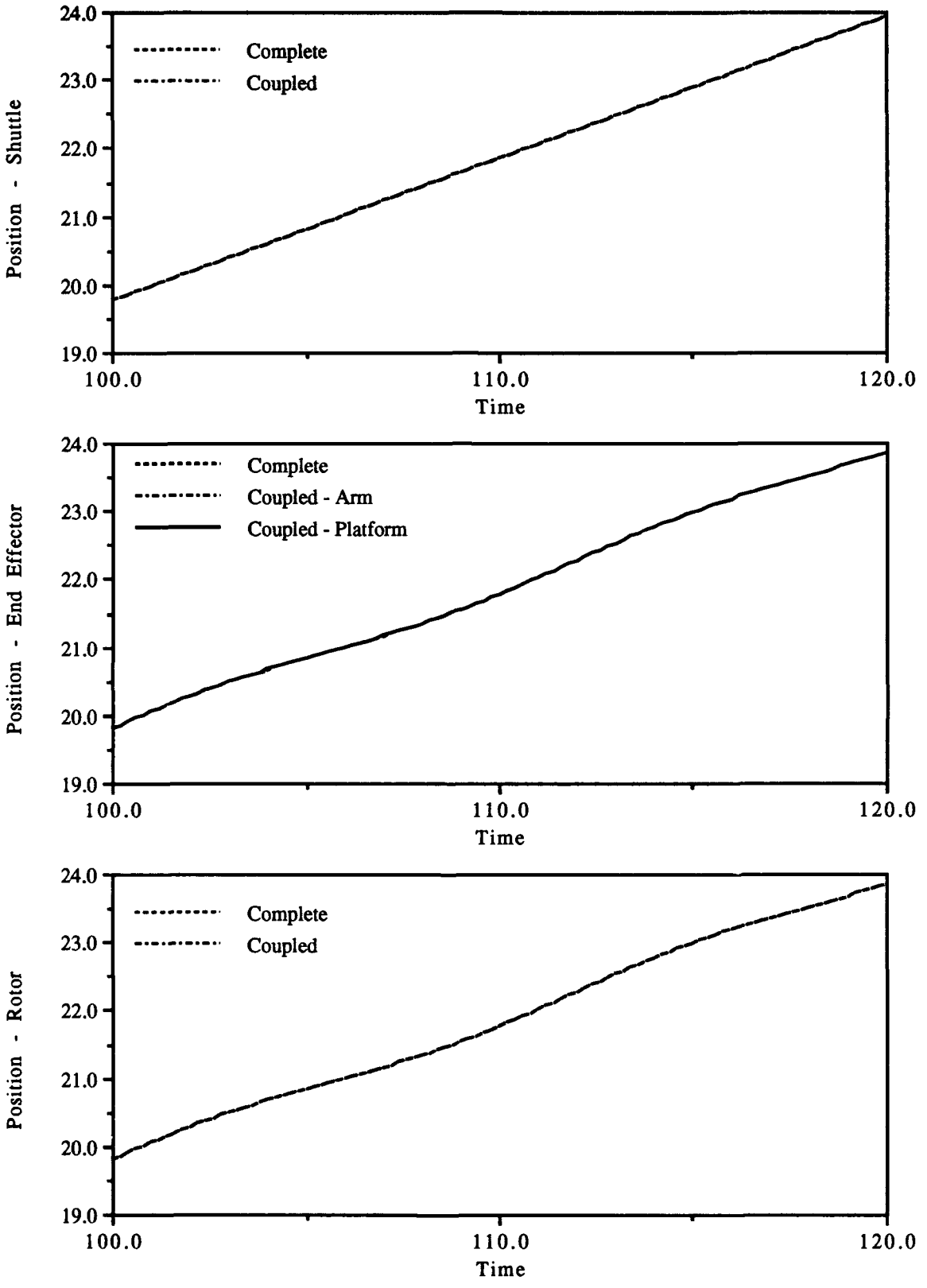

Figure 5.2-4 Shuttle-Satellite Example Long Term Response

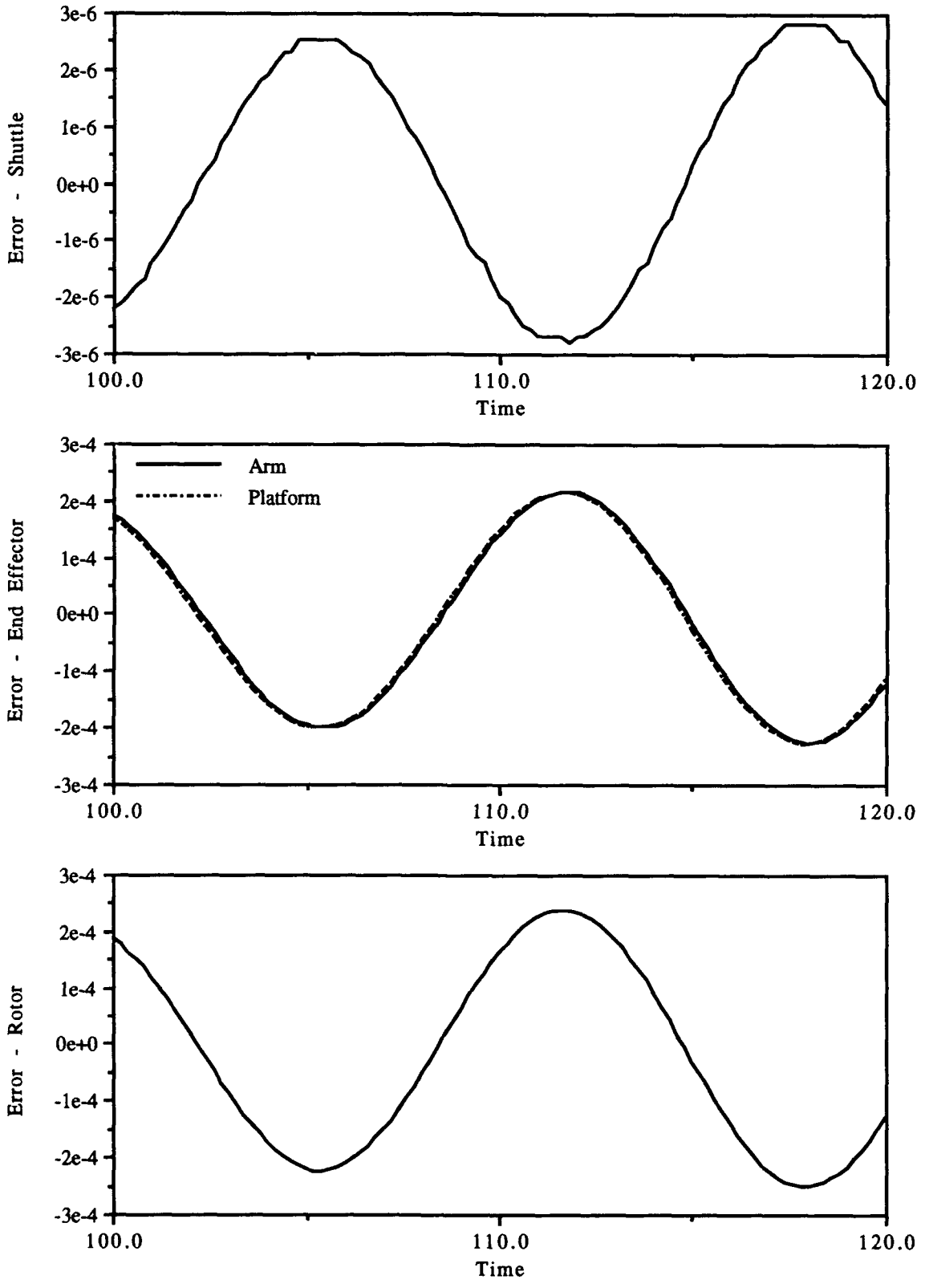

Figure 5.2-5 Shuttle-Satellite Example Long Term Error

5.3 Free Floating Rigid Body Example

The final simple example is a return to the satellite described in Section 5.1 and illustrated in Figure 5.1-1. This example, however, will consider all six DOFs, $\mathbf{R}_0 = [\ X\ Y\ Z\ ]^T$ and $\theta = [\ \theta_1\ \theta_2\ \theta_3\ ]^T$. The translations express displacement from the inertial frame in inertial coordinates and the angles represent Euler angles of a 2-1-3 rotation from the body frame to the inertial frame. The equations of motion for a rigid system with these specified DOFs are derived in many dynamics texts (see [5.4]).

For the fully rigid case there are six active constraints. Three translational constraints require the point where the rotor joins the platform to have the same inertial position. Three rotational constraints require the Euler angles for the platform orientation and the rotor orientation to be equal. The two sets of constraints are distinct enough to justify having a unique α and κ for the translations and the rotations.

5.3.1 Analysis of Rigid Body Example: Translational DOFs

Each body frame is fixed at the body CM with the z axis oriented along the spin axis indicated in Figure 5.1-1. If $\mathbf{r}^a$ is the position of the joint between the platform and the rotor with respect to the CM of frame a in frame a coordinates. With this definition the constraints on the translational DOFs are

$$\Phi = \mathbf{R}_0^r - \mathbf{R}_0^p + {}^I\mathbf{C}_B^r\,\mathbf{r}^r - {}^I\mathbf{C}_B^p\,\mathbf{r}^p \qquad (5.3\text{-}1)$$

where ${}^{I}C_B$ is the matrix representing an orthogonal 2-1-3 rotation from body to inertial frames. Taking the first two derivatives gives

$$\frac{d\Phi}{dt} = \dot{R}_o^r - \dot{R}_o^p + {}^{I}\dot{C}_B^r r^r - {}^{I}\dot{C}_B^p r^p + {}^{I}C_B^r(\omega^r \times r^r) - {}^{I}C_B^p(\omega^p \times r^p) \qquad (5.3\text{-}2)$$

and

$$\begin{aligned}\frac{d^2\Phi}{dt^2} = {} & \ddot{R}_o^r - \ddot{R}_o^p + {}^{I}\ddot{C}_B^r r^r - {}^{I}\ddot{C}_B^p r^p + {}^{I}\dot{C}_B^r(\omega^r \times r^r) - {}^{I}\dot{C}_B^p(\omega^p \times r^p) \\ & + {}^{I}C_B^r(\dot{\omega}^r \times r^r) - {}^{I}C_B^p(\dot{\omega}^p \times r^p) + {}^{I}C_B^r(\omega^r \times (\omega^r \times r^r)) - {}^{I}C_B^p(\omega^p \times (\omega^p \times r^p))\end{aligned} \qquad (5.3\text{-}3)$$

These terms are used to form the constraint correction force, f_c, and the constraint error equation.

The translational equations of motion for these two bodies are

$$\ddot{R}_o^r = \frac{1}{m_r}{}^{I}C_B^r R^r + \frac{1}{m_r} f_c \quad \text{and} \quad \ddot{R}_o^p = -\frac{1}{m_p} f_c \qquad (5.3\text{-}4)$$

Taking the difference of these equations and substituting e for Φ and $-\alpha\left[\frac{d\Phi}{dt} + \kappa\Phi\right]$ for f_c leaves

$$\ddot{R}_o^r - \ddot{R}_o^p = \frac{1}{m_r}{}^{I}C_B^r R^r - \frac{m_r + m_p}{m_r m_p}\alpha[\dot{e} + \kappa e] \qquad (5.3\text{-}5)$$

Adding the additional terms to form $\ddot{e}$ and the constraint error equation

$$\ddot{e} + \frac{m_r + m_p}{m_r m_p}\alpha\,\dot{e} + \frac{m_r + m_p}{m_r m_p}\alpha\,\kappa e = \frac{1}{m_r}{}^{I}C_B^r R^r + f^* \qquad (5.3\text{-}6)$$

where f^* includes the nonlinear terms treated as applied forces

$$\begin{aligned} f^* = {} & {}^{I}\ddot{C}_B^r r^r - {}^{I}\ddot{C}_B^p r^p + {}^{I}\dot{C}_B^r(\omega^r \times r^r) - {}^{I}\dot{C}_B^p(\omega^p \times r^p) + {}^{I}C_B^r(\dot{\omega}^r \times r^r) \\ & - {}^{I}C_B^p(\dot{\omega}^p \times r^p) + {}^{I}C_B^r(\omega^r \times (\omega^r \times r^r)) - {}^{I}C_B^p(\omega^p \times (\omega^p \times r^p)) \end{aligned} \qquad (5.3\text{-}7)$$

In order to keep the analysis linear, the nonlinear forcing term is assumed to be much smaller than the actual forcing. This leaves the vector form of the error equation found in (5.1-4). Given the same error limits and desired damping (steady state error less than 10^{-7} and damping of 30%), the penalty constants and time step limit found in the first example will still hold. These numbers are

$$\alpha = 2{,}400.0 \qquad \kappa = 125.0 \qquad h \leq 0.008 \tag{5.3-8}$$

5.3.2 Analysis of Rigid Body Example: Rotational DOFs

As described earlier the rotational constraints require the Euler 2-1-3 angles for each frame to be equal

$$\Phi = \theta^r - \theta^p \tag{5.3-9}$$

Taking the first two derivatives gives

$$\frac{d\Phi}{dt} = \dot{\theta}^r - \dot{\theta}^p = S_r^{-1}\omega^r - S_p^{-1}\omega^p \tag{5.3-10}$$

and

$$\frac{d^2\Phi}{dt^2} = \ddot{\theta}^r - \ddot{\theta}^p = S_r^{-1}\dot{\omega}^r - S_p^{-1}\dot{\omega}^p + \dot{S}_r^{-1}\omega^r - \dot{S}_p^{-1}\omega^p \tag{5.3-11}$$

where S_r is a non-orthogonal transformation from Euler angle rates to angular velocity coordinates (see [5.4]). These terms are used to form the constraint correction torques, τ_c, and the constraint error equation.

The rotational equations of motion for these two bodies are

$$\dot{\omega}^r = \mathbf{I}_r^{-1}\tau^r - \mathbf{I}_r^{-1}(\omega^r \times \mathbf{I}_r\omega^r) + \mathbf{I}_r^{-1}\tau_c^r$$
$$\dot{\omega}^p = -\mathbf{I}_p^{-1}(\omega^p \times \mathbf{I}_p\omega^p) - \mathbf{I}_p^{-1}\tau_c^p \qquad (5.3\text{-}12)$$

Premultiplying by the appropriate form of $\mathbf{S}_a^{-1}$ and taking the difference of these equations, as well as substituting $e = \Phi$ and $\tau_c^a = -\mathbf{S}_a\alpha\left[\frac{d\Phi}{dt} + \kappa\Phi\right]$ leaves

$$\mathbf{S}_r^{-1}\dot{\omega}^r - \mathbf{S}_p^{-1}\dot{\omega}^p = \mathbf{S}_r^{-1}(\mathbf{S}_r + \mathbf{S}_p)\mathbf{S}_p^{-1}\mathbf{I}_r^{-1}(\mathbf{I}_r + \mathbf{I}_p)\mathbf{I}_p^{-1}(\omega^p \times \mathbf{I}_p\omega^p - \omega^r \times \mathbf{I}_r\omega^r)$$
$$- \mathbf{S}_r^{-1}(\mathbf{S}_r + \mathbf{S}_p)\mathbf{S}_p^{-1}\mathbf{I}_r^{-1}(\mathbf{I}_r + \mathbf{I}_p)\mathbf{I}_p^{-1}(\mathbf{S}_r + \mathbf{S}_p)\alpha[\dot{e} + \kappa e] + \mathbf{S}_r^{-1}\mathbf{I}_r^{-1}\tau^r \qquad (5.3\text{-}13)$$

Adding the additional terms to form $\ddot{e}$ for the constraint error equation and making the following definitions: $\mathbf{S} = \mathbf{S}_r^{-1}(\mathbf{S}_r + \mathbf{S}_p)\mathbf{S}_p^{-1}$ and $\mathbf{I} = \mathbf{I}_r^{-1}(\mathbf{I}_r + \mathbf{I}_p)\mathbf{I}_p^{-1}$, leaves

$$\ddot{e} + \mathbf{S}\,\mathbf{I}(\mathbf{S}_r + \mathbf{S}_p)\alpha\dot{e} + \mathbf{S}\,\mathbf{I}(\mathbf{S}_r + \mathbf{S}_p)\alpha\,\kappa e = \mathbf{S}_r^{-1}\mathbf{I}_r^{-1}\tau^r + \tau^* \qquad (5.3\text{-}14)$$

where τ^* includes the nonlinear terms

$$\tau^* = \mathbf{S}\,\mathbf{I}(\omega^p \times \mathbf{I}_p\omega^p - \omega^r \times \mathbf{I}_r\omega^r) + \dot{\mathbf{S}}_r^{-1}\omega^r - \dot{\mathbf{S}}_p^{-1}\omega^p \qquad (5.3\text{-}15)$$

Two assumptions are made to keep the analysis linear. First, the nonlinear forcing term, τ^*, is assumed to be small with respect to the actual forcing. Additionally, since the error between the Euler angles is forced to be small, the transformation matrix for the two body frames is assumed to be the same, $\mathbf{S}_{rp}$. This will reduce the matrix $\mathbf{S}$ to $2\mathbf{S}_{rp}^{-1}$. Rearranging the remaining linear terms leaves

$$\mathbf{S}_{rp}^{-1}\mathbf{I}^{-1}\mathbf{S}_{rp}\ddot{e} + 4\alpha\dot{e} + 4\alpha\kappa e = \mathbf{S}_{rp}^{-1}\mathbf{I}_p(\mathbf{I}_r + \mathbf{I}_p)^{-1}\tau^r \qquad (5.3\text{-}16)$$

Using this equation and desired values for steady state error and damping ratio, the penalty constants can be found in the same manner as the first and second examples. With a steady state error of 10^{-4} degrees and and damping ratio of 0.1 the constants are α = 375.0 and κ = 40.0.

To find the maximum stable time step the complete equations of motion must be formed. Combining (5.3-12) and the fact the S_a relates Euler angle rates to angular velocity, the complete first order unforced equation of motion can be formed

$$\begin{Bmatrix} \dot{\omega}^r \\ \dot{\theta}^r \\ \dot{\omega}^p \\ \dot{\theta}^p \end{Bmatrix} = \begin{bmatrix} 0 & 0 & 0 & 0 \\ S_{rp}^{-1} & 0 & 0 & 0 \\ 0 & 0 & 0 & 0 \\ 0 & 0 & S_{rp}^{-1} & 0 \end{bmatrix} \begin{Bmatrix} \omega^r \\ \theta^r \\ \omega^p \\ \theta^p \end{Bmatrix} - \begin{Bmatrix} I_r^{-1}(\omega^r \times I_r \omega^r) \\ 0 \\ I_p^{-1}(\omega^p \times I_p \omega^p) \\ 0 \end{Bmatrix}$$
$$- \begin{bmatrix} 0 & I_r^{-1} & 0 & -I_r^{-1} \\ 0 & 0 & 0 & 0 \\ 0 & -I_p^{-1} & 0 & I_p^{-1} \\ 0 & 0 & 0 & 0 \end{bmatrix} S_{rp} \alpha \left[\begin{Bmatrix} \dot{\omega}^r \\ \dot{\theta}^r \\ \dot{\omega}^p \\ \dot{\theta}^p \end{Bmatrix} + \kappa \begin{Bmatrix} \omega^r \\ \theta^r \\ \omega^p \\ \theta^p \end{Bmatrix} \right] \qquad (5.3\text{-}17)$$

or redefining terms

$$\dot{\Theta} = \mathbf{K}\Theta - \tau^* - G\alpha\left[\dot{\Theta} + \kappa\Theta\right] \qquad (5.3\text{-}18)$$

Using the trapezoidal rule and a last value predictor, an amplification matrix similar to the one in (5.2-14) can be formed. With $\mathbf{K}_{Eff}$ defined as $\mathbf{I}^{(12)} - \delta\mathbf{K}$, the matrix is

$$\begin{bmatrix} \mathbf{K}_{Eff}^{-1}[\delta\mathbf{K} - \alpha\mathbf{G}] & \mathbf{K}_{Eff}^{-1}[\mathbf{K} - \alpha\mathbf{G}\kappa] \\ \mathbf{K}_{Eff}^{-1}[\delta\mathbf{I}^{(12)} - \delta\alpha\mathbf{G}] & \mathbf{K}_{Eff}^{-1}[\mathbf{I}^{(12)} - \delta\alpha\mathbf{G}\kappa] \end{bmatrix} \qquad (5.3\text{-}18)$$

By requiring the eigenvalues of this amplification matrix to be within the unit circle the critical time step is found to be h = 0.03.

5.3.3 Response of Rigid Body Example

For the response the penalties used are

	α	κ
Translation	2400.0	125.0
Rotation	375.0	40.0

The maximum time step is 0.008 seconds and the actual time step used is 0.005 seconds. The satellite (rotor and platform) is given an initial spin rate of 0.5 rpm. The complete set of plots, all degrees of freedom and errors, is given in Appendix A.

The first case reflects a constant force input of 1 N in the z axis. Due to the satellite's symmetry this forcing only excites the z axis translation. The error response is exactly as shown in the first example, with constraint error damping out at two seconds to the steady state value of 10^{-7} meters. The second case is similar with a constant torque input of 10 N-m about the z axis. Again only the θ_3 DOF shows any response. This response damps out after four seconds to a steady state value of 10^{-4} degrees. These responses show that the simulation will perform as desired under the simplest of forcing conditions.

Although the earlier cases verify performance of the coupling algorithm the more interesting cases are those designed to show the cross-coupling effects between the translation and rotation DOFs. The third case, a 1 N force along each axis shows one new effect. The constant spin about the third axis produces a long period displacement error in the x and y axes. This displacement is a

maximum at $1.5x10^{-6}$ meters, larger than the desired value but still small enough that the penalty constants do not need to be changed. Had this value not been sufficient the constants may be changed easily. For instance, if the maximum allowable error is 10^{-6} meters then by raising κ by a factor of 1.5 and α by $\sqrt{1.5}$ then maximum is reduced while still still maintaining reasonable damping. Additionally, if the penalties are changed by a significant amount it may also be necessary to adjust the time step.

The final case involves applying a 0.1 second 1 N-m torque to one of the non-spinning axes. In this case the nonlinear terms which were ignored in the analysis of Section 5.3.2 start to have a significant impact on the motion. The original constants must be altered to account for this nutation of the spinning satellite and ensure the stability of the simulation coupling process. Running several different penalty combinations, simply adding a large amount of damping seems the most effective correction for nutation effects. After achieving stability, the penalties are modified to keep the steady state errors small. The total of these two corrections raises α by a factor of forty and κ by a factor of four. The time step is dropped during this process to 0.0025, again to ensure stability.

There is one final effect of a rigid body simulation to discuss. When using Euler angles it is possible to encounter singularities where the three angles condense to one DOF. This continues to be the case in a simulation coupling process. The most successful way to correct for this effect is to switch to a different Euler angle combination when close to a singularity. Although this will

successfully avoid the singularity problems, for this example the initial conditions were altered instead to avoid any singularities.

5.4 Conclusions from Simple Examples

These examples should show that for small cases it is possible to write an error equation to find appropriate penalties and to complete a linear stability analysis to find a time step for the simulation coupling algorithm. Both rigid and flexible problems display unique difficulties to watch for as larger, more involved problems are attempted.

For rigid cases the most difficult problem to handle is the singularities Each simulation handles them differently and it may be necessary to change constraints and even penalties to account for the singularity. The only other noteworthy problem is how to deal with the coupling between displacement and rotation DOFs which may occur due to rotating frames, nutation, or simple geometry considerations. However, by making small adjustments in the penalty constants and time step these difficulties can usually be handled.

Simulation coupling of flexible cases presents the unique problem of an additional dissipative force in the penalty stabilization scheme. Care should be taken not to significantly alter the system damping ratio, otherwise the constraint error will damp out but the response will not converge to the correct solution.

Finally, both flexibility and rotation effects produce significant long period error responses. This long period motion is usually much

larger than predicted steady state maximum values and a check should always be made for this sort of constraint error mode.

Chapter Six

Space Station Example

The Space Station Assembly Complete model used in this example consists of 3852 degrees of freedom and 1577 elements. It is made up of three primary bodies: the center span and two articulating "wings". The individual bodies are separated at the alpha joints pictured in Figure 6.1 and the gamma and beta joints are modelled as fixed. Since it is possible to set up the complete three-body multibody problem for comparison the Space Station makes a good test case for the validity of simulation coupling as an alternative simulation strategy.

For the purpose of simulation coupling the response of each body is calculated according to the single flexible body equations presented in [6.1]. One individual rigid-flex one-body simulation is used for each of the separate bodies. The simulation makes use of a popular fourth order Runge-Kutta integration scheme instead of the linear multi-step methods which are suggested in Chapter Three. Additionally, the Space Station is too large for a flexible analysis like

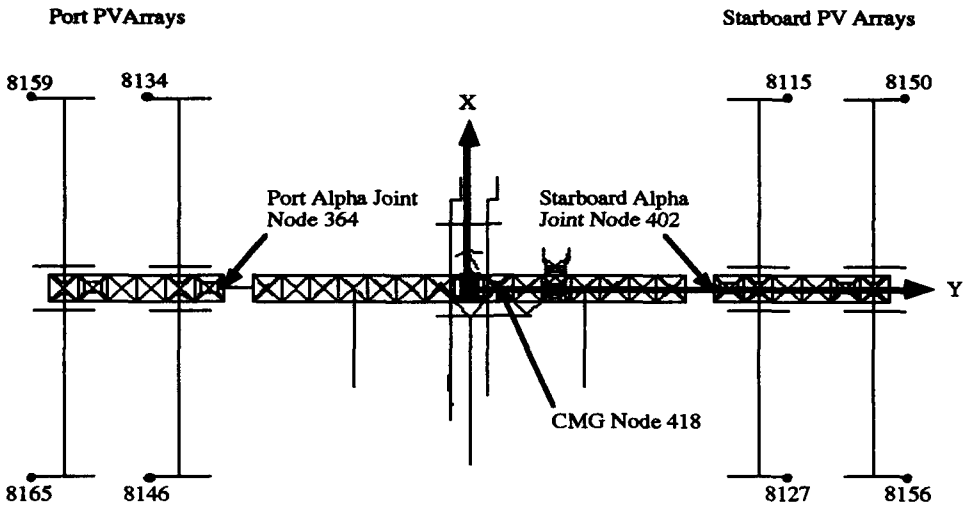

Figure 6.1. Space Station Freedom Assembly Complete

the one used in Section 5.2 to be done. Because of these two factors the approach taken is slightly different than the examples of the previous chapter.

For the non-articulated simulations all 6 DOFs at each alpha joint are rigidly constrained. The articulated simulations allows free rotation about the y axis (θ_2 degree of freedom). The penalties, α and κ are to be designed to keep the translation constraint violation less then 10^{-8} feet and the rotation constraint violation less than 10^{-6} degrees.

6.1 Analysis for the Space Station Example

As has been mentioned the flexible model of the Space Station is too large for a full analysis. It is still reasonable, however, to do the rigid body analysis. This will allow a first guess at the complete model penalties using the rigid body penalties. If this guess should prove unacceptable then further adjustments can be made based on the error responses.

The analysis of the Space Station is broken into two two-field problems: the interaction between the left wing and center span and the interaction between the right wing and center span. The constraint error equations for a rigidly coupled two-field problem derived in Section 5.3 are

Translation $$\ddot{\mathbf{e}} + \frac{m_c + m_w}{m_c m_w}\alpha\dot{\mathbf{e}} + \frac{m_c + m_w}{m_c m_w}\alpha\kappa\mathbf{e} = \frac{1}{m_c}{}^{I}\mathbf{C}_B^c\mathbf{R}^c + \mathbf{f}^* \qquad (6.1\text{-}1)$$

and

Rotation $$\ddot{\mathbf{e}} + \mathbf{S}_I(\mathbf{S}_c + \mathbf{S}_w)\alpha\dot{\mathbf{e}} + \mathbf{S}_I(\mathbf{S}_c + \mathbf{S}_w)\alpha\kappa\mathbf{e} = \mathbf{S}_c^{-1}\mathbf{I}_c^{-1}\tau^c + \tau^* \qquad (6.2\text{-}2)$$

were center (c) and wing (w) properties and attendant matrices replace the previous rotor and platform ones.

Using these equations and again assuming the nonlinear terms are much smaller than the applied forcing the penalty constants for both the starboard and port wings are

	α	κ
Translation	90,000	8,000
Rotation	1,150,000	90.0

The translational penalties limit the time step at 0.0001 seconds.

6.2 Response for the Space Station Example

Due to the the type and location of the reaction jet clusters there are two forcing conditions commonly used for comparison of the Space Station model. They are a one second 100 lb force in the z direction and a 0.2 sec torque about the x axis of 2500 ft-lb. Using the two forcing conditions there are three cases to be considered: a

rigid non-articulated case, a rigid articulated case, and a flexible case with articulation. The plots for all cases are shown in Appendix B.

Running the rigid non-articulated case shows two areas where the penalties must be adjusted to ensure the proper response. First, the penalties on the rotations must be raised substantially to counter the coupling which the inertia matrix provides. Overall, κ is raised by a factor of eight and α is doubled before the error response is acceptable. Also, the non-primary responses need additional damping. Primary responses are the DOF being directly forced and the articulation DOF, which corresponds to θ_2. By overdamping the other error responses coupling between error terms is virtually eliminated. The overdamping involved raising α by additional factor of ten and lowering κ by a factor of twenty.

One numerical effect of simulation coupling seems to be the creation of alternate response paths which solve the error equations but do not provide the correct solution for the coupled equations of motion. For the Space Station one of these paths is the unconstrained response of the center span. Under certain penalty values the error will decay rapidly to zero, leaving the center span 'blind' to the wing on either side. In fact, the basic penalties listed in Section 6.1 converged to the unconstrained solution.

After correcting the penalties the other rigid cases have little new information to offer. There are a few small errors between the multibody solution and the simulation coupling solution but all are within acceptable limits. The constraint errors on the average are much smaller than specified due to the overdamping effects.

The flexible model includes 10 flexible modes for each single body. The included modes are the first ten based on frequency. When switching to the flexible case the penalties do not need to be changed significantly but the time step is cut in half to account for the flexibility. Unfortunately, the same accuracy seen in the rigid cases is not maintained in the flexible cases.

The flexible case shows mosts of the errors expected form simulation coupling. There are some noticable frequency shift effects as well as significant artifical damping effects present. These effects can normally be reduced by tightening the penalties used. In the simple example of Section 5.3 these effects were not serious because the error was kept small. In this case the penalties cannot be raised to a sufficent level to counter these effects for two reasons. First, pushing the penalties higher seriously limits the time step, making it unreasonably small. Also, the penalties needed to remove most of these effects ends up causing overflow problems for the computer on which the code was written. Some of these difficulties may be solved using the numerical improvements discussed in Appendix C.

The largest difference in the flexible cases appears as a frequency shift in the lowest frequency mode. In the x torque case, for instance, this shift is most evident in the θ_3 DOF. This error also causes a slow drift in the other angular DOFs as well as reinforcing the low frequency motion in the translational DOFs. The same sort of error is also present in the z force case. Also, the z force case appears unstable, however, the actual response shows the first mode grow in magnitude for ten seconds before it begins to decay.

Chapter Seven

Conclusion

Simulation coupling is a procedure which allows individual existing simulations of separate fields to be combined for the solution of coupled field problems. It is a potentially time and cost saving method for dealing with these problems. If the constraints which couple the separate fields are adequately dealt with this method can be very accurate.

7.1 Summary

The coupled field problem has been introduced with the available solution methods. Simulation coupling was introduced as an branch of partitioned solution methods, where the partitions are created to decoupled the dynamics into single fields. This allowed the use of constraints and single field simulation tools to solve coupled field problems.

Integration methods were examined in detail, focusing on linear multistep methods. Operator expressions were introduced to

provide a compact notation for the analysis tools developed. These expressions were applied to integration methods and predictors to find expressions for the stability and accuracy of complex integration schemes.

Numerical methods of dealing with constraints were discussed, focusing on the classical Lagrange mulipliers and the newer stabilization schemes. These methods were used along with the integration tools to develop the simulation coupling algorithm. Although two methods of simulation coupling were introduced the concurrent evaluation was given considerably more attention. The validity of the method and the analysis tools developed was examined in a series of small scale problems before applying the theory to the Space Station simulation.

This theory is in no way meant to be suggested as superior to any other methods of solving coupled field problems. It is introduced here as a possible alternative to preforming large scale analysis of complex problems such as multibody dynamics.

7.2 Significant Findings and Results

Simulation coupling has proven to be worthy of further consideration as an alternative solution process for coupled field problems. It shows considerable success on small flexible and rigid body problems. It allows a considerable savings in time and effort to set up the simulation for and find the solution of large coupled problems. It is not at the time a perfect alternative and needs

further investigation in several areas before application to larger problems. However, the potential shown warrants this effort.

7.3 Future Work

Of the several areas that require more work, the one with the most potential for aiding the success of simulation coupling as a viable solution form is prediction methods. Only the simplest form of prediction has been used in this thesis but current research suggests that large gains in time step limits and accuracy can be made through more advanced predictors. Work done in the past on other partitioned solution forms suggests that 'optimal' predictors may exist and that they have large impact on a method's success.

More work needs to be done in the area of handling and incorporating constraints. This area is essential to the success of simulation coupling. At the current time there is still a great deal of debate as to which of the many possibilities is most suitable for widescale application.

Finally, an area with enormous potential for application of the simulation coupling algorithm is parallel computing. Seperate simulation elements could be tasked to the various processors with one to oversee data management and execution. This would make simulation coupling a potentially cost saving method not only in effort required to create simulation codes, but also in real time necessary to run simulations. Simulation coupling readily lends itself to such a multitasking enviroment.

Appendix A

Satellite Rigid Body Plots

As mentioned in Section 5.3.3 this Appendix contains all of the plots for the third simple numerical example. The particular forcing conditions for each of the four cases are described within the appropriate section. The third and fourth cases have long and short duration runs. The units for all translations degrees are meters and meters per second, rotations are degrees and degrees per second, and time is in seconds.

A.1 First Case - Z Axis Forcing

A constant forcing of 1 N is applied in the direction of the z axis. There is an initial spin rate of 0.5 rpm about the z axis. Due to symmetry only a z axis translation results. Responses included are rotor and platform translational displacements as well as the constraint error responses. Angular responses are not included since the only angular displacement that occurs is a constant increase about the z axis.

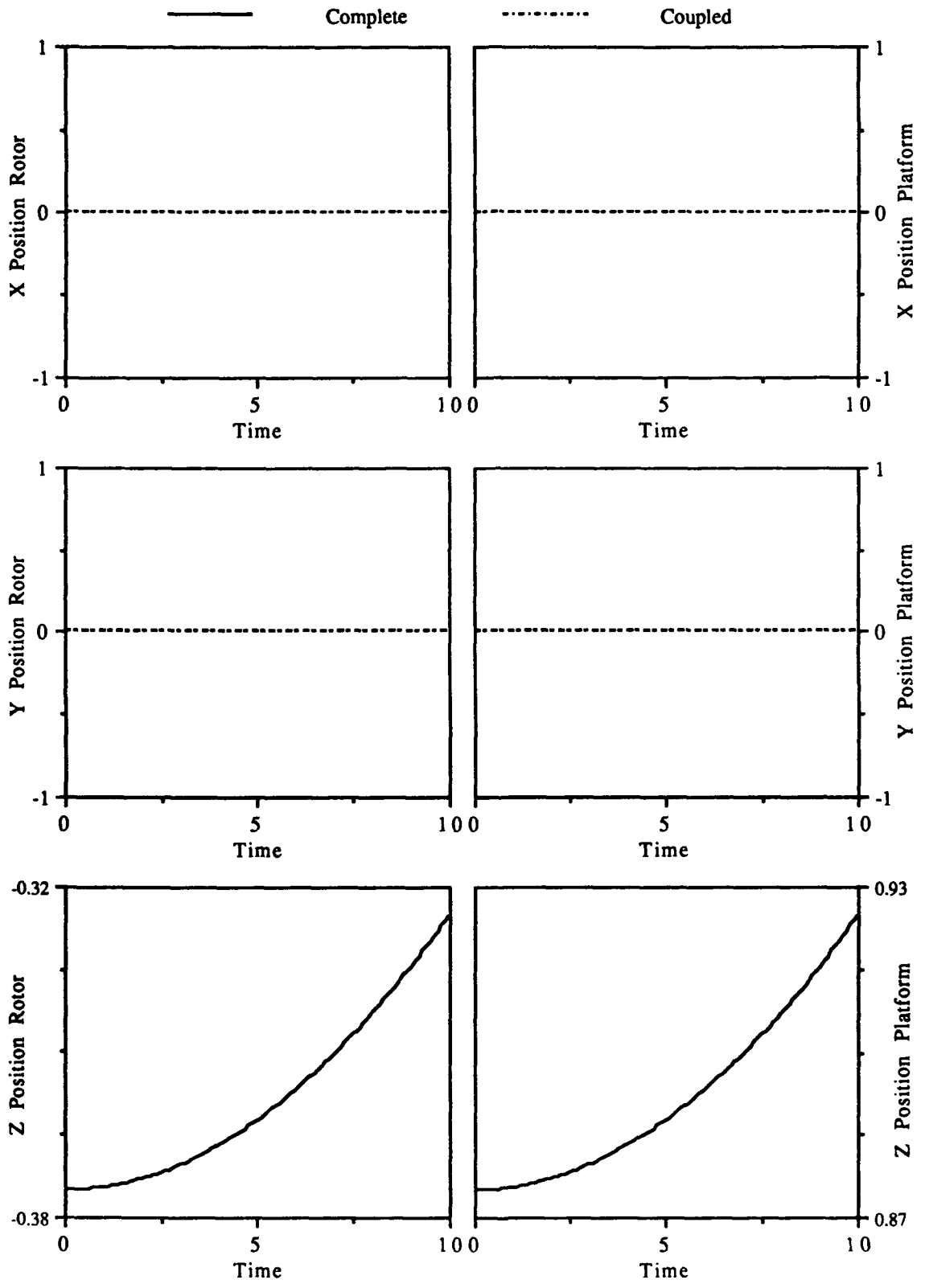

Figure A.1-1 Translational Response for Case 1

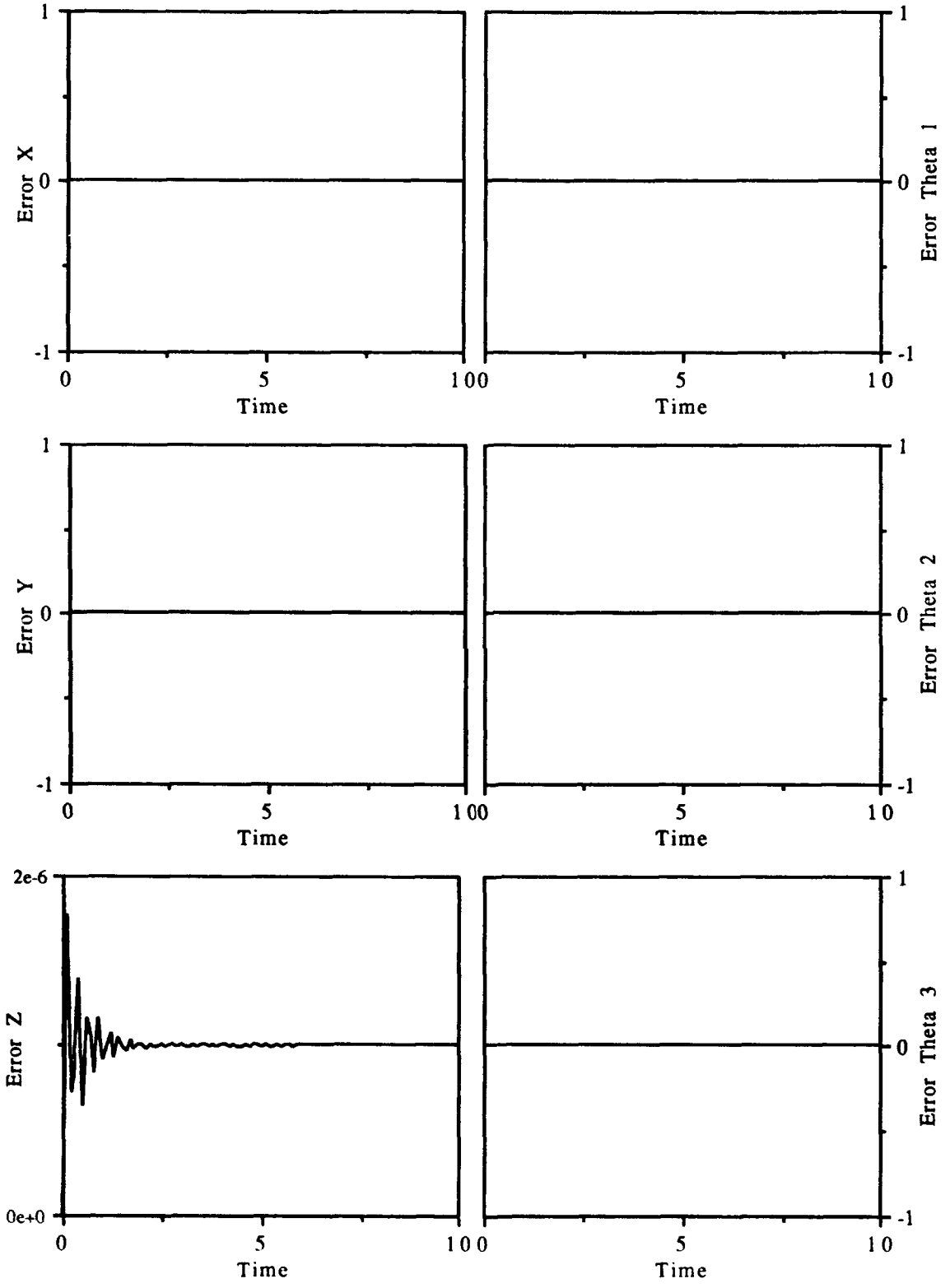

Figure A.1-2 Constraint Error Response for Case 1

A.2 Second Case - Z Axis Torque

A constant forcing of 10 N-m torque is applied about the z axis. There is an initial spin rate of 0.5 rpm about the z axis. Due to symmetry only a z axis rotation results. Responses included are rotor and platform rotational displacements as well as the constraint error responses. Translational responses are not included since all displacements are zero.

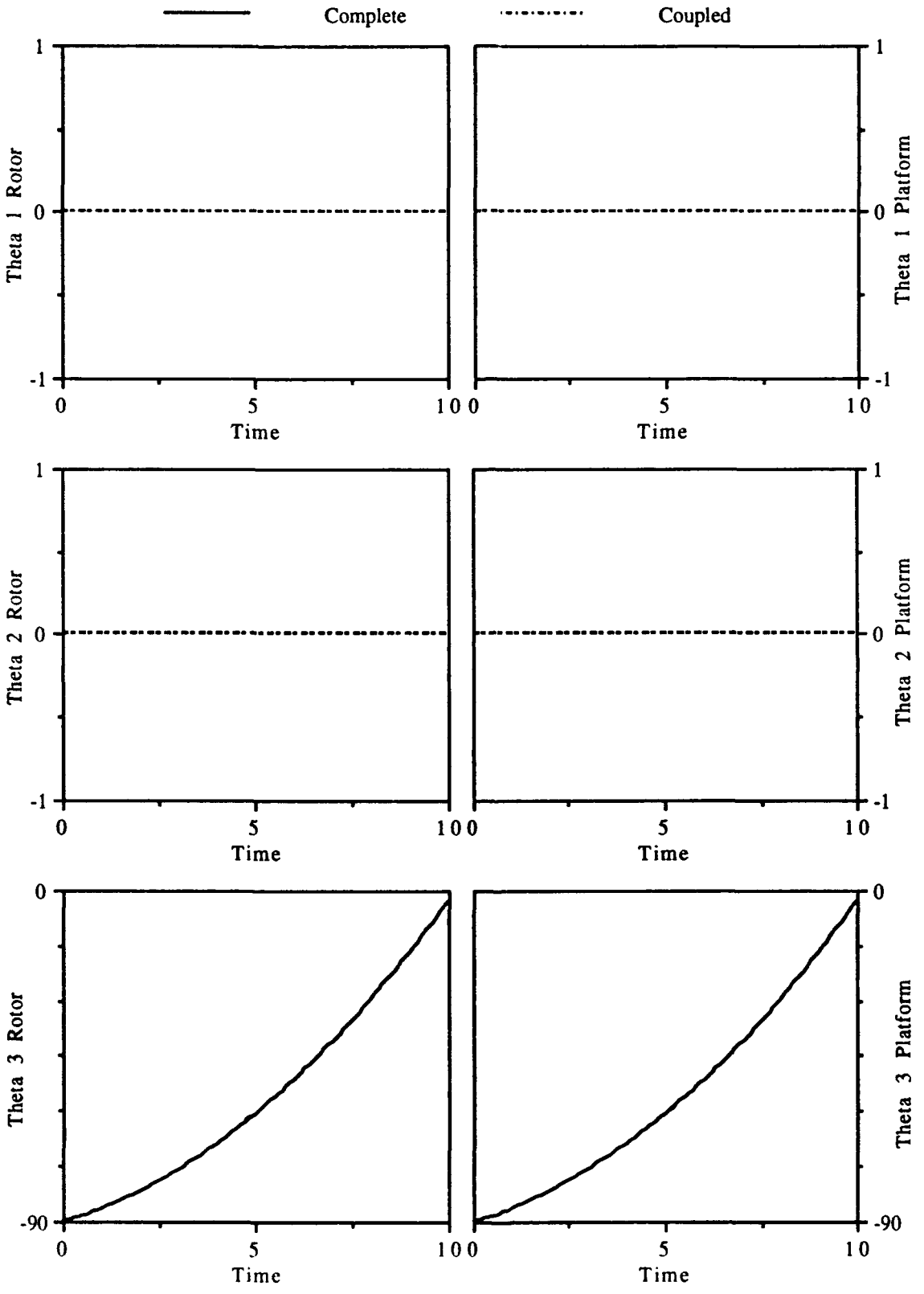

Figure A.2-1 Rotational Response for Case 2

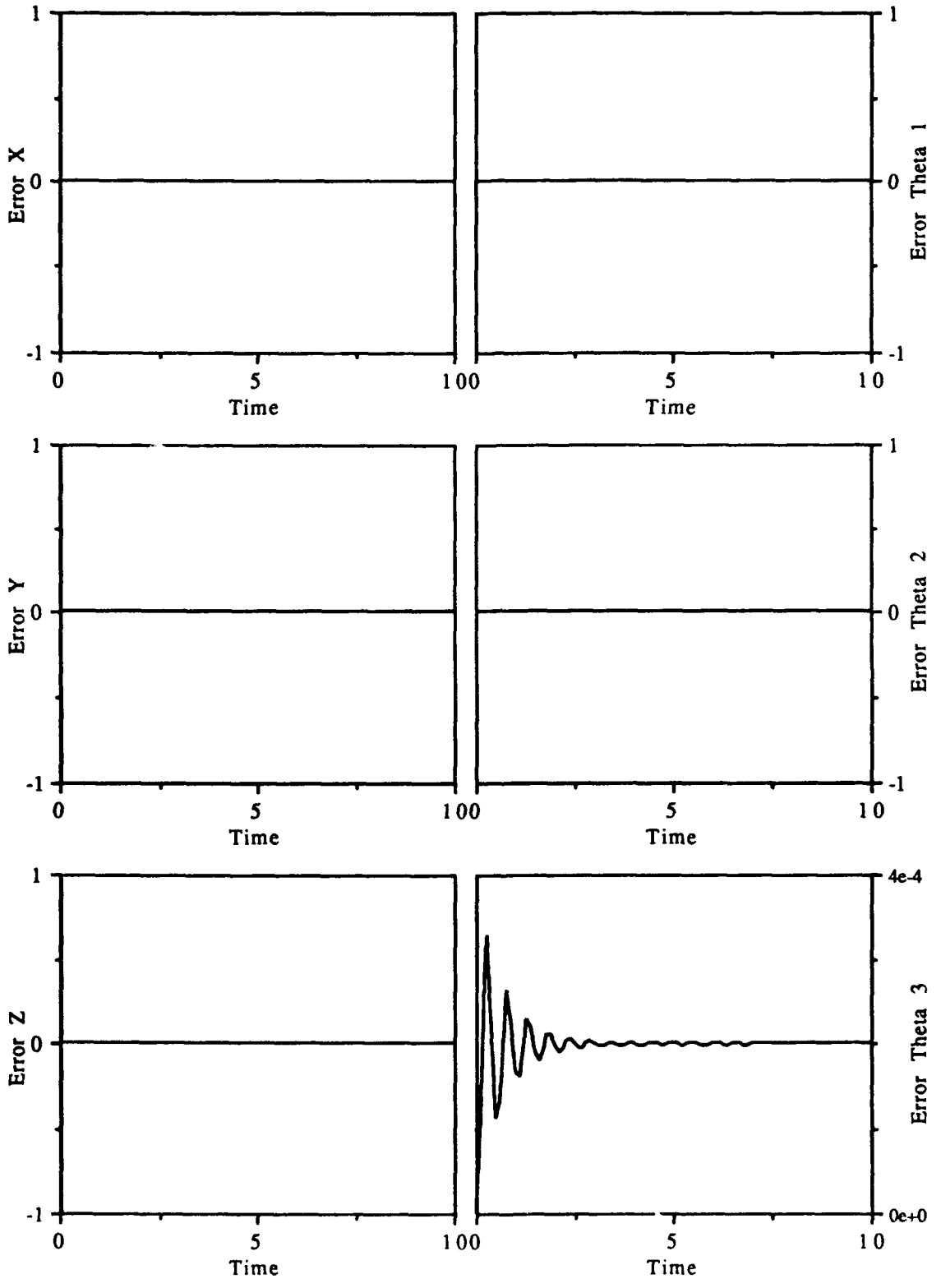

Figure A.2-2 Constraint Error Response for Case 2

A.3 Third Case - Tri-Axis Forcing

A constant forcing of 1 N is applied to all three axes. There is an initial spin rate of 0.5 rpm about the z axis. Due to symmetry there is no coupling into the rotational DOFs and only the constant z axis rotation results. Responses included are rotor and platform translational displacements and velocities as well as the constraint error responses. Rotational responses are not included.

A ten second run and a four minute run are included. The ten second run displays the initial damping of the constraint error. The longer run shows two cycles of a longer period error induced from the constant rotation about the z axis.

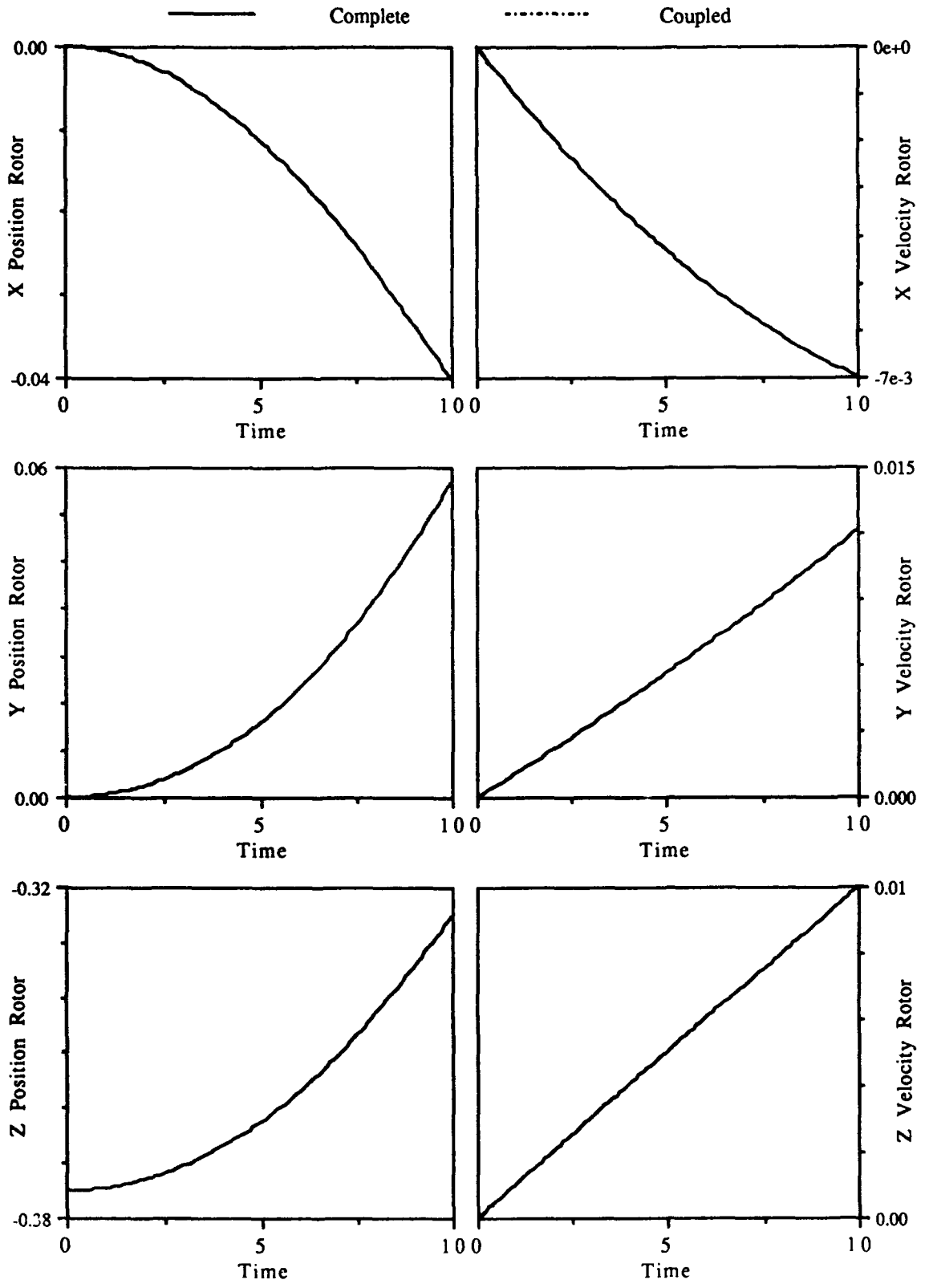

Figure A.3-1 Translational Rotor Response, Short Run, Case 3

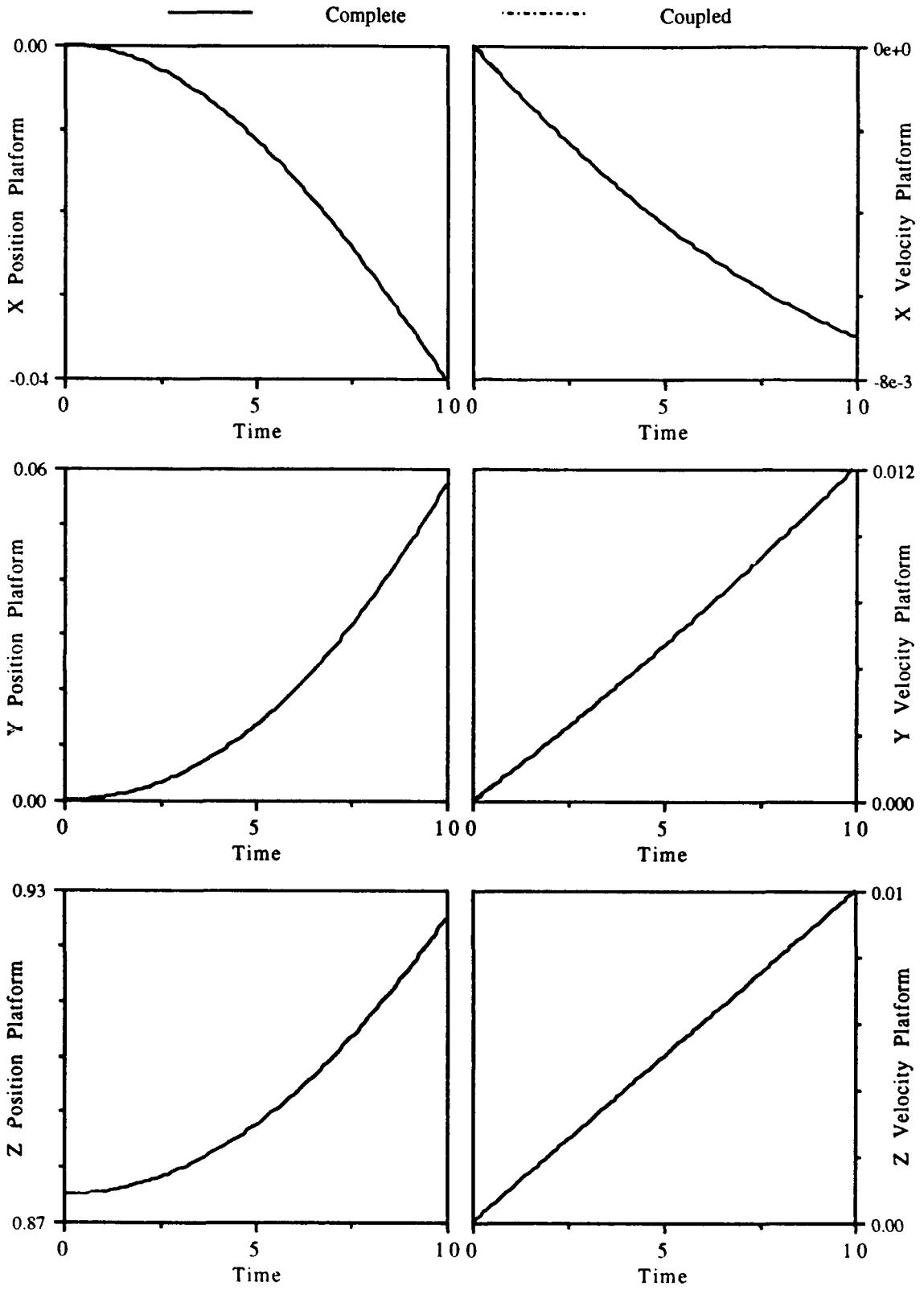

Figure A.3-2 Translational Platform Response, Short Run, Case 3

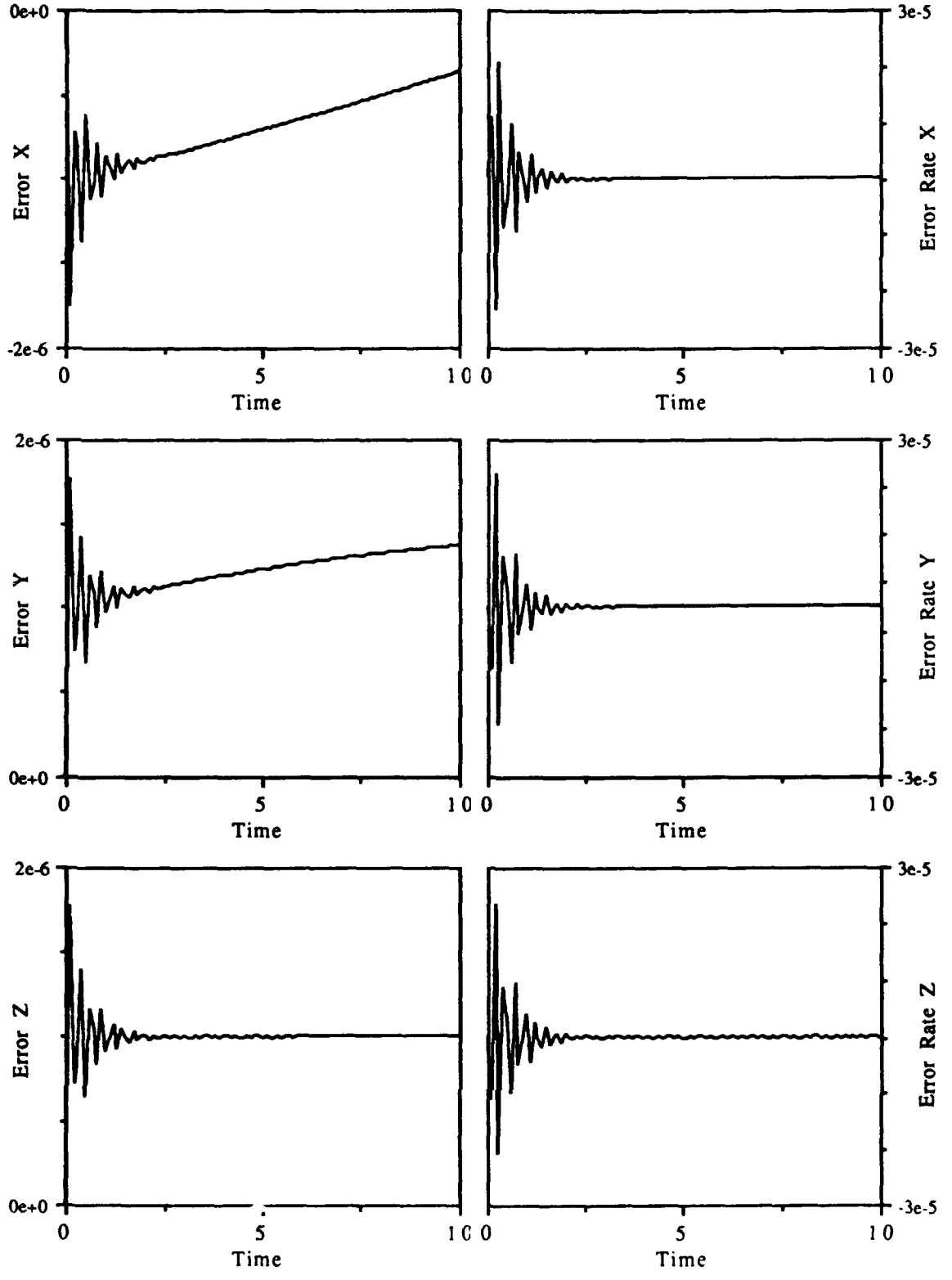

Figure A.3-3 Translational Error Response, Short Run, Case 3

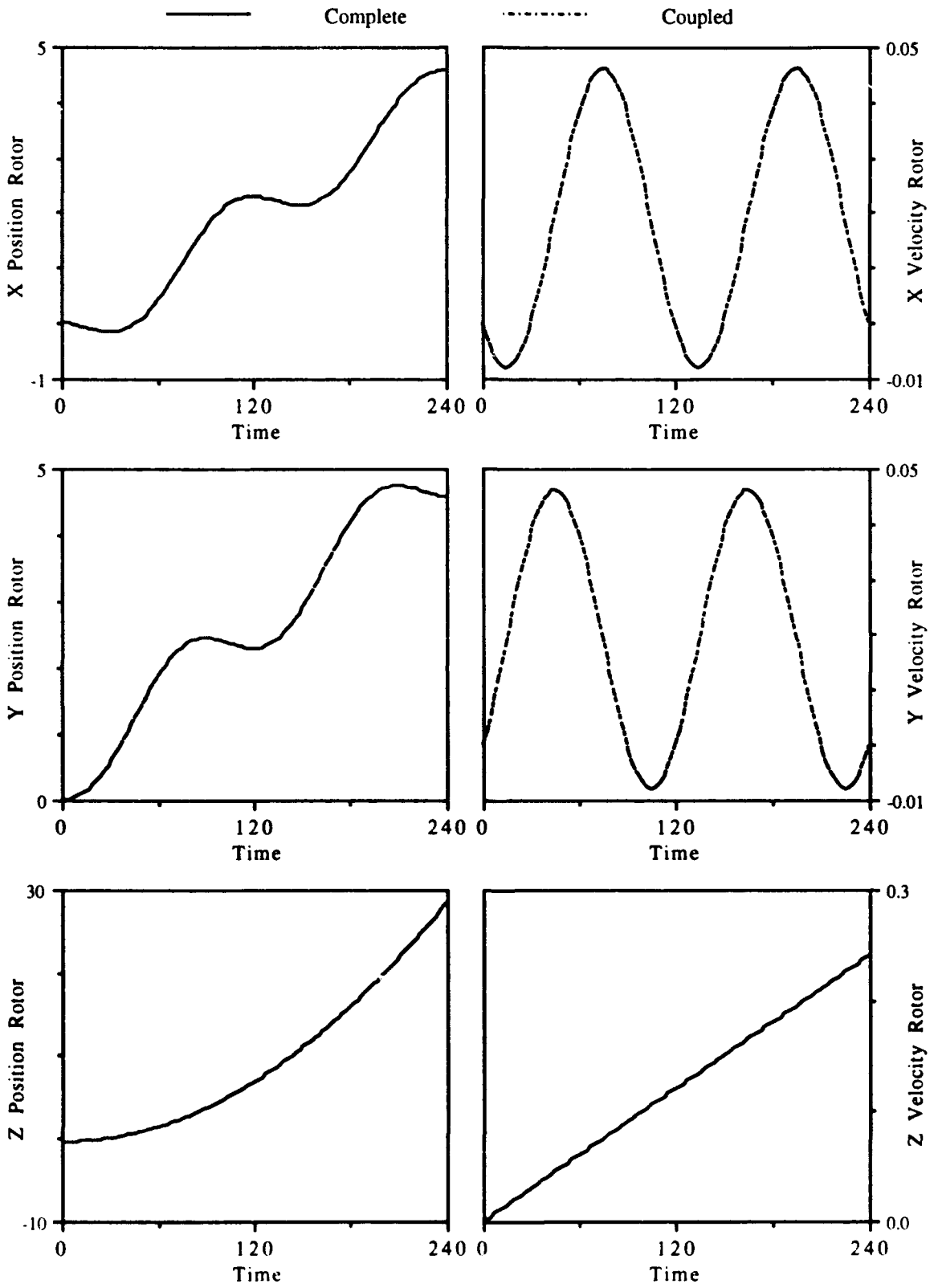

Figure A.3-4 Translational Rotor Response, Long Run, Case 3

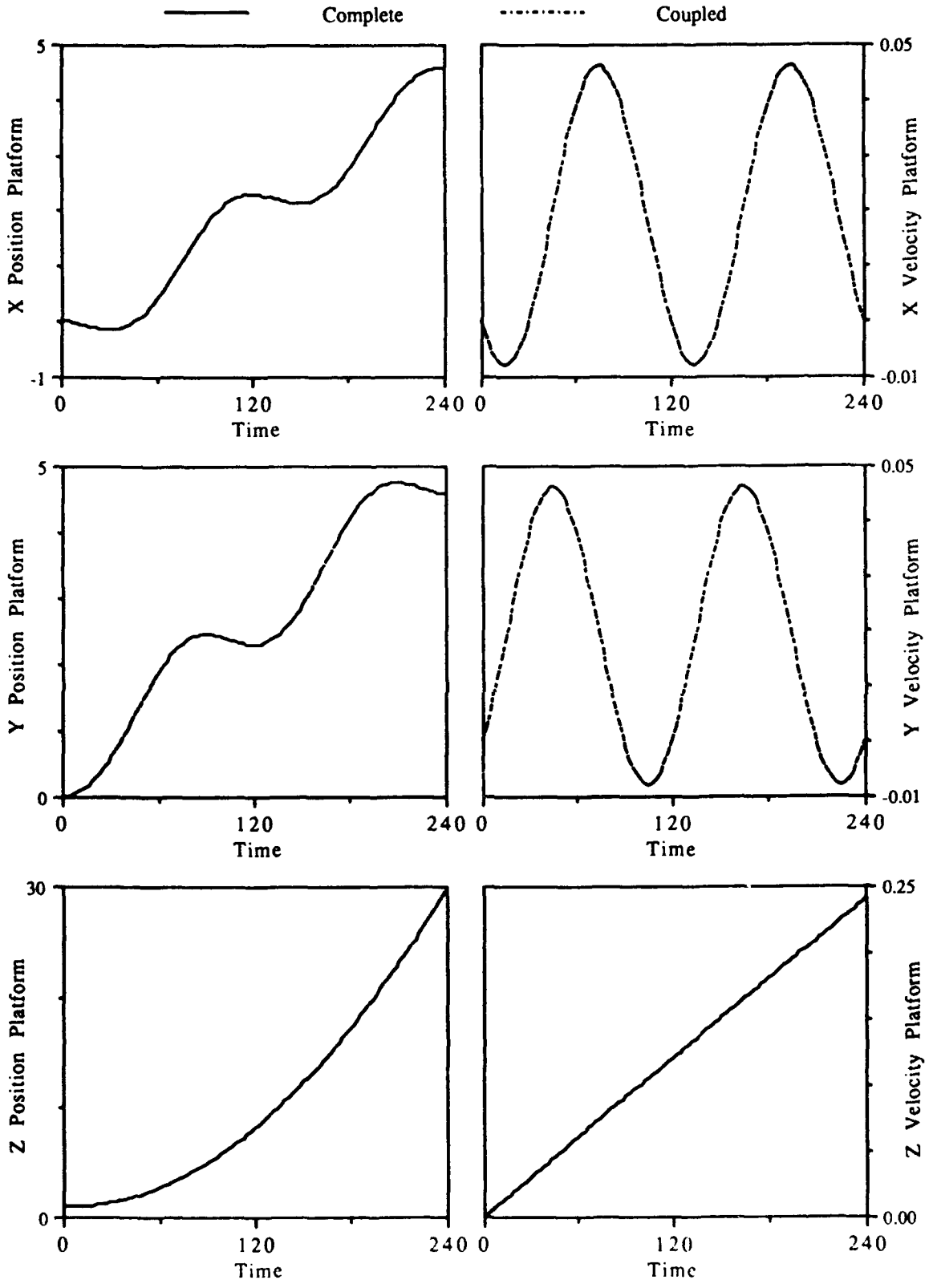

Figure A.3-5 Translational Platform Response, Long Run, Case 3

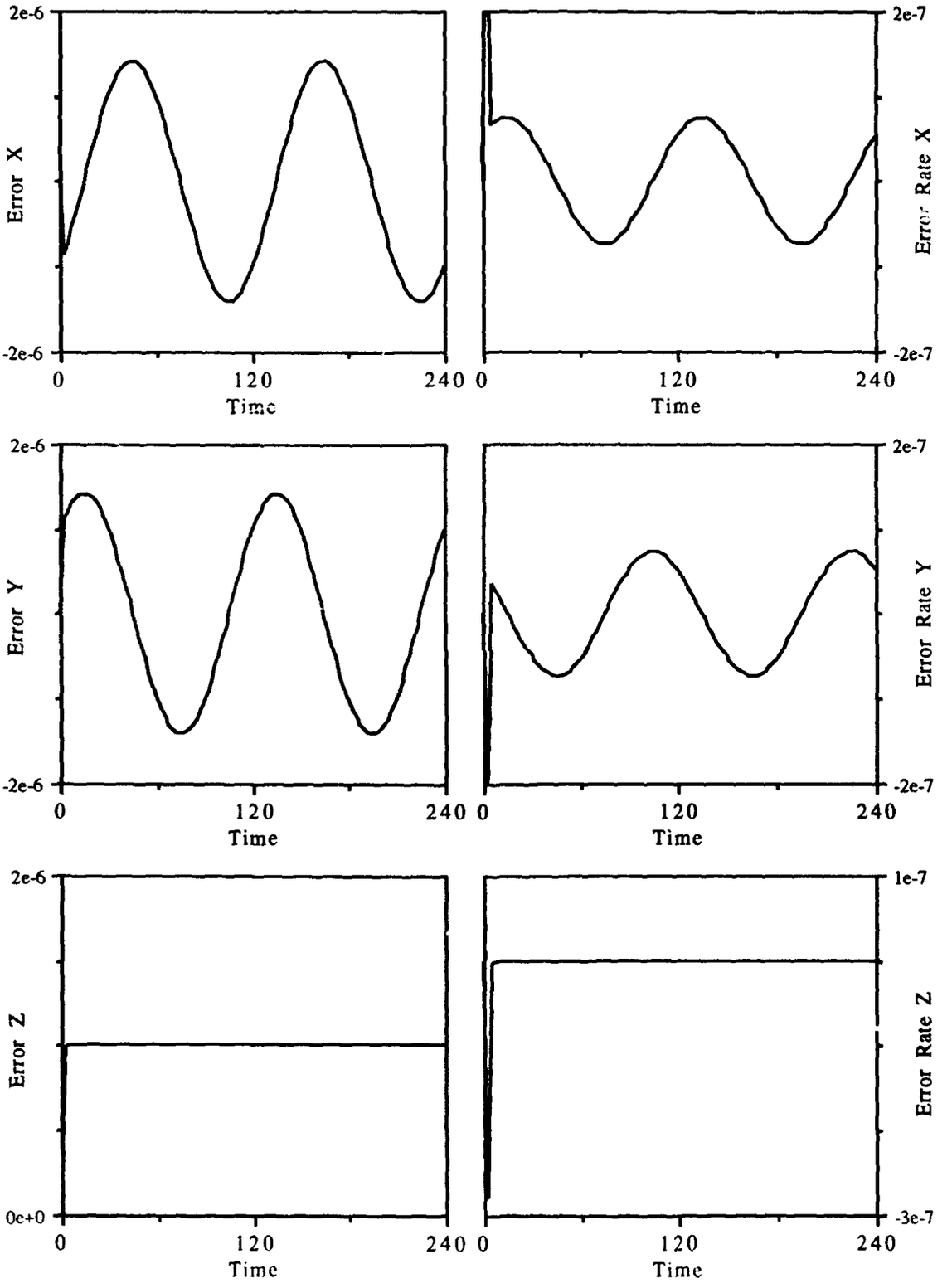

Figure A.3-6 Translational Error Response, Long Run, Case 3

A.4 Fourth Case - Non-Spin Axis Torque

A 0.1 second torque of 1 N-m is applied about a non-spin axis. There is an initial spin rate of 0.5 rpm about the z axis. For the first time there is significant coupling between the translational and rotational DOFs. Responses included are rotor and platform translational displacements and velocities as well as the rotational displacements and velocities. Constraint error responses are also included.

A ten second run and a sixty second run are included. The ten second run displays the initial damping of the constraint error. The longer run shows a longer period error induced from the rotations and the effects of cross-coupling. The error responses take on a slightly different form than seen previously due to the fact that the forcing is cycled so quickly.

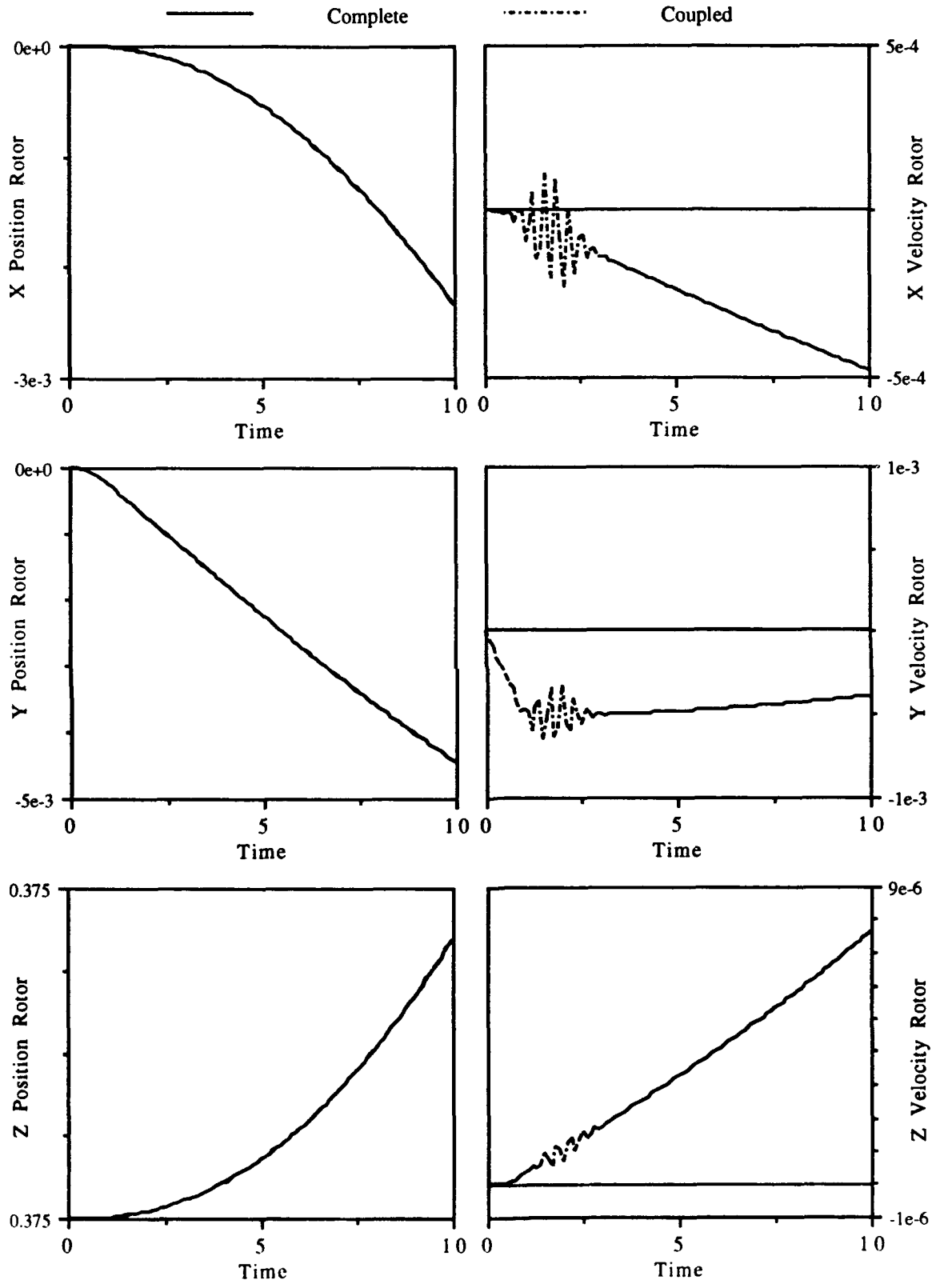

Figure A.4-1 Translational Rotor Response, Short Run, Case 4

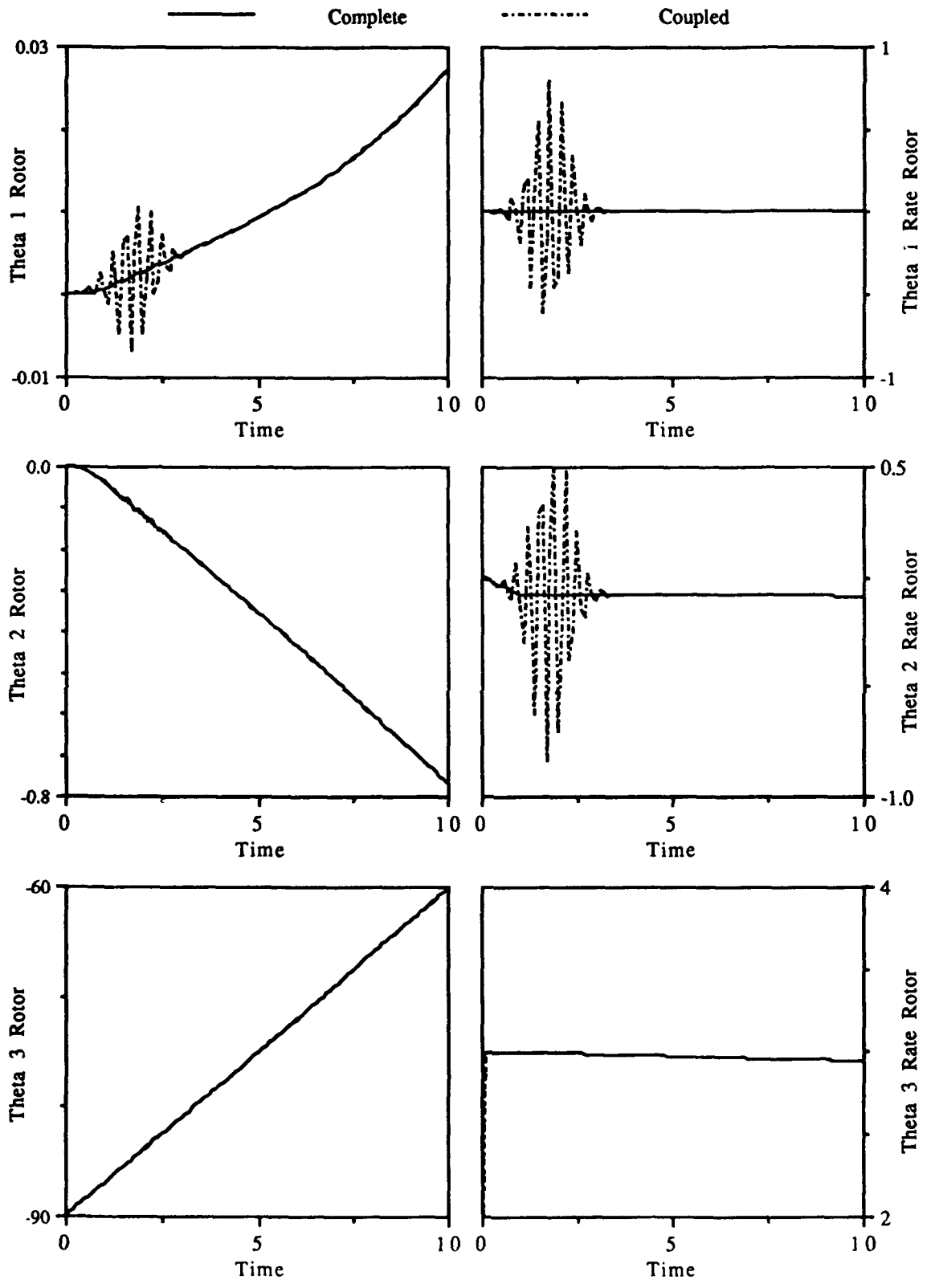

Figure A.4-2 Rotational Rotor Response, Short Run, Case 4

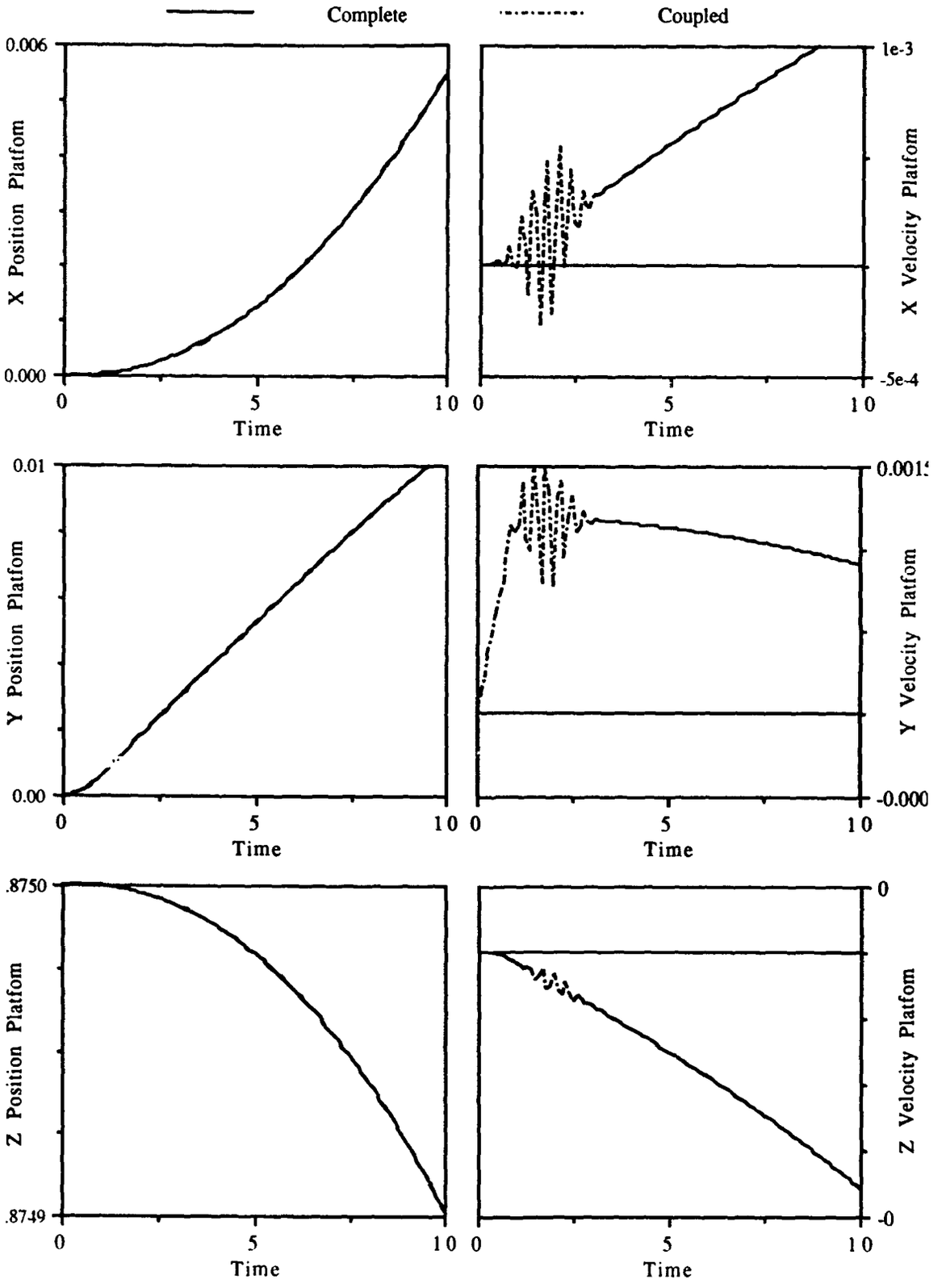

Figure A.4-3 Translational Platform Response, Short Run, Case 4

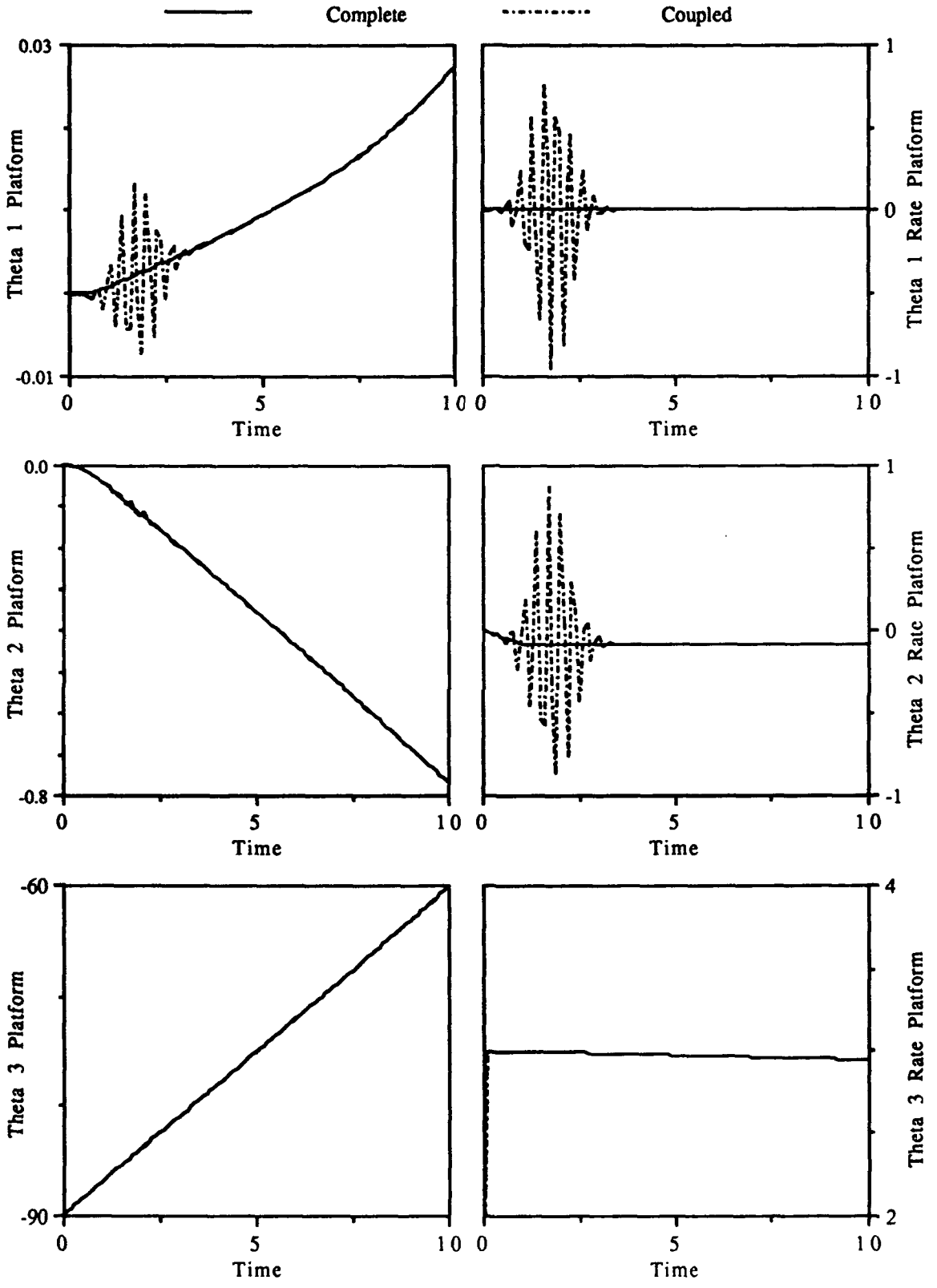

Figure A.4-4 Rotational Platform Response, Short Run, Case 4

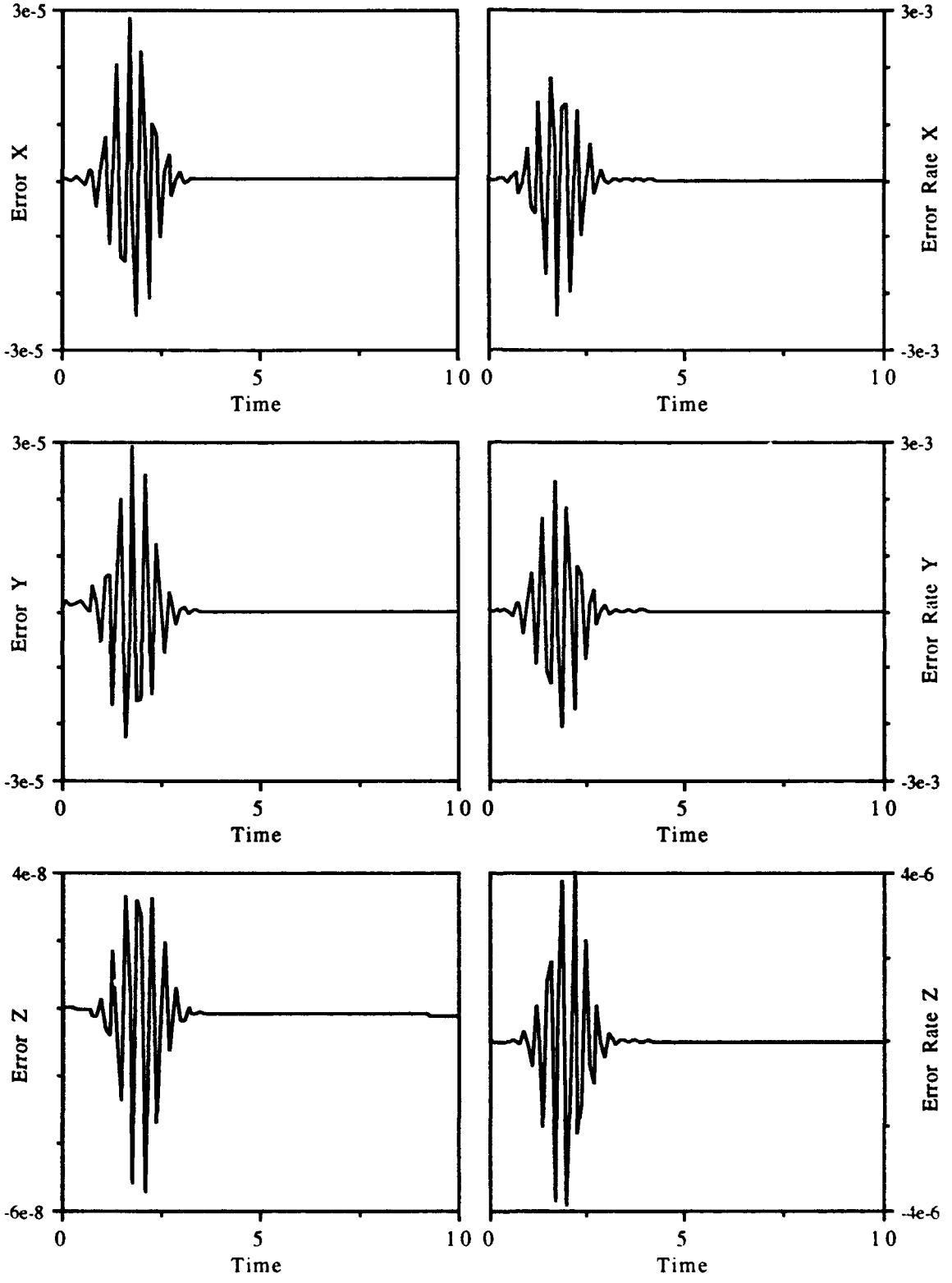

Figure A.4-5 Translational Error Response, Short Run, Case 4

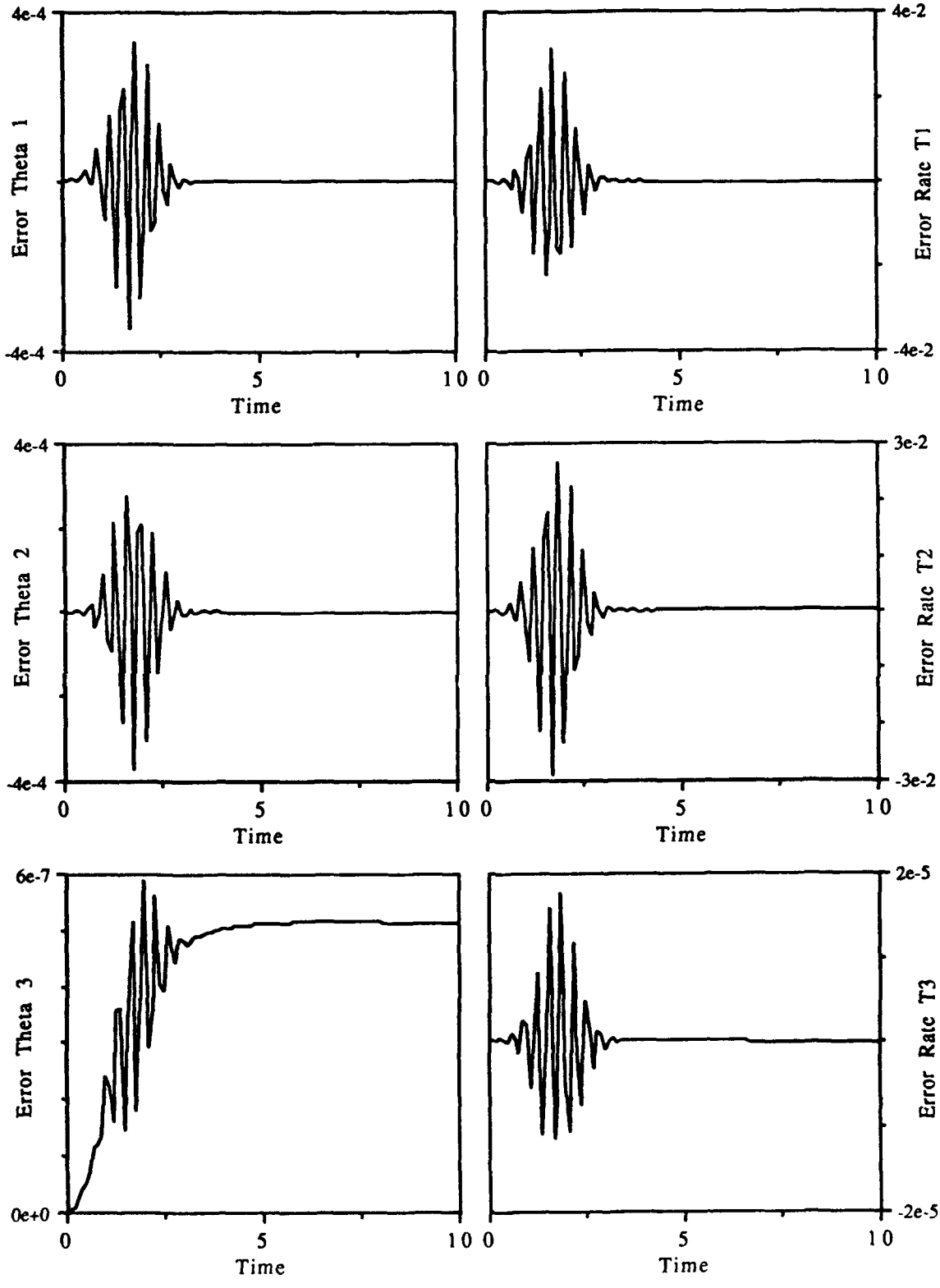

Figure A.4-6 Rotational Error Response, Short Run, Case 4

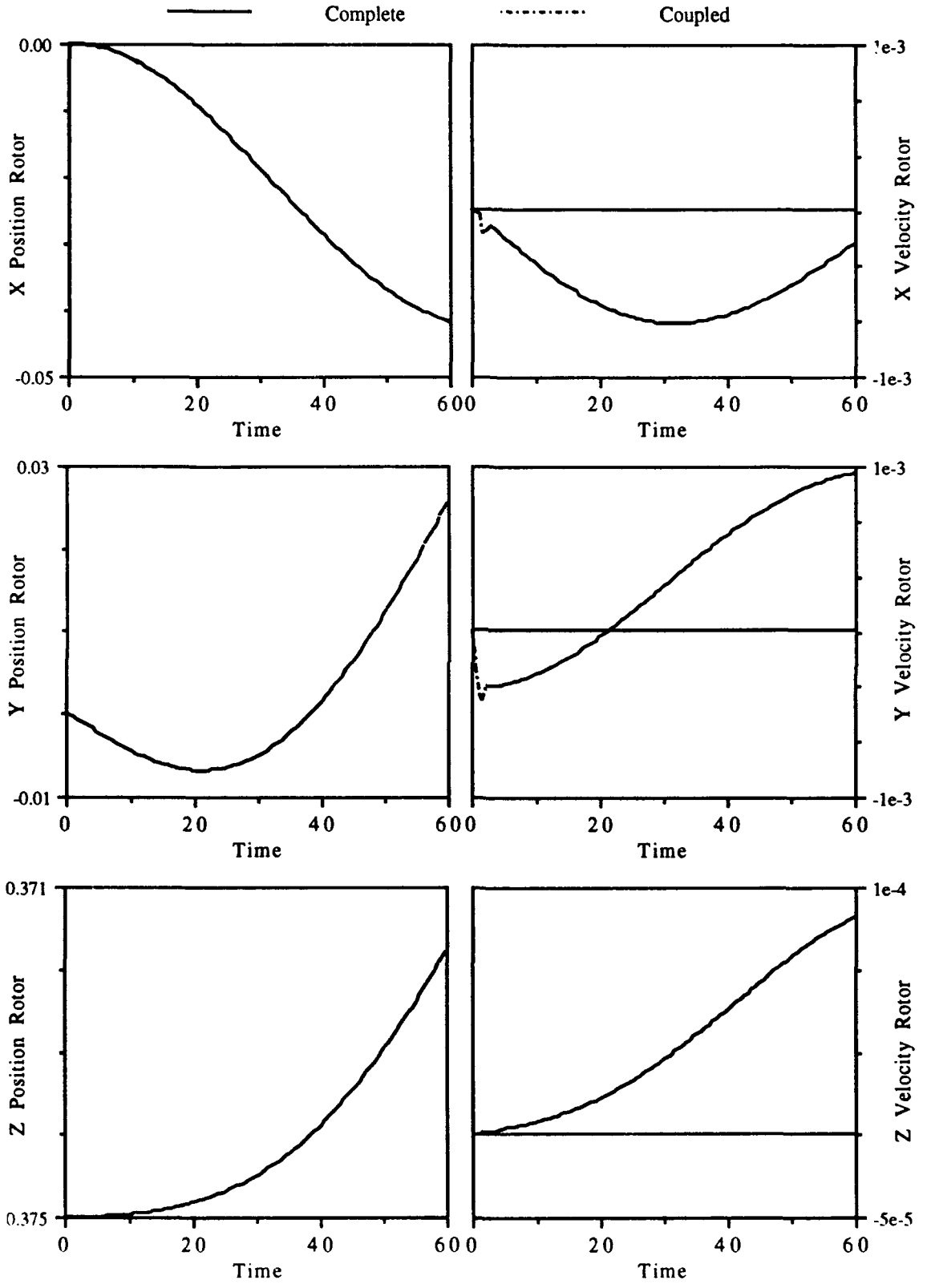

Figure A.4-7 Translational Rotor Response, Long Run, Case 4

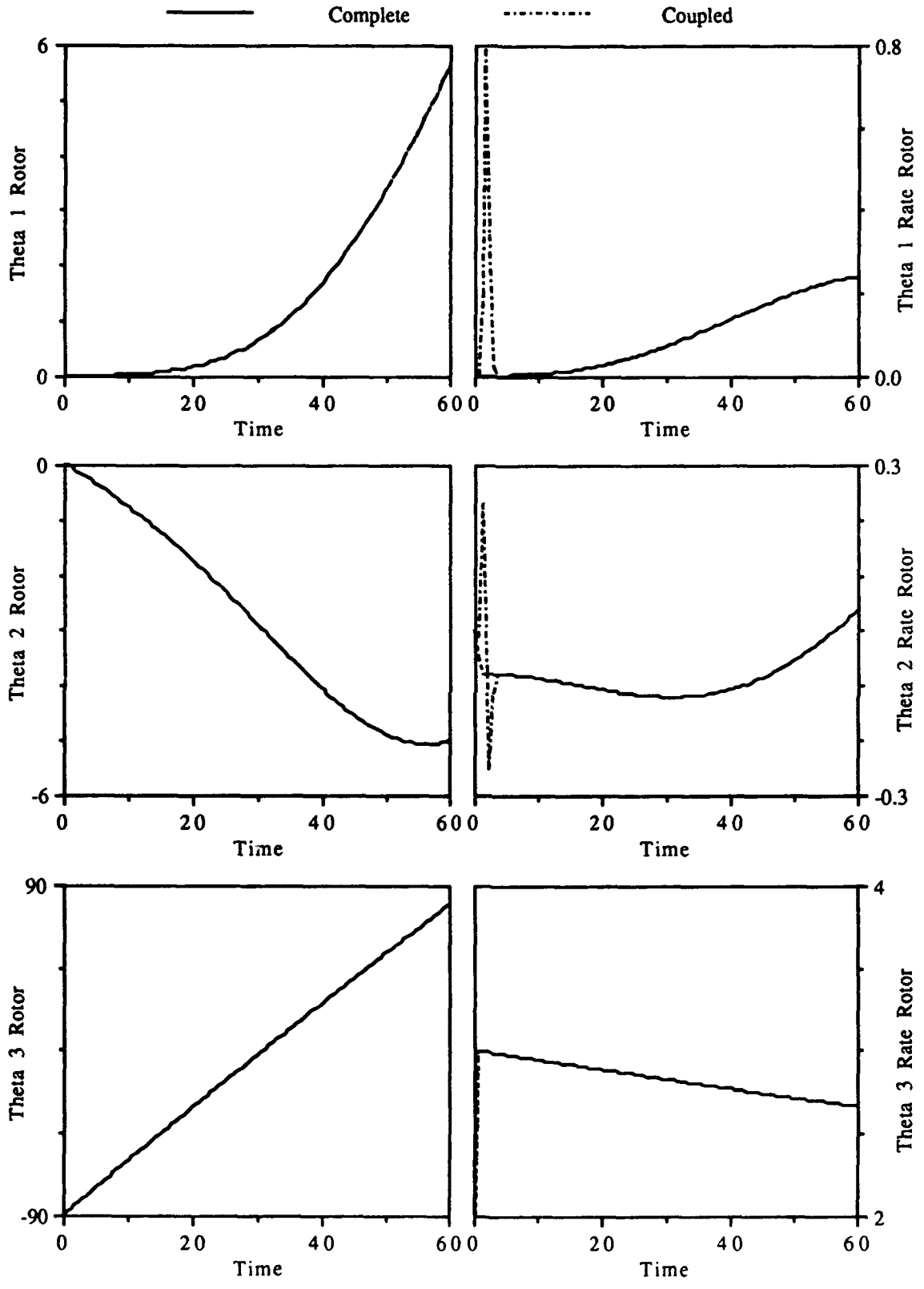

Figure A.4-8 Rotational Rotor Response, Long Run, Case 4

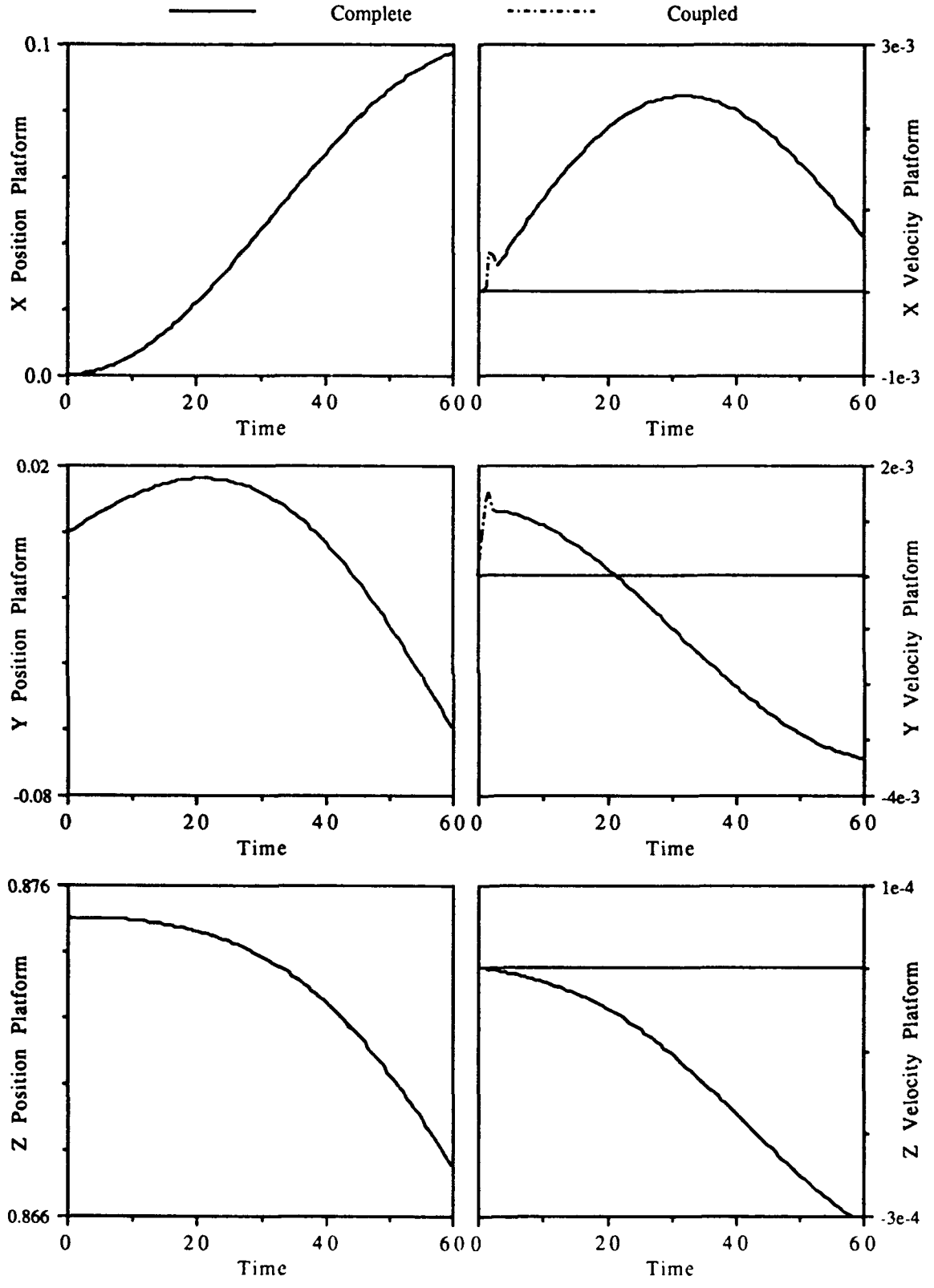

Figure A.4-9 Translational Platform Response, Long Run, Case 4

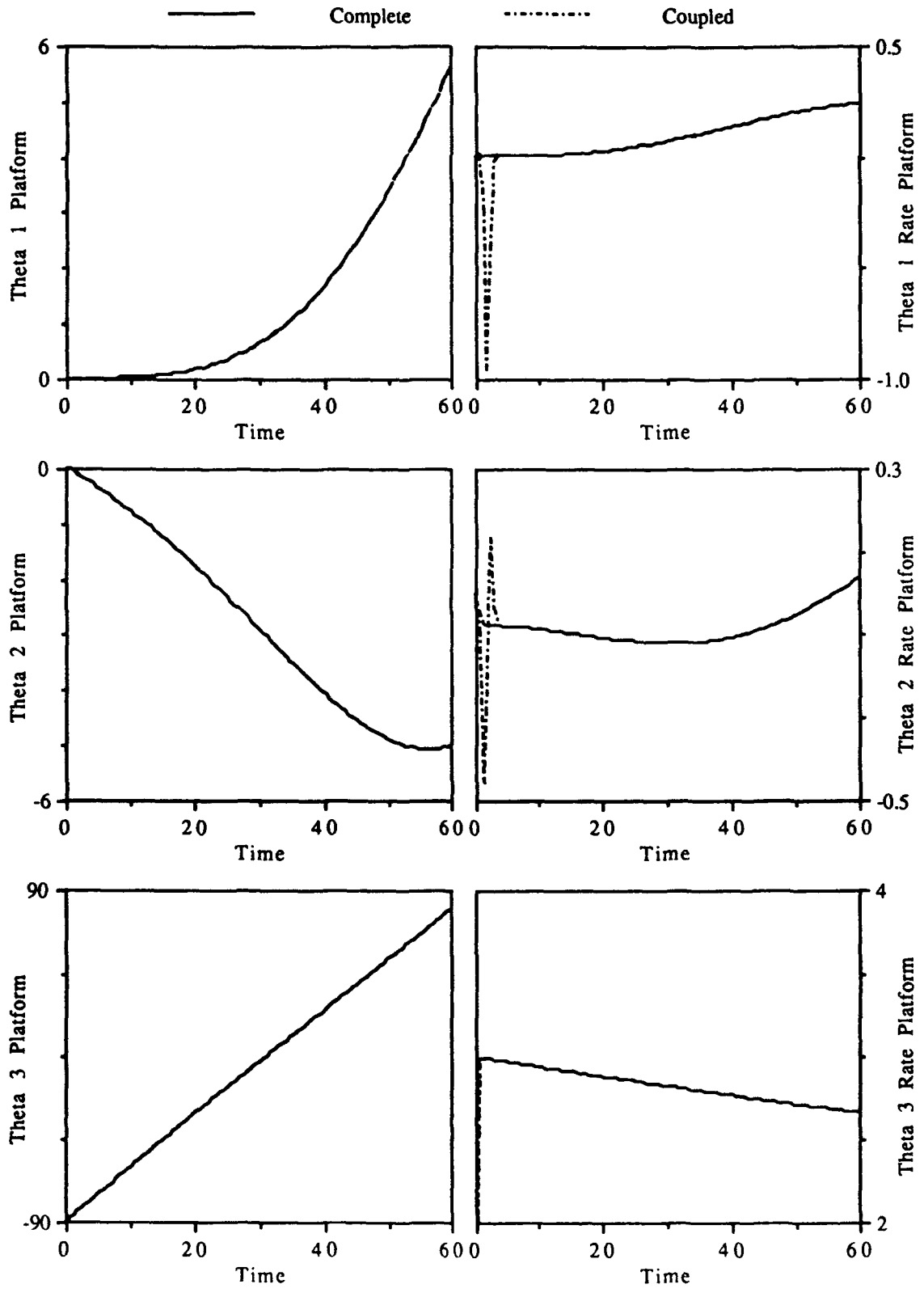

Figure A.4-10 Rotational Platform Response, Long Run, Case 4

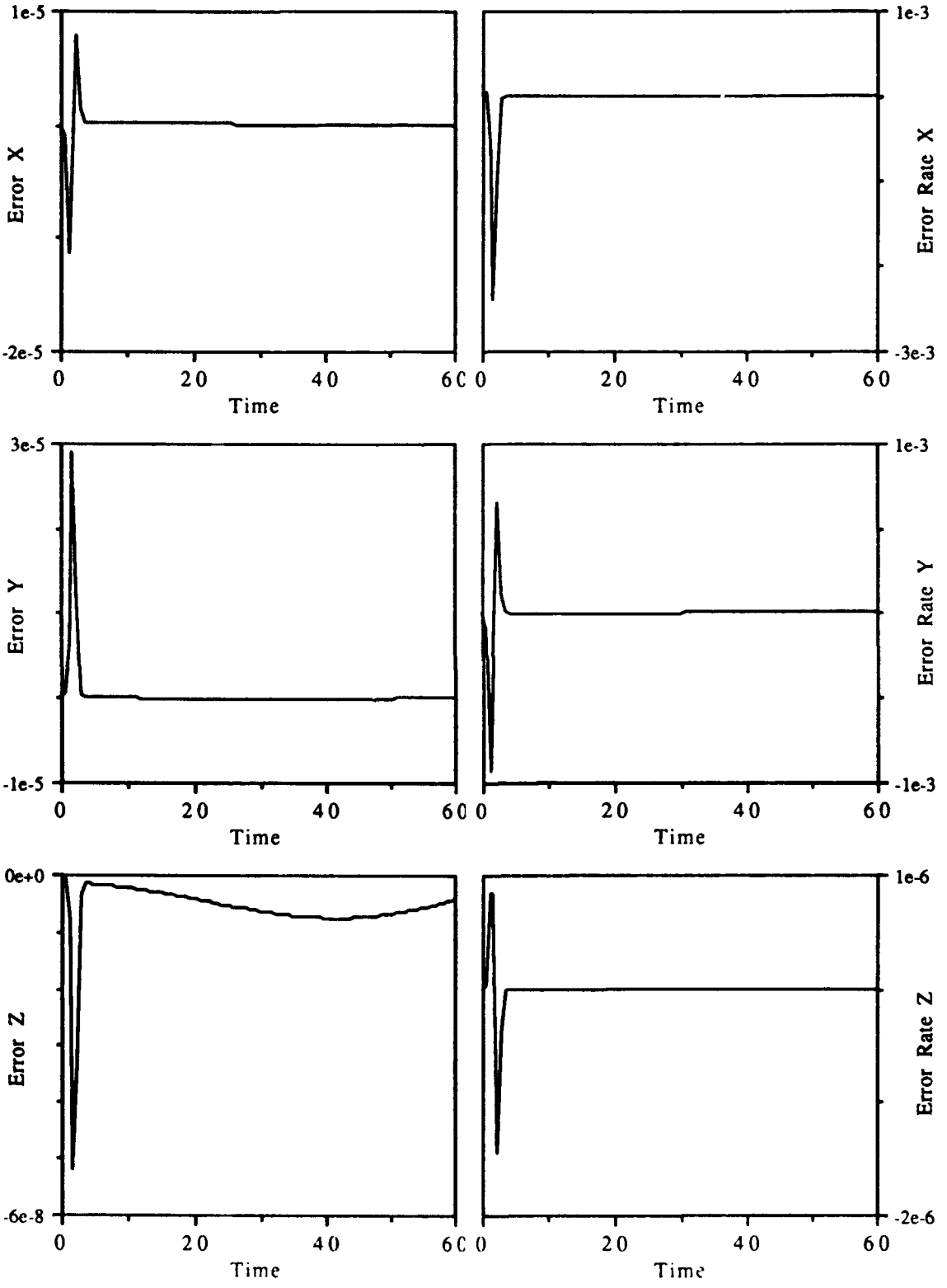

Figure A.4-11 Translational Error Response, Long Run, Case 4

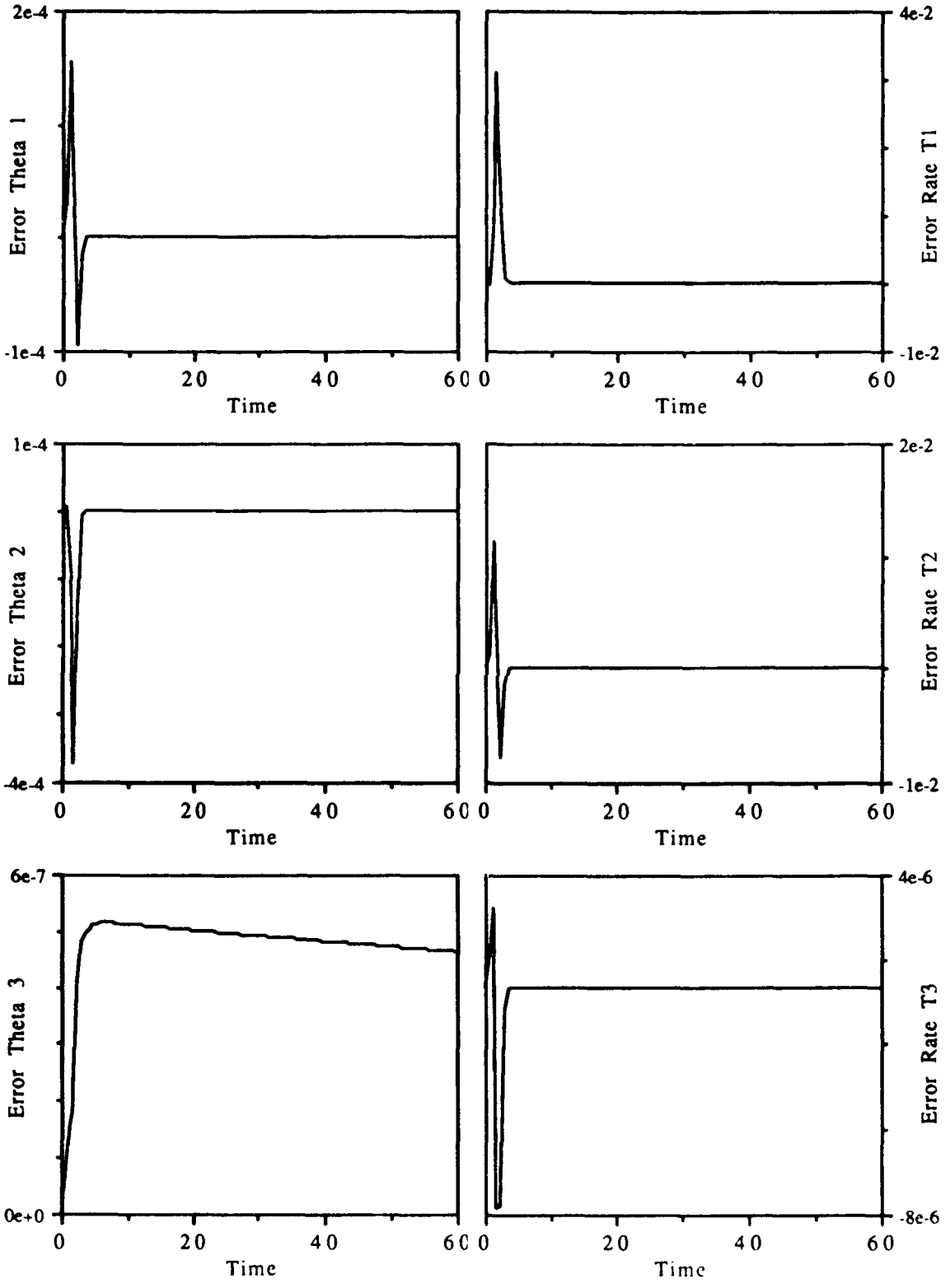

Figure A.4-12 Rotational Error Response, Long Run, Case 4

Appendix B

Space Station Plots

As mentioned in Section 7.2 this Appendix contains the plots for the Space Station example. The Appendix is split into two sections, one for the rigid body model and one for the flexible model. The individual cases are described in each section. In all plots the dotted line represents the 'truth' model response. The truth model is actually the repsonse taken using a three body mulitibody solution.

B.1 Rigid Model Plots

This section includes four separate cases, a non-articulated and an articulated case for each of the two forcing conditions. The two forcings are a 100 lb force in the direction of the z axis and a 2500 ft-lb torque about the x axis. In addition to the four case responses there are plots representing a typical error response for the rigid cases. The particular case these error plots were taken from is the non-articulated z forced case.

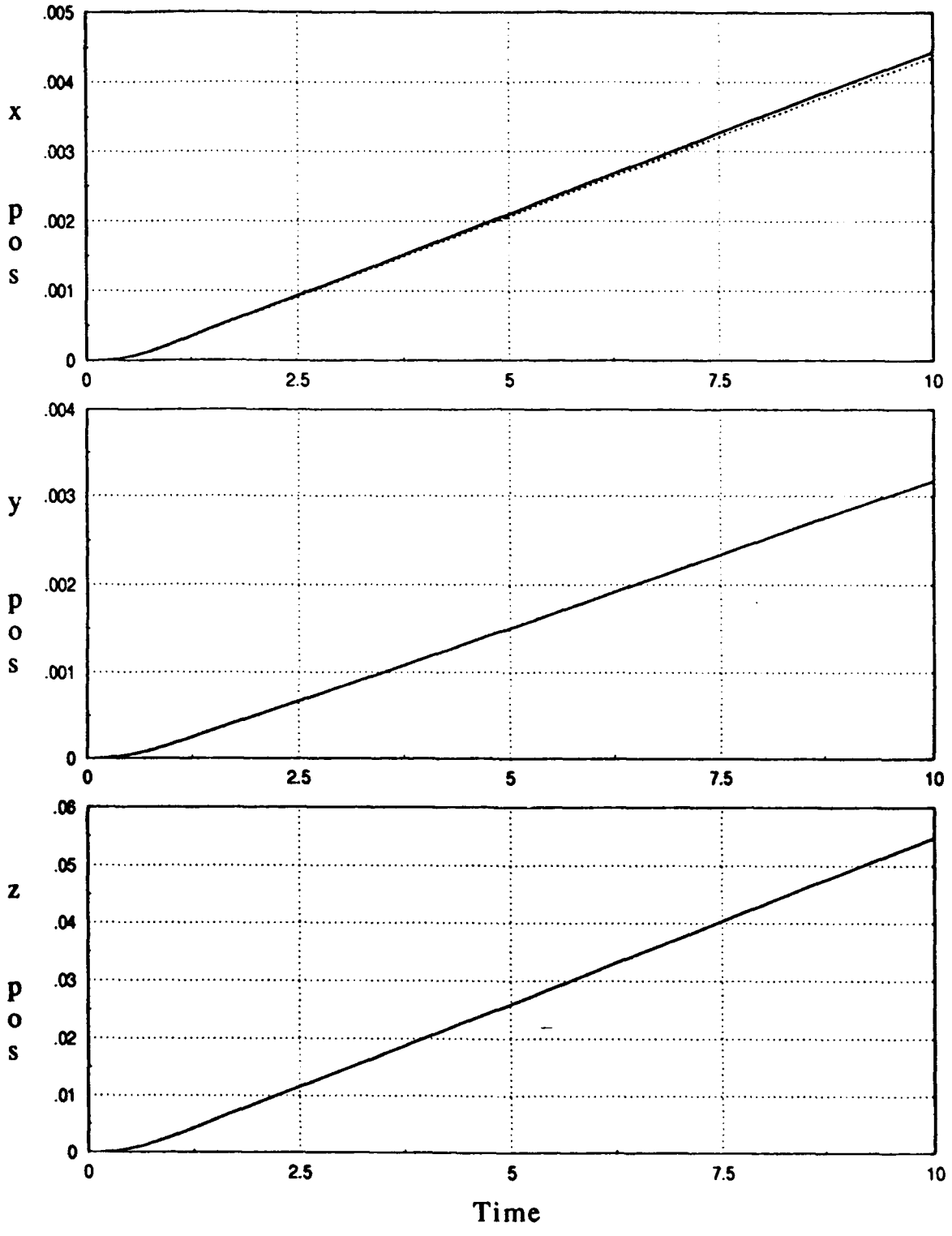

Figure B.1-1 Z Force Response for Rigid Nonarticulated Case

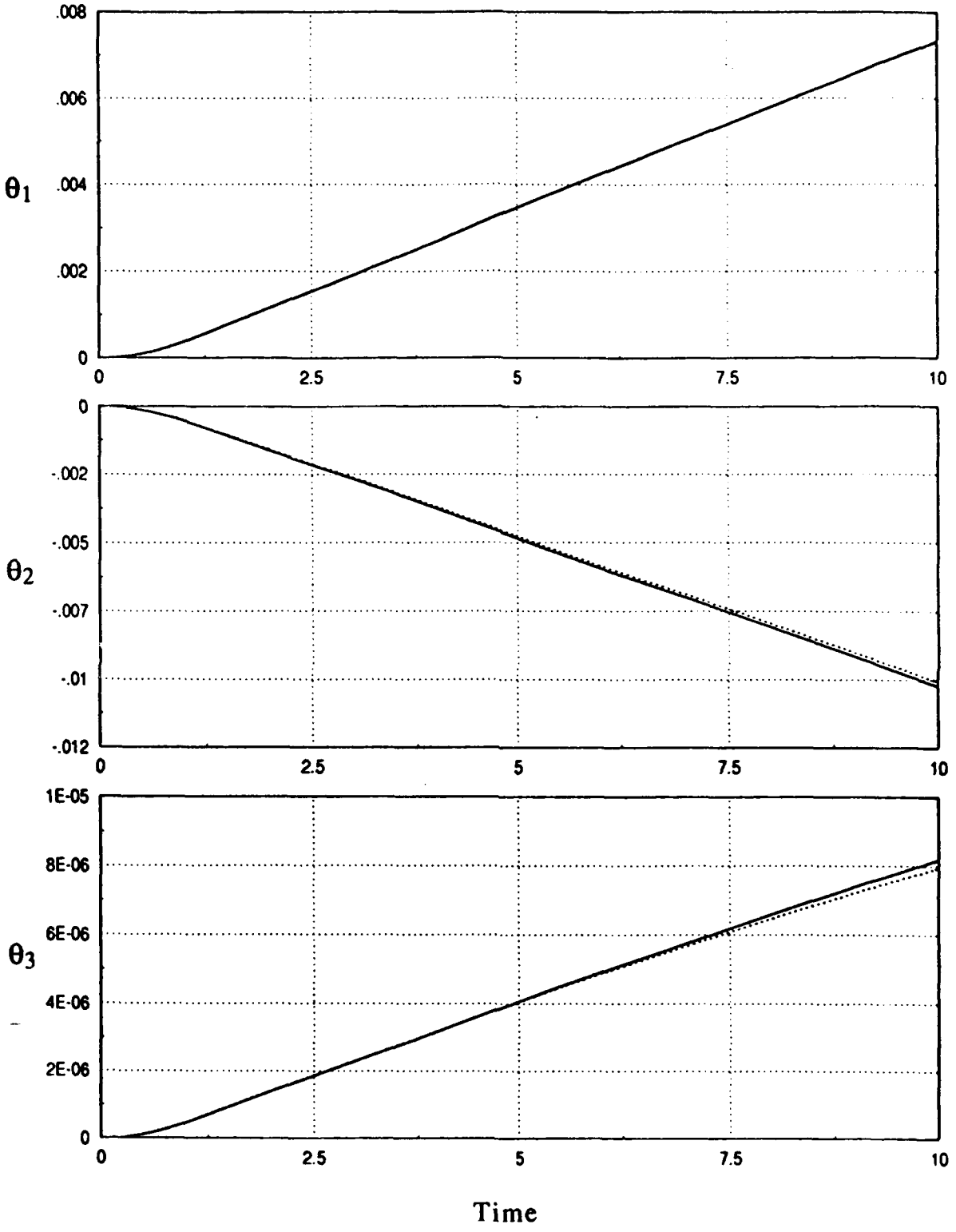

Figure B.1-2 Z Force Response for Rigid Nonarticulated Case

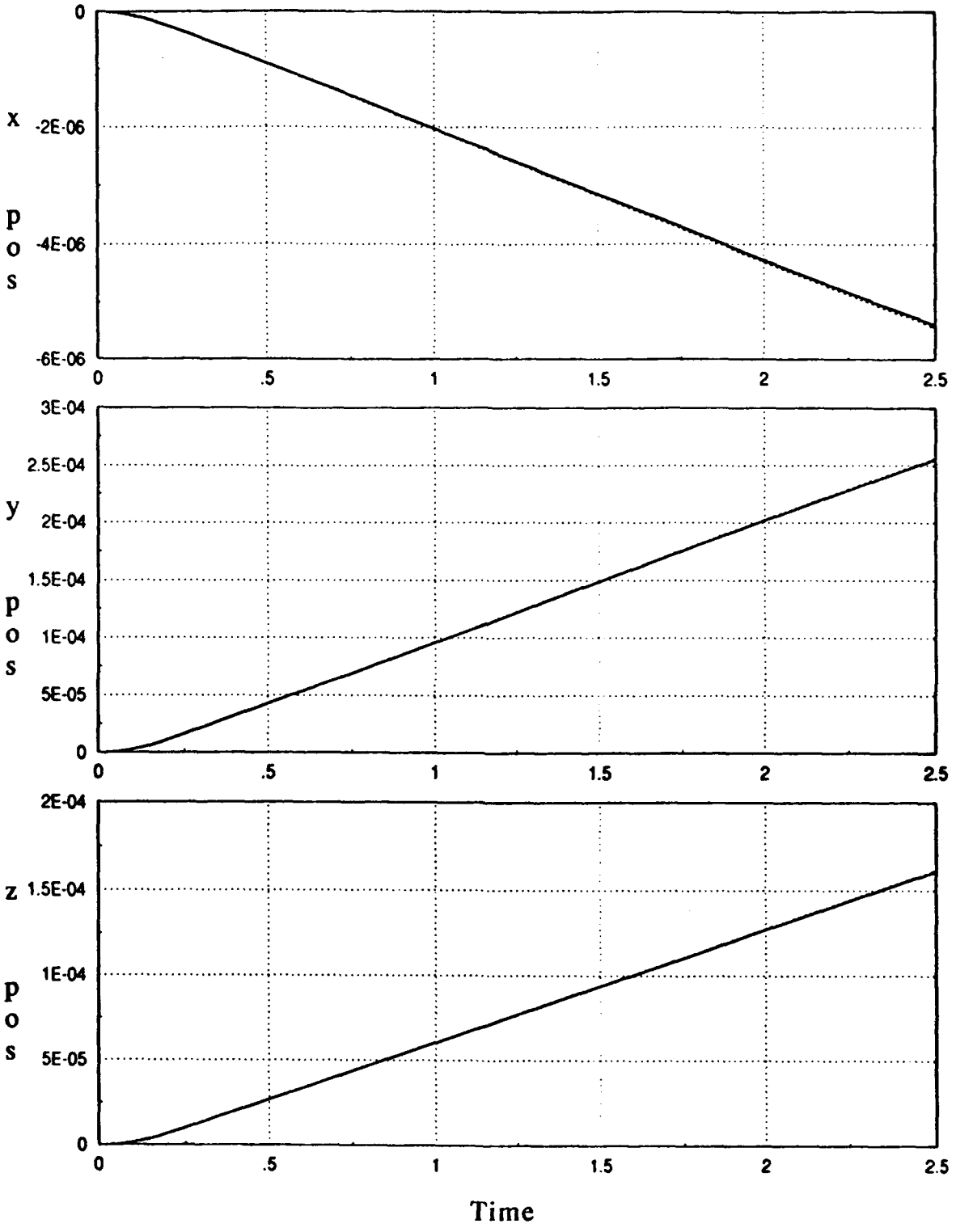

Figure B.1-3 X Torque Response for Rigid Nonarticulated Case

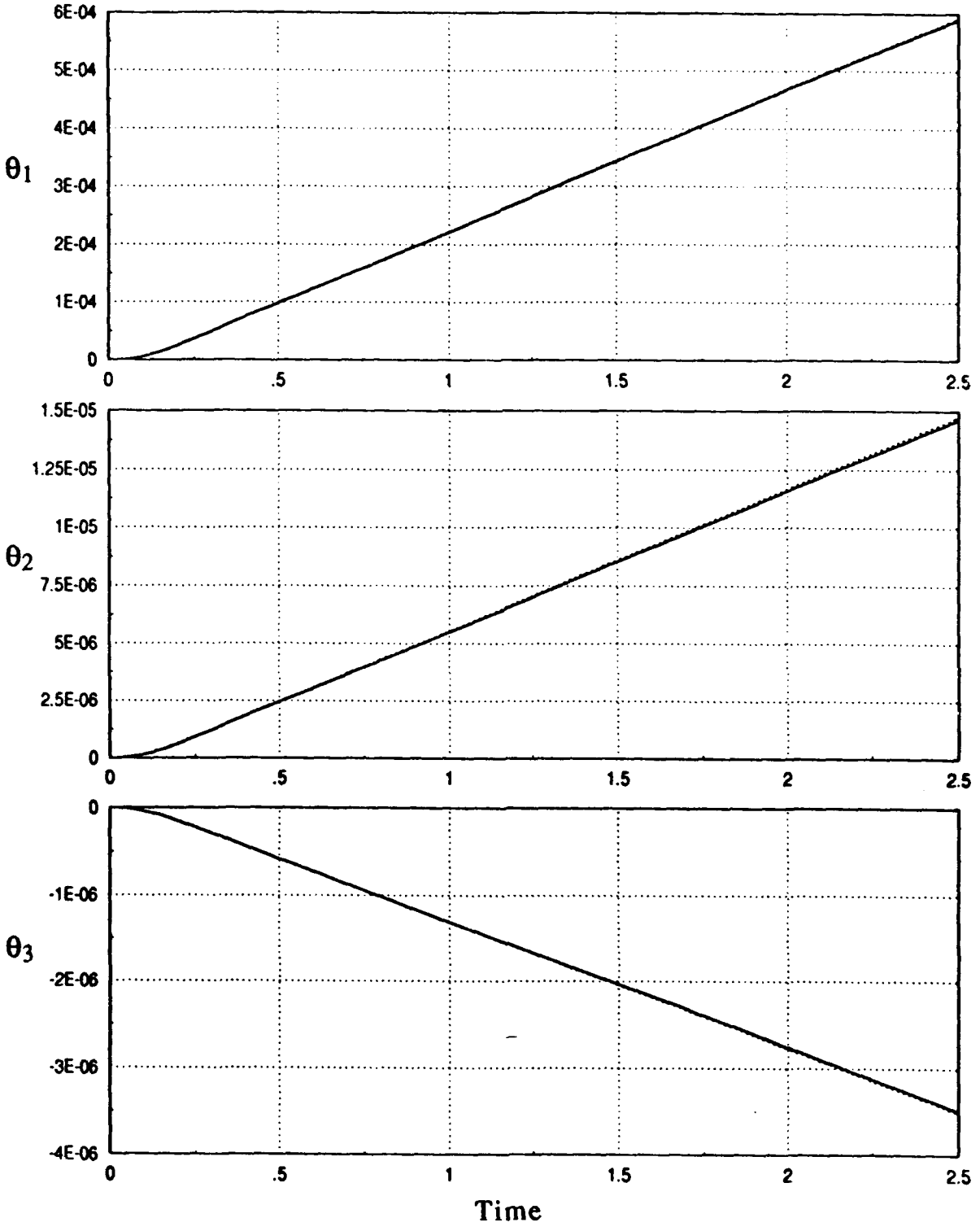

Figure B.1-4 X Torque Response for Rigid Nonarticulated Case

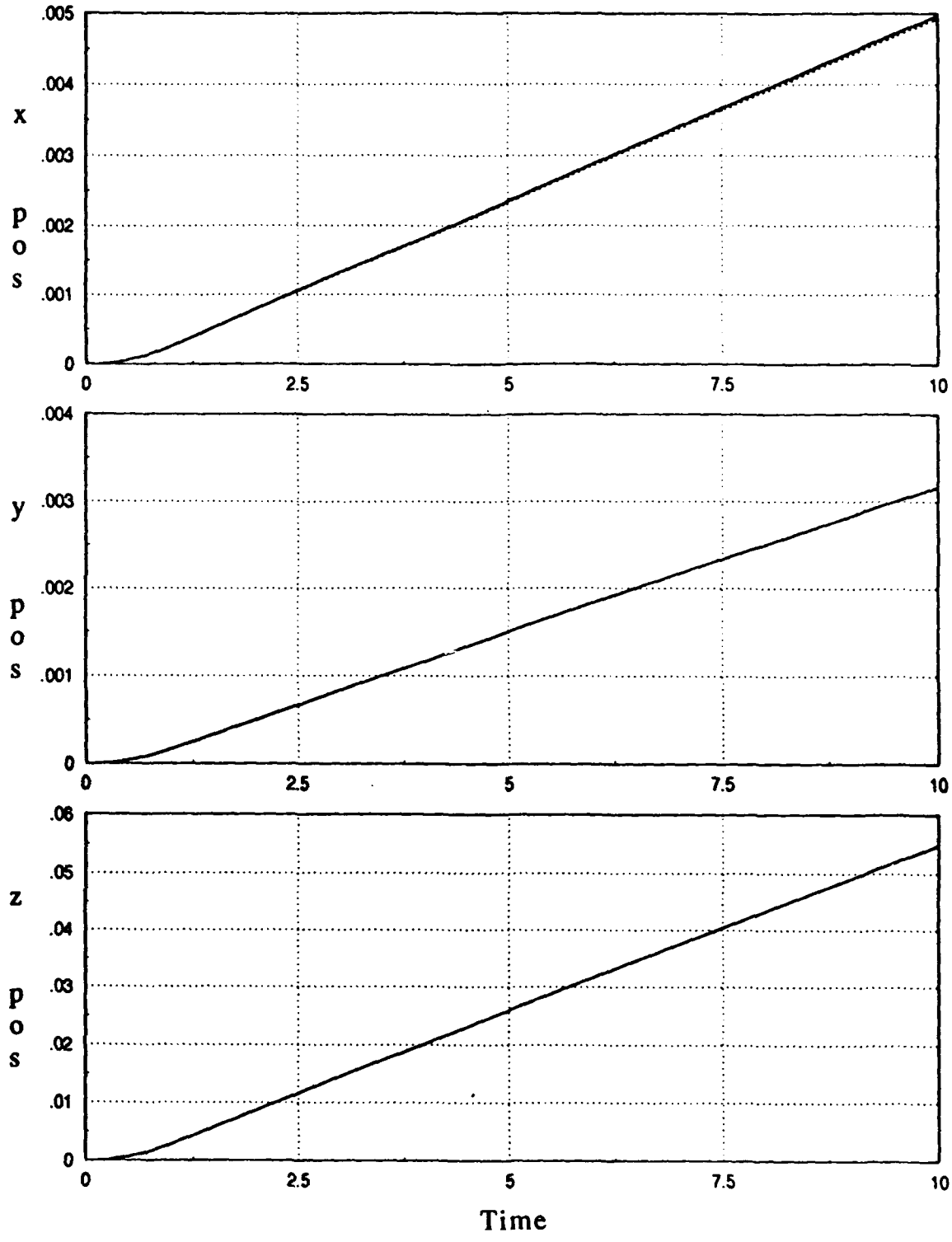

Figure B.1-5 Z Force Response for Rigid Articulated Case

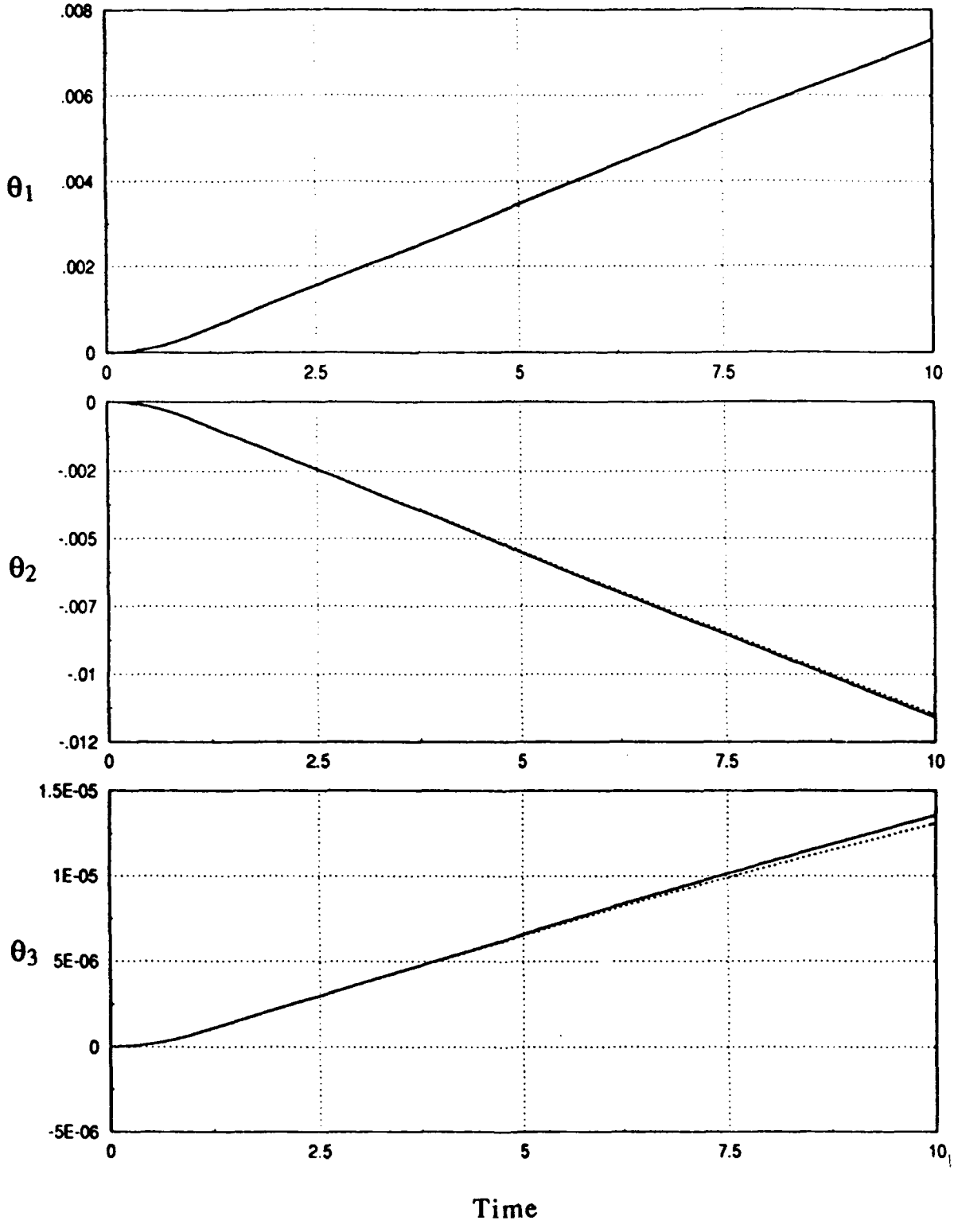

Figure B.1-6 Z Force Response for Rigid Articulated Case

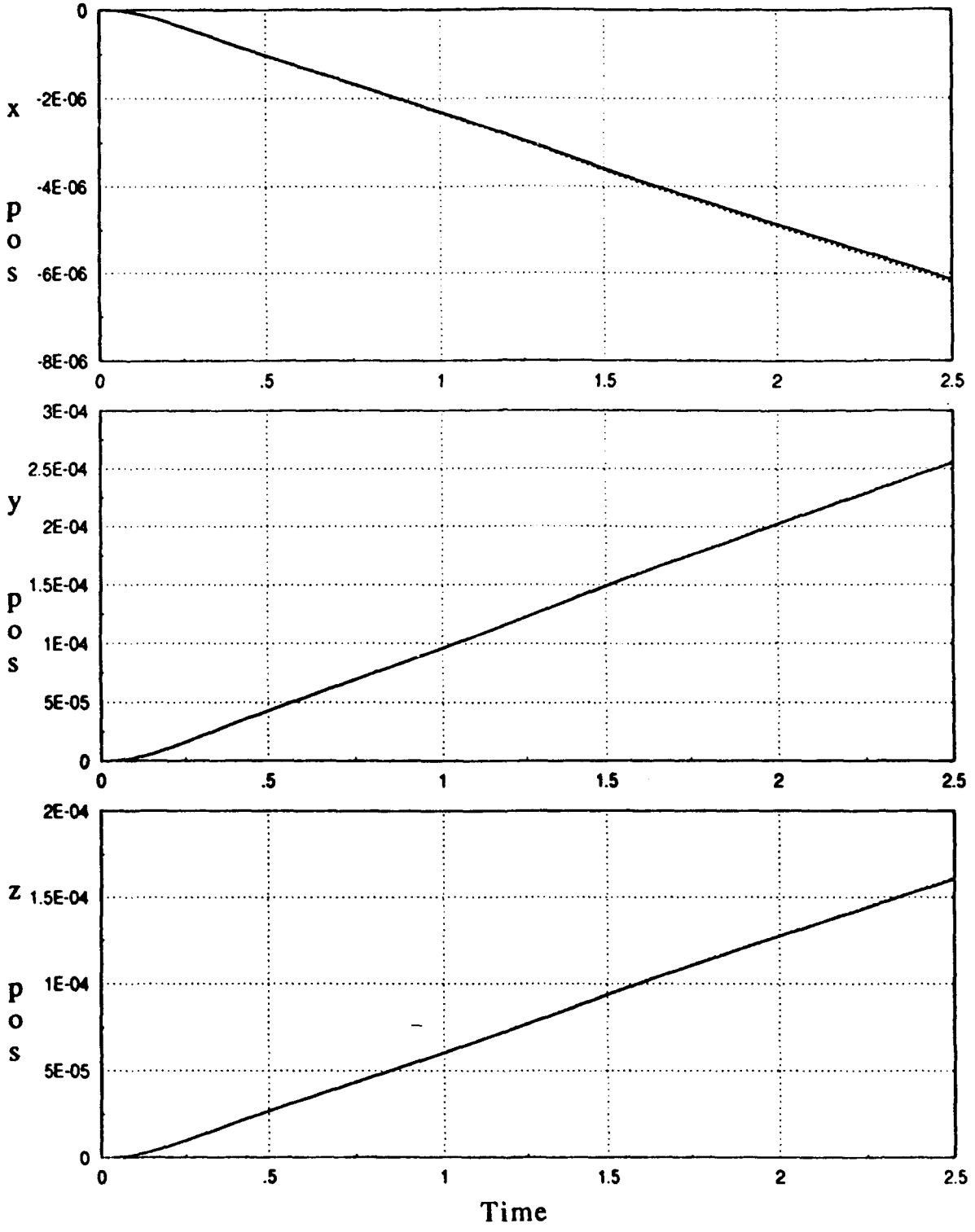

Figure B.1-7 X Torque Response for Rigid Articulated Case

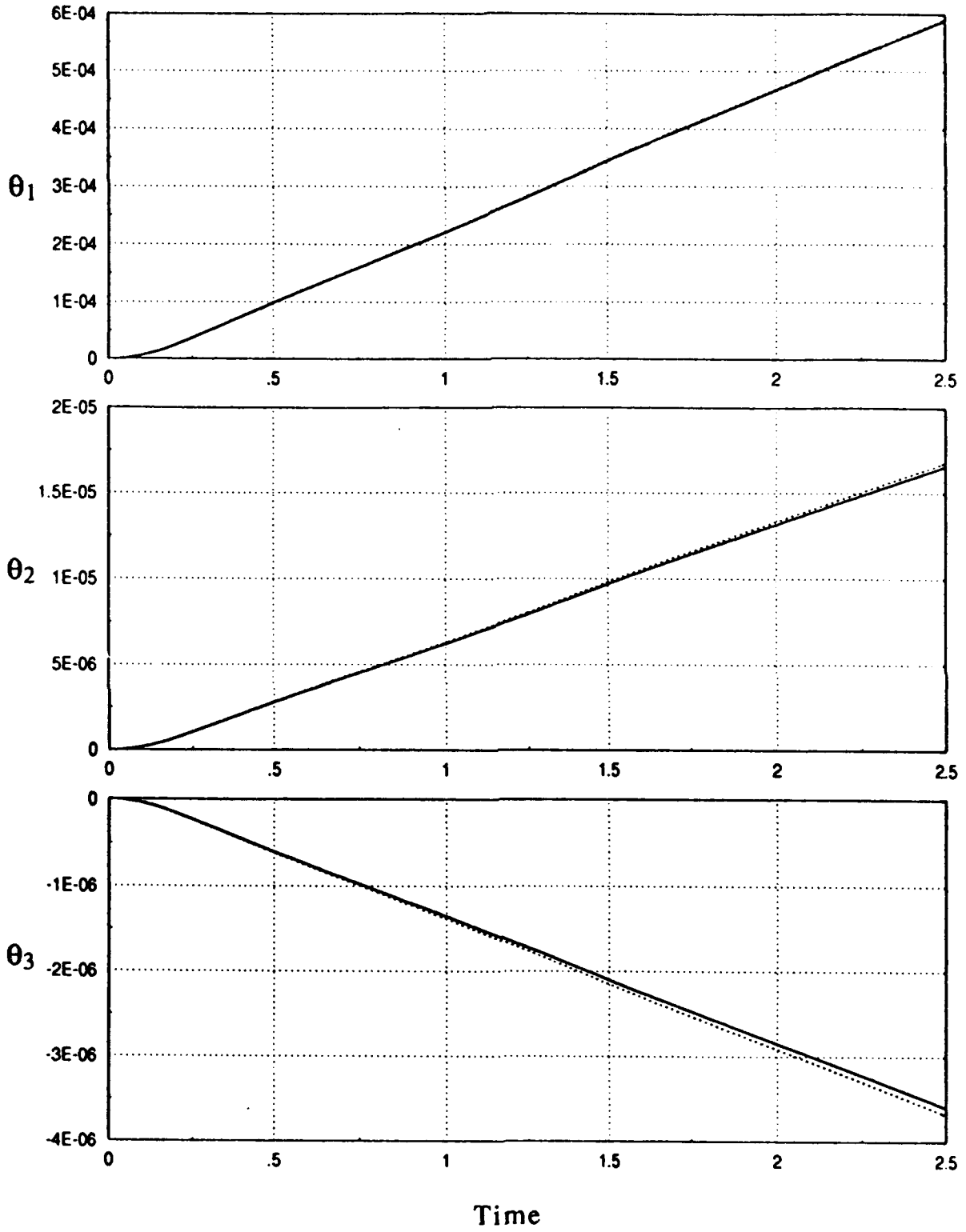

Figure B.1-8 X Torque Response for Rigid Articulated Case

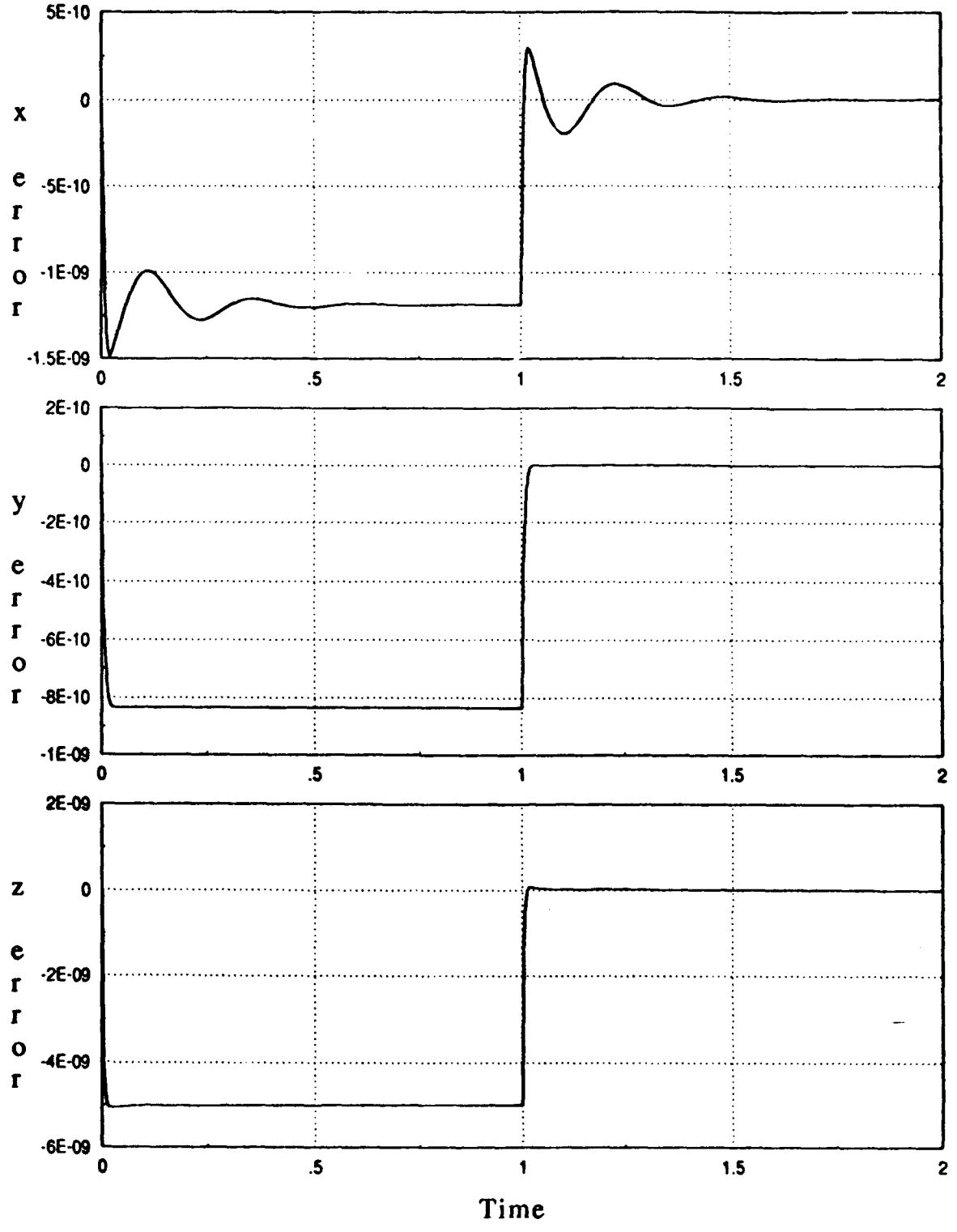

Figure B.1-9 Translation Errors for Rigid Nonarticulated Case

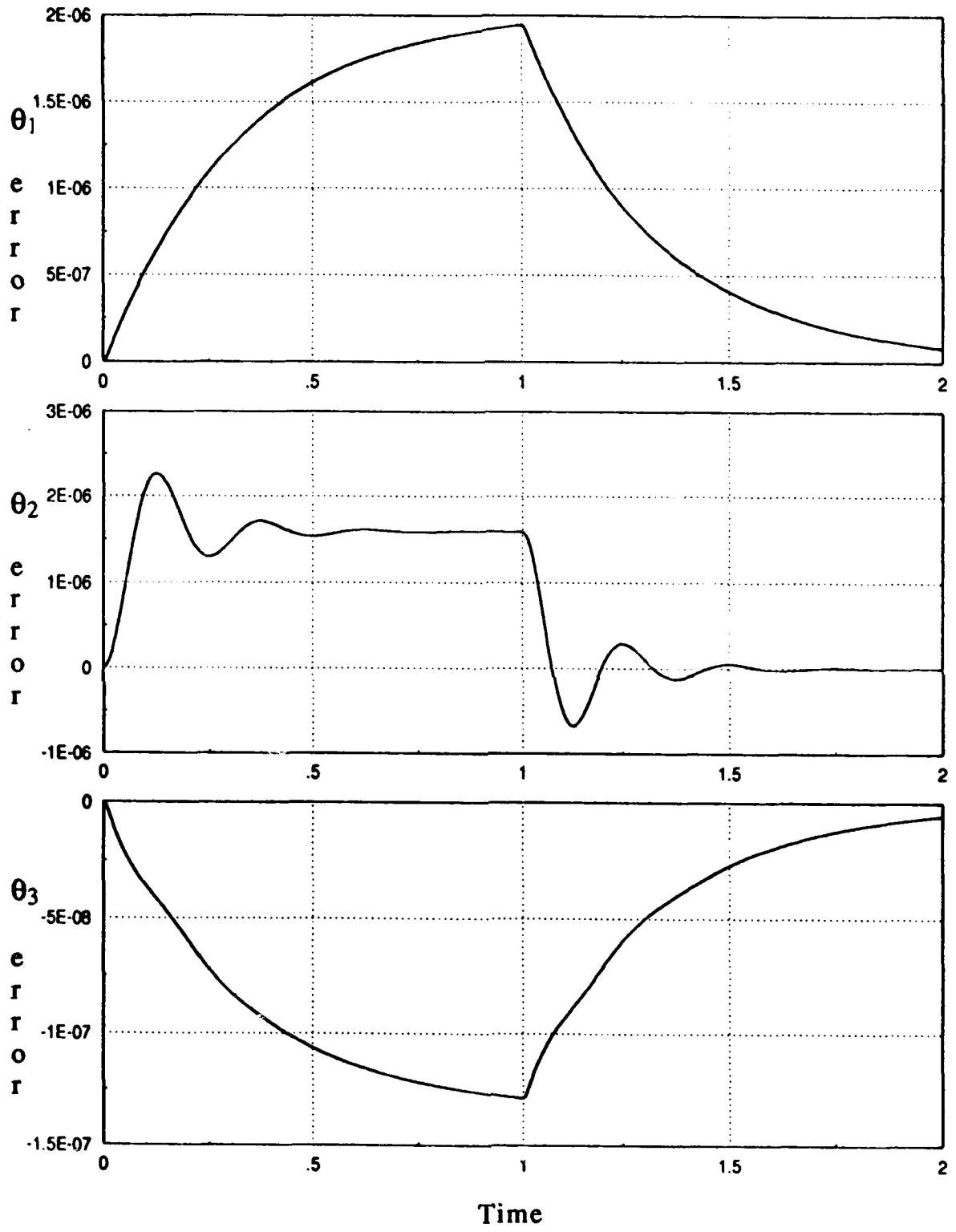

Figure B.1-10 Rotation Errors for Rigid Nonarticulated Case

B.2 Flexible Model Plots

The flexible model was run with 10 modes for each subdomain. The responses are included for each forcing case as well as the error plots for the x torque case. The error plots for the z force case are not significantly different and are not included.

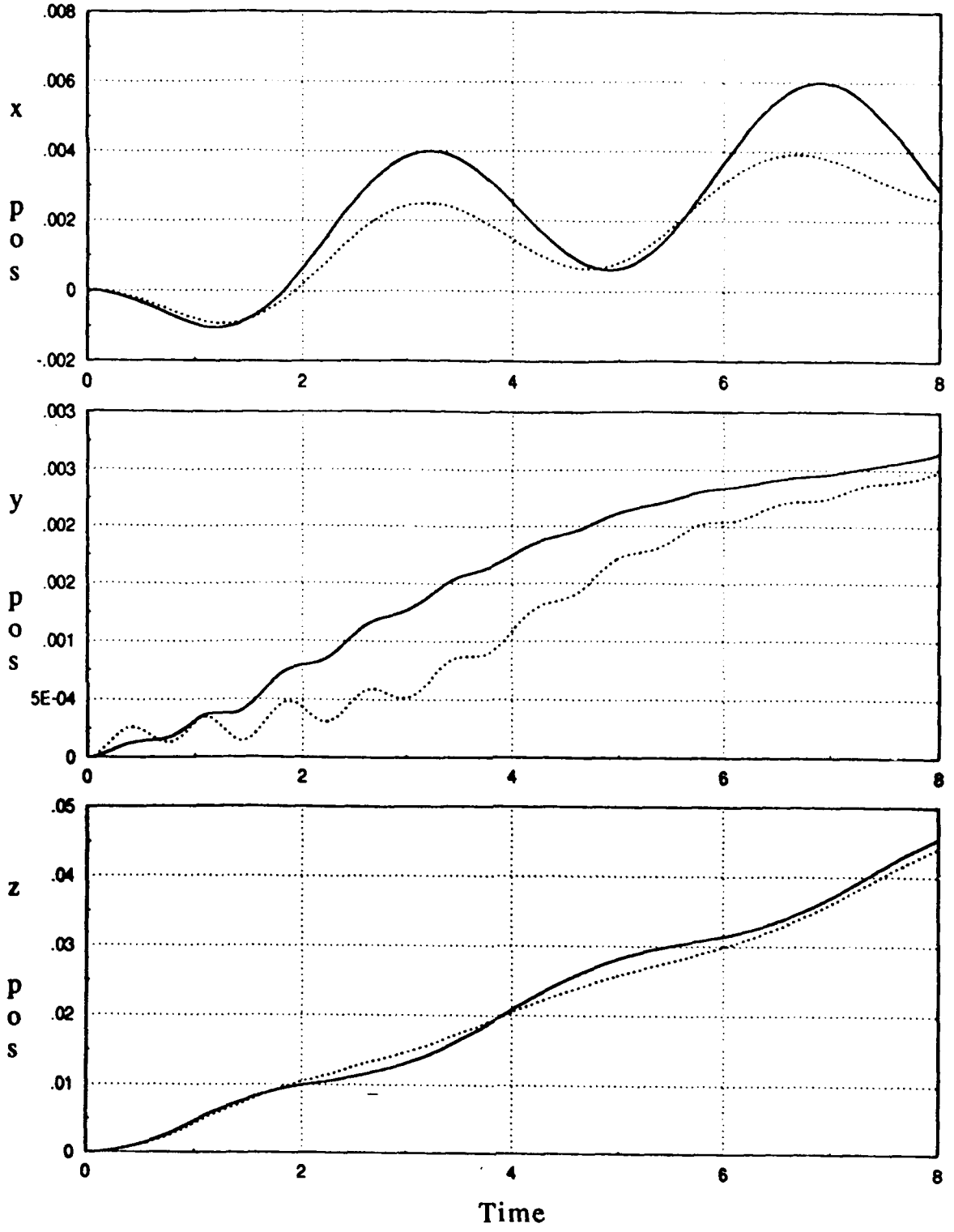

Figure B.2-1 Z Force Response for Flexible Articulated Case

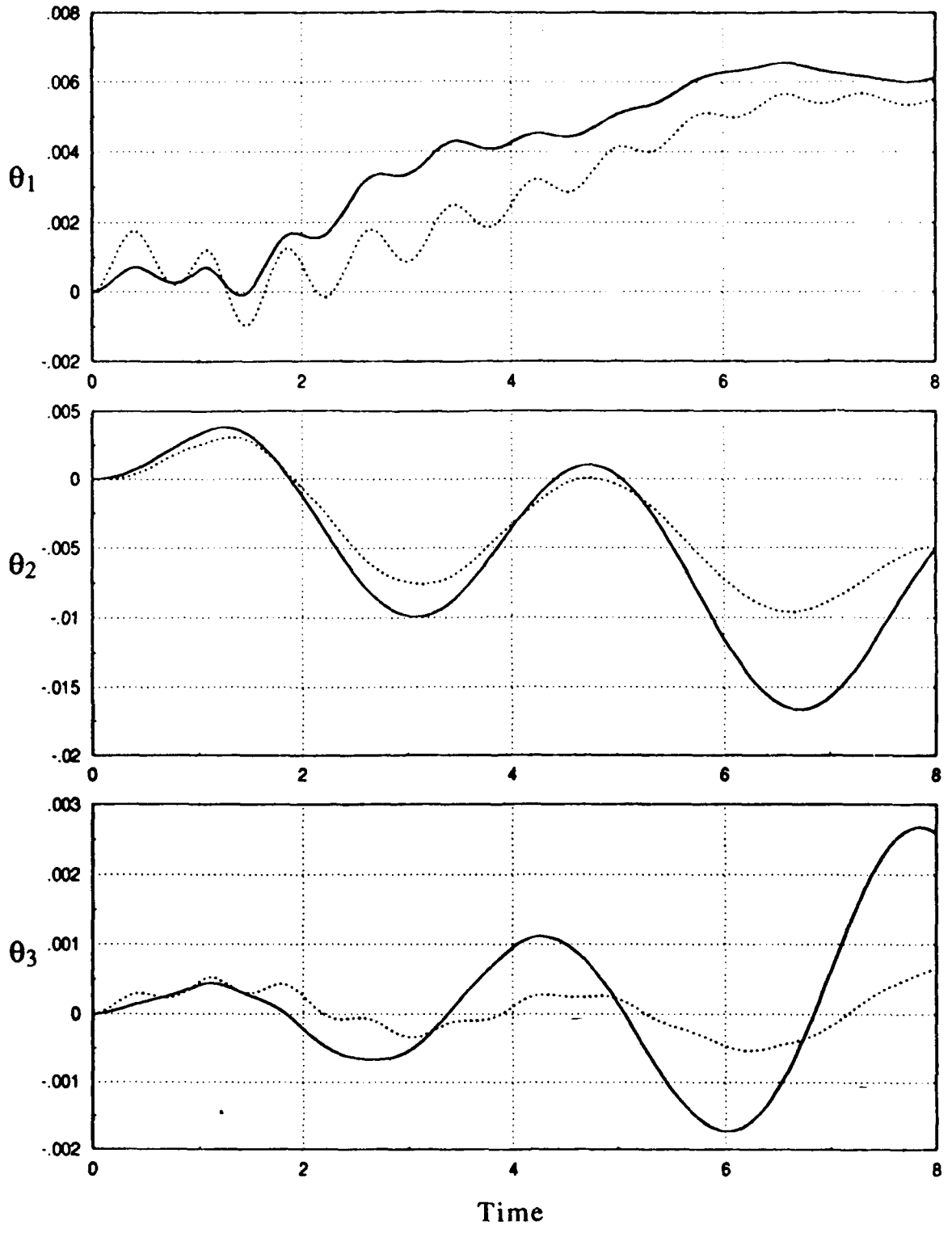

Figure B.2-2 Z Force Response for Flexible Articulated Case

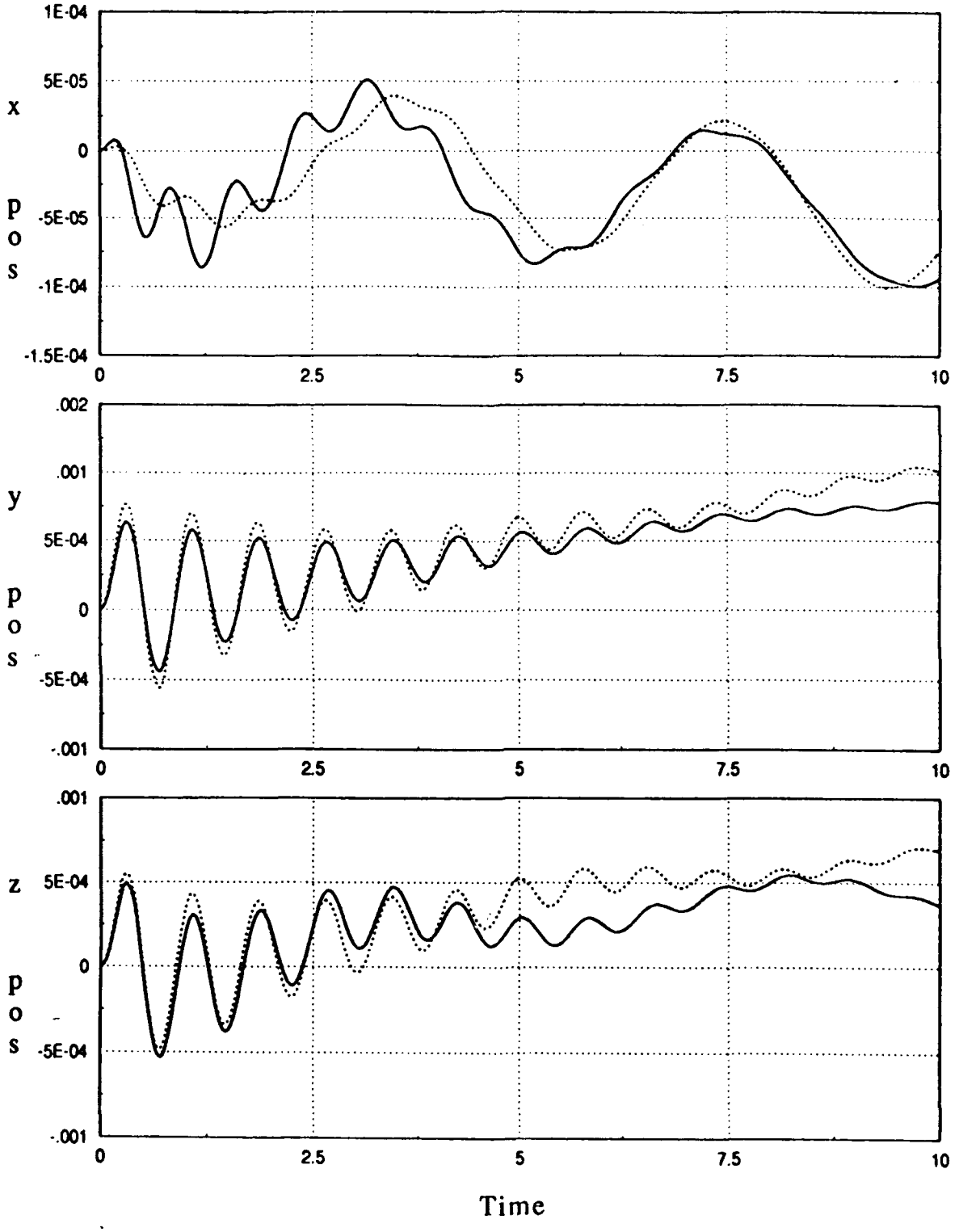

Figure B.2-3 X Torque Response for Flexible Articulated Case

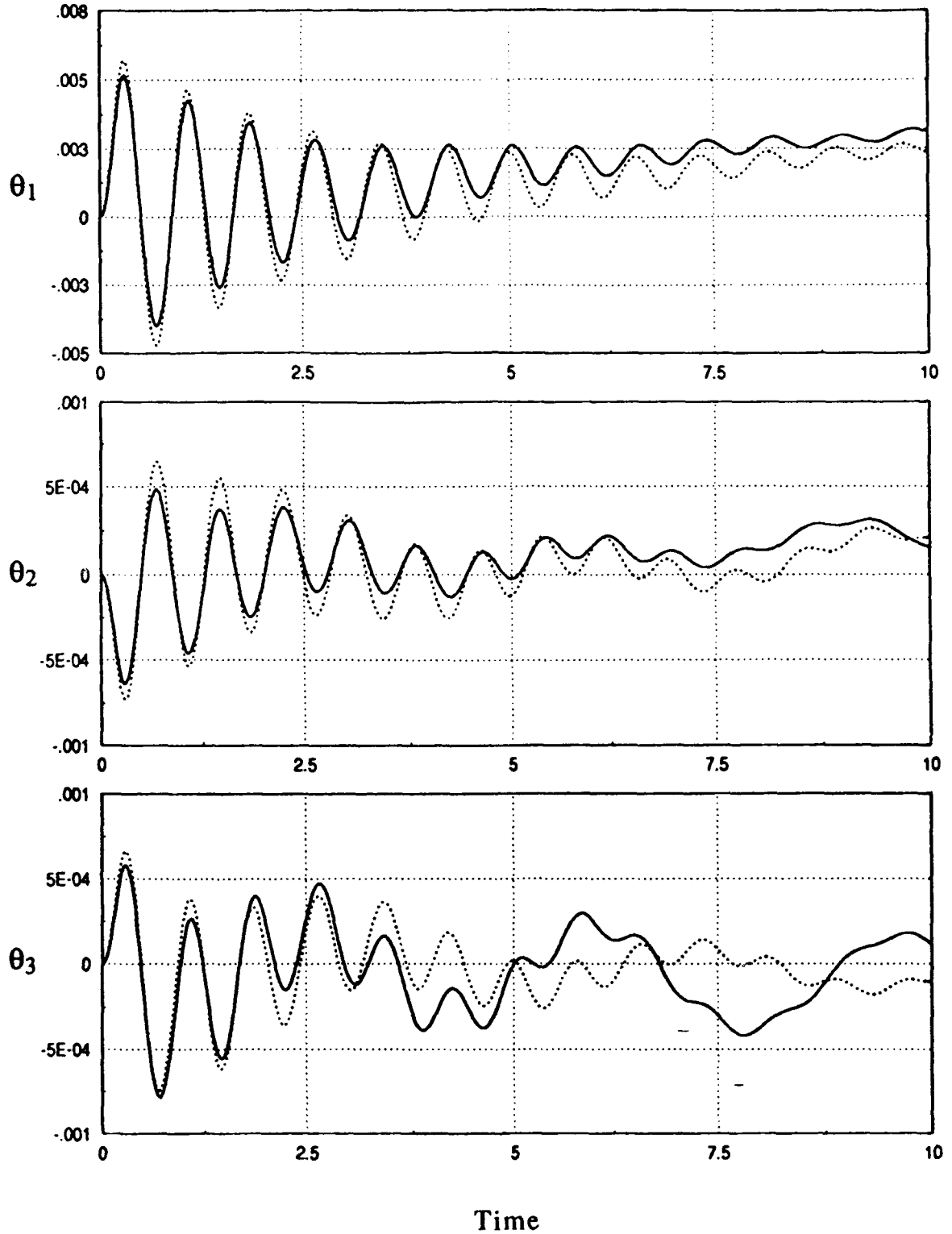

Figure B.2-4 X Torque Response for Flexible Articulated Case

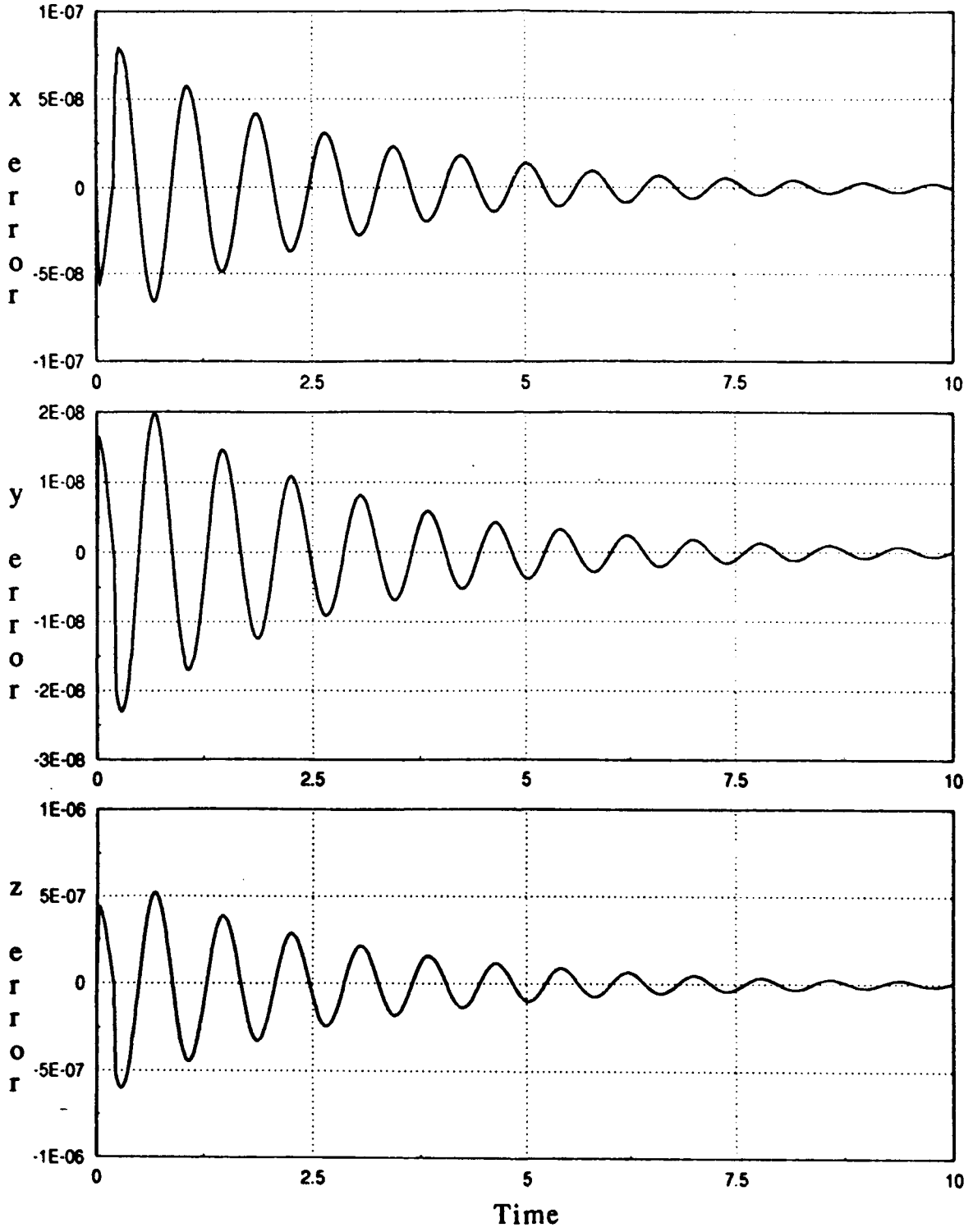

Figure B.2-5 Error Response for Flexible Nonarticulated Case

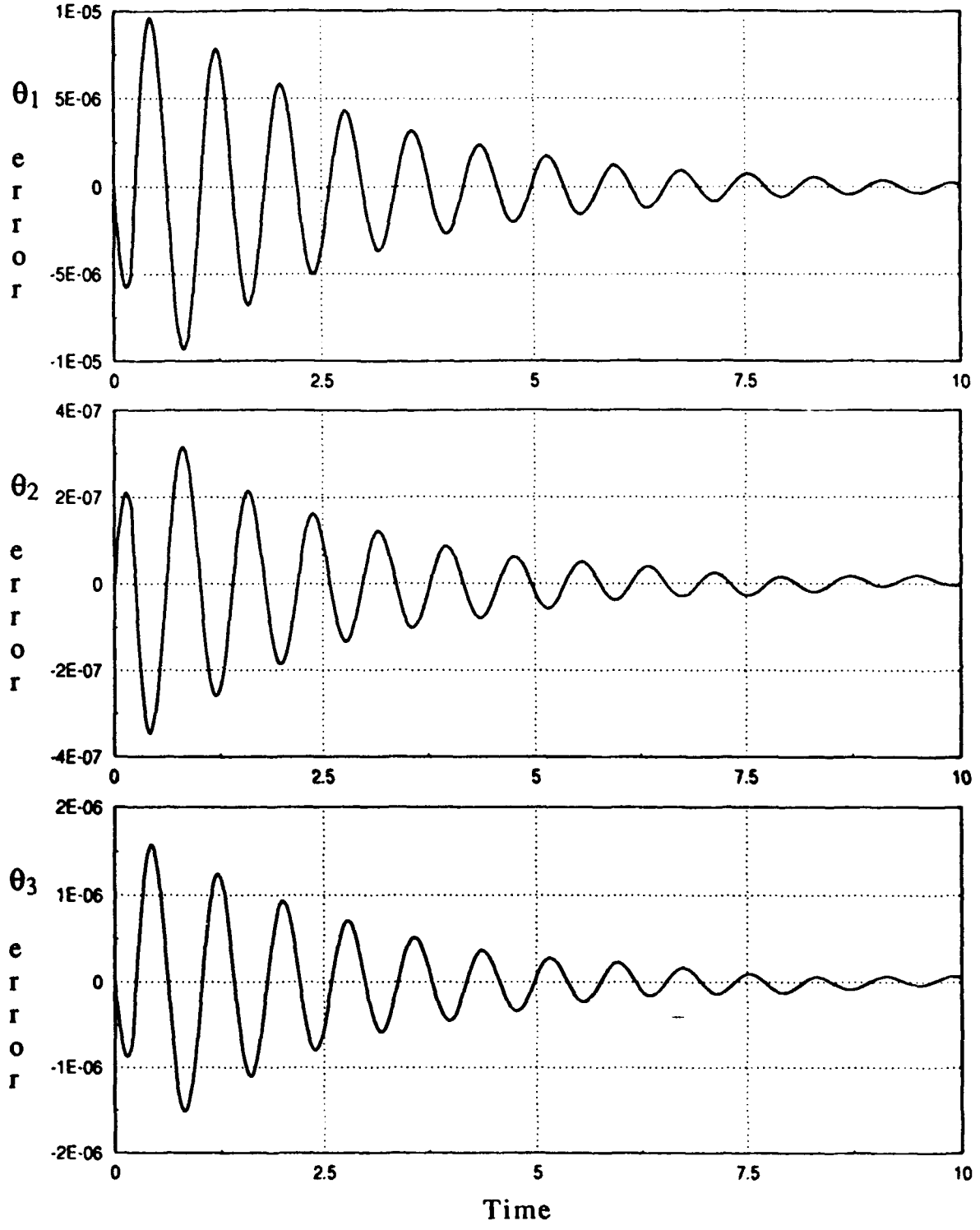

Figure B.2-6 Error Response for Flexible Nonarticulated Case

Appendix C

Numerical Improvements for Simulation Coupling

Since the computational dynamist has so few free parameters available to him some addition measures are sometimes necessary to aid in achieving the desired stability and accuracy. The most common of these measures are additional prediction steps and iteration loops.

C.1 Use of Rigid Body Predictors

One main difficulty with simulation coupling is that the corrective forces represent a delayed feedback of information. A force applied to one body takes one full time step before its effects can be felt at a connecting body. One easy correction for coupled structural problems is the use of a rigid body predictor step. Consider as an exampie the simple two field problem illustrated in Figure C.1-1.

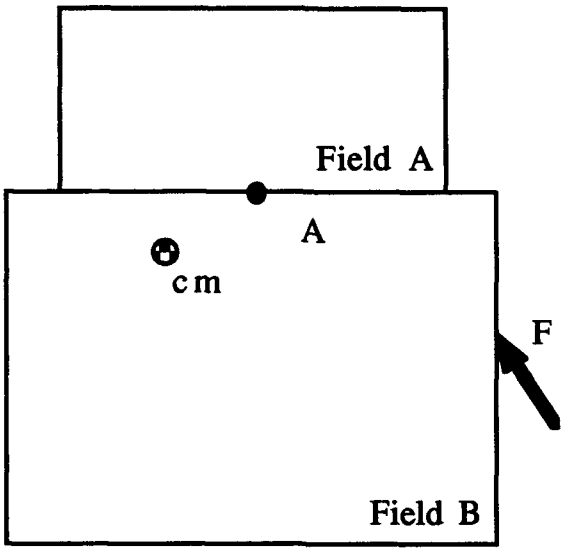

Figure C.1-1 Two Field Rigid Body

Given knowledge of the geometry of the problem and the mass/inertia matrices of the separate fields a global rigid body mass matrix, $\mathbf{M}_G$, is easily assembled. Using this matrix and the total force applied to the coupled domain, the rigid body accelerations may be found by solving the matrix form of $\mathbf{f} = \mathbf{M}\,\ddot{\mathbf{u}}_{cm}$. These accelerations are used along with basic kinematics to solve for the accelerations any point in the system. The accelerations at the boundary, point A, are

$$\ddot{\mathbf{u}}_A = \ddot{\mathbf{u}}_{cm} + \omega \times \dot{\mathbf{u}}_{cm} + \dot{\omega} \times \mathbf{r}_A + \omega \times (\omega \times \mathbf{r}_A) \qquad \text{(C.1-1)}$$

Using these values and the mass/inertia matrix of field A, the forces are found which, when applied at point A produce the accelerations $\ddot{\mathbf{u}}_A$. To maintain dynamic equilibrium, an equal and opposite set of forces must be applied to field B. These forces represent the set of d'Alembert forces which act at the boundary to ensure the constraints are met under rigid conditions. This force balance is presented in Figure C.1-2.

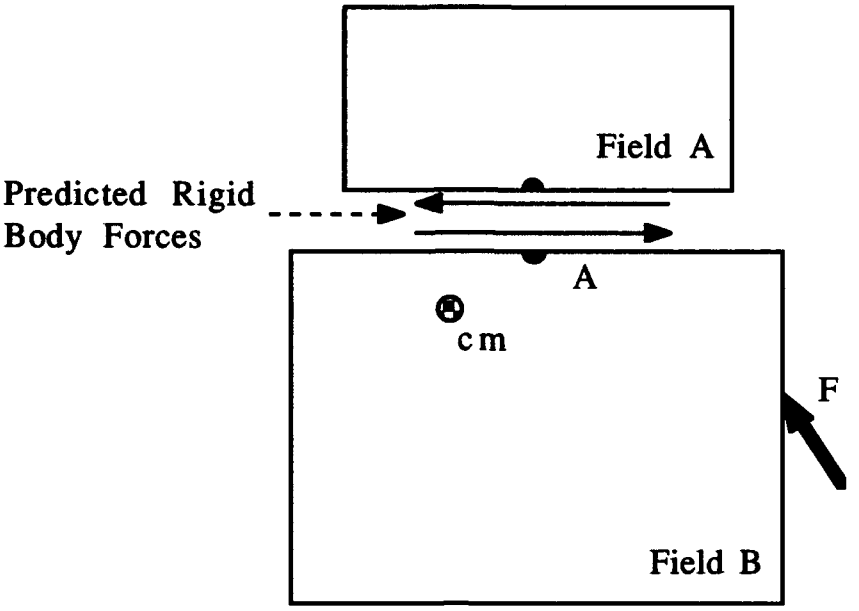

Figure C.1-2 Force Balance Using Rigid Body Prediction

The overall effect of using a rigid body predictor is to appropriately distribute the forces applied at given time to all the coupled fields. In this manner the effects of a force on a body are felt immediately across the entire domain. In this way the problems associated with time delayed information are avoided. An additional benefit comes from the fact that the rigid body predictor keeps the simulation coupled solution close to the actual solution. Because of this smaller penalties and larger time steps than without the predictor may be used.

C.2 Example of Rigid Body Prediction

As an example using a rigid body predictor the Space Station rigid model with articulation is used. The penalties required to keep translation errors less than 10^{-8} meters and angular errors less than 10^{-6} degrees are

	α	κ
Translation	100,000	100.0
Rotation	50,000	10.0

Since the penalties are so much lower than without using a rigid body predictor, the time step could be lowered from 0.0001 to 0.005. The case is run using a 100 lb force in the z direction. The plots for rigid body translations and rotations are included as Figures C.2-1 and C.2-2. In this example all responses are basically overlays with a small drift in the θ_3 angle.

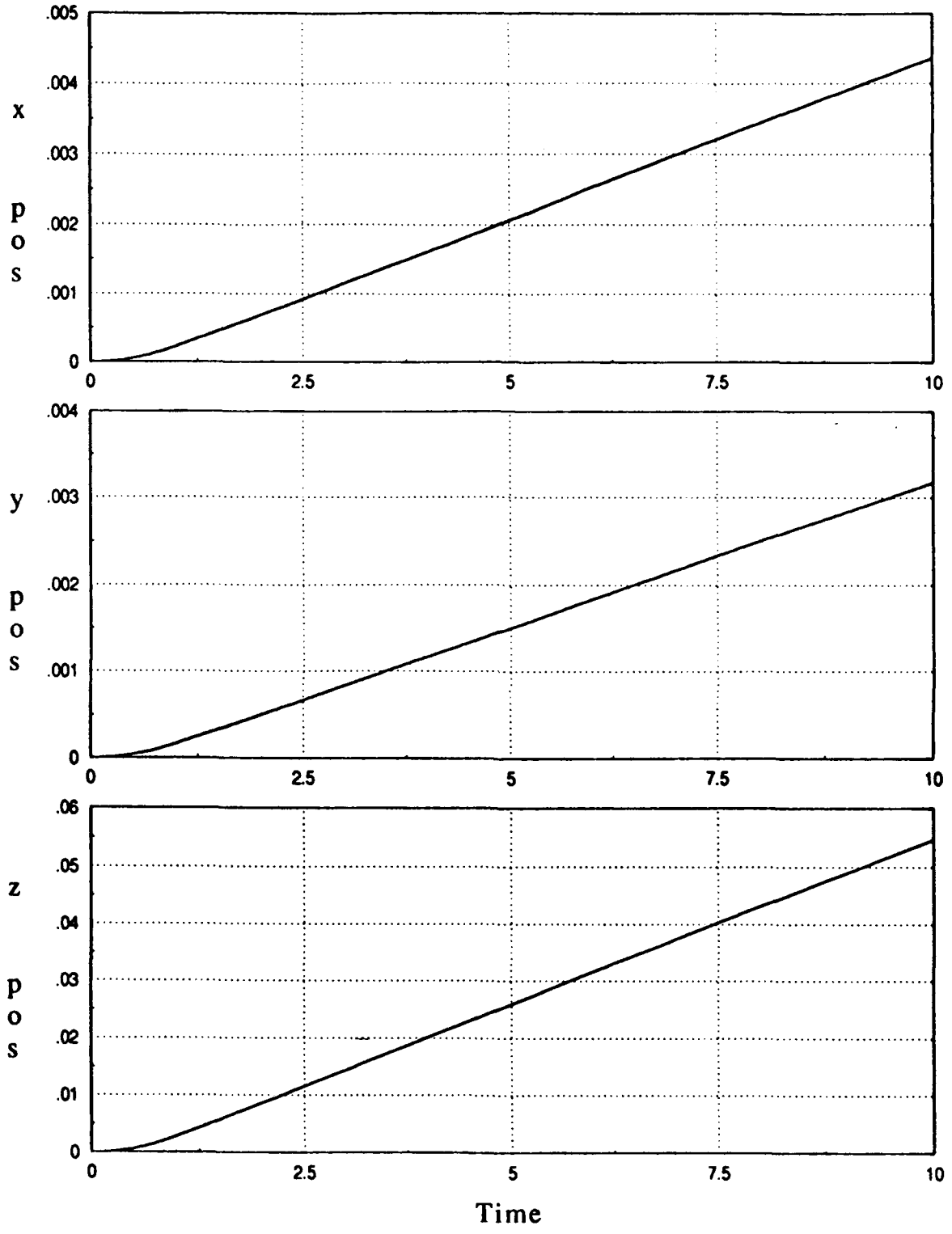

Figure C.2-1 Z Force Response for Rigid Articulated Case

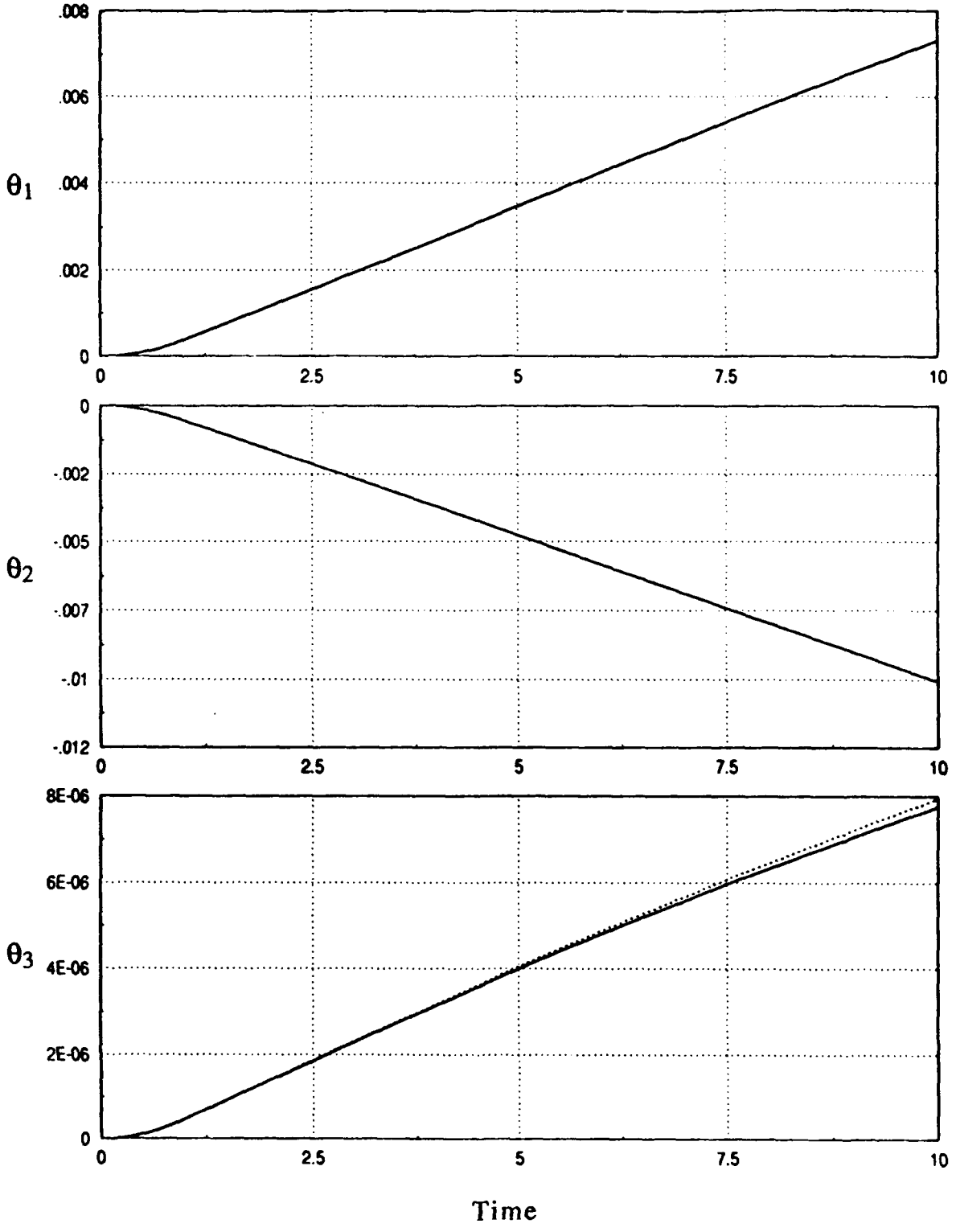

Figure C.2-2 Z Force Response for Rigid Articulated Case

References

[2.1] Belytschko, T., and Mullen, R., "Mesh Partitions of Explicit-Implicit Time Integration," *Formulation and Computational Algorithms in Finite Element Analysis*, eds. J. Bathe., et al, MIT Press, 1977, pp. 674-690.

[2.2] Belytschko, T., and Mullen, R., "Stability of Explicit-Implicit Mesh Partitions in Time Interaction," *International Journal of Numerical Methods in Engineering*, Vol. 12, 1978, pp. 1575-1586.

[2.3] Hughes, T.J.R., and Liu, W.K., "Implicit-Explicit Finite Elements in Transient Analysis: Stability Theory," *Journal of Applied Mechanics*, Vol. 45, 1978, pp. 371-374.

[2.4] Hughes, T.J.R., and Liu, W.K., "Implicit-Explicit Finite Elements in Transient Analysis: Implementation and Numerical Examples," *Journal of Applied Mechanics*, Vol. 45, 1978, pp. 375-378.

[2.5] Hughes, T.J.R., and Belytschko, T., "A Precis of Developments in Computational Methods for Transient Analysis," *Journal of Applied Mechanics*, Vol. 50, 1983, pp. 1033-1041.

[2.6] Felippa, C.A., and Park, K.C., "Staggered Transient Analysis Procedures for Coupled Mechanical Systems," *Computer Methods in Applied Mechanics and Engineering*, Vol. 24, 1980, pp. 61-111.

[2.7] Park, K.C. "Partitioned Analysis Procedures for Coupled-Field Problems: Stability Analysis," *Journal of Applied Mechanics*, Vol. 47, 1980, pp. 370-378.

[2.8] Park, K.C., and Belvin, W.K., "Partitioned Procedures for Control-Structure Interaction Analysis," *Computational Mechanics '88*, eds. S.N. Atluri and G. Yagawa, Vol. 2, Springer-Verlag, 1988, pp. 64.iii.1-4.

[2.9] Park, K.C., Chiou, J.C., and Downer, J.D., "Explicit-Implicit Staggered Procedure for Multibody Dynamic Analysis," *Journal of Guidance, Control, and Dynamics*, Vol. 13, No. 3, May-June 1990, pp. 562-570.

[2.10] Park, K.C., Felippa, C.A., and DeRuntz, J.A., "Stabilization of Staggered Solution Procedures for Fluid-Structure Interaction Analysis," *Computational Methods for Fluid-Structure Interaction Problems*, eds. T. Belytschko and T.L. Geers, ASME, AMD Vol. 26, New York, N.Y., 1977, pp. 95-124.

[3.1] Jensen, P.S., "Transient Analysis of Structures by Stiffly Stable Methods," *Computers and Structures*, Vol. 4, 1974, pp. 615-626.

[3.2] Felippa, C.A., and Park, K.C., "Computational Aspects of Time Integration Procedures in Structural Dynamics, Part 1: Implementation," *Journal of Applied Mechanics*, Vol. 45, 1978, pp. 595-602.

[3.3] Felippa, C.A., and Park, K.C., "Computational Aspects of Time Integration Procedures in Structural Dynamics, Part 2: Error Propagation," *Journal of Applied Mechanics*, Vol. 45, 1978, pp. 602-611.

[3.4] Geradin, M., "A Classification and Discussion of Integration Operators for Transient Structural Response," AIAA Aerospace Sciences Meeting, Washington, D.C., Jan. 1974.

[3.5] Gear, C.W., *Numerical Initial Value Problems in Ordinary Differential Equations*, Prentice-Hall, Englewood Cliffs, N.J., 1975.

[4.1] Baumgarte J.W., "Stabilization of Constraints and Integrals of Motion in Dynamical Systems," *Computational Methods in Applied Mechanics and Engineering*, Vol. 1, 1972, pp. 1-16.

[4.2] Baumgarte, J.W., "A New Method of Stabilization for Holonomic Constraints," *Journal of Applied Mechanics*, Vol. 50, 1983, pp. 869-870.

[4.3] Wehage, R.A. and Haug, E.J., "Generalized Coordinate Partitioning for Dimension Reduction in Analysis of Constrained Dynamic Systems," *Journal of Mechanical Design*, Vol. 104, 1982, pp. 247-255.

[4.4] Nikravesh, P.E., "Some Methods for Dynamic Analysis of Constrained Mechanical Systems: A Survey," *Computer Aided Analysis and Optimization of Mechanical System Dynamics*, ed. E.J. Haug, NATO ASI Series, F9, Springer-Verlag, Berlin, 1984, pp. 351-367.

[4.5] Park, K.C., "Stabilization of Computational Procedures for Constrained Dynamical Systems," *Journal of Guidance, Control, and Dynamics*, Vol. 11, No. 4, July-August 1988, pp. 365-370.

[4.6] Bayo, E. J., et al., "A Modified Lagrangian Formulation for the Dynamic Analysis of Constrained Mechanical Systems," *Computational Methods in Applied Mechanics and Engineering*, Vol. 71, 1988, pp. 183-195.

[4.7] Bathe, K. J. "Analysis of Direct Integration Methods," *Finite Element Procedures in Engineering Analysis*, Prentice-Hall, Englewood Cliffs, N.J., 1975.

[5.1] Wertz, J. R. and Larson, W. J., *Space Missions Analysis and Design*, Kluwer Publishers, Norwell, Ma, 1991.

[5.2] *NASA Space Systems Technology Model*, NASA TM 88174, NASA Publishing, Washington, D.C., June 1985.

[5.3] Roberts, D. T., "Assessment of Finite Element Approximations for Nonlinear Flexible Multibody Dynamics," CS Draper Labs Document T-1077, Cambridge, Ma, 1991.

[5.4] Hughes, P.C., "Motion Equations for a Rigid Body, $\mathcal{R}$," *Spacecraft Attitude Dynamics*, Wiley and Sons, New York, 1986.

[6.1] Clark, H.T. and Kang, D.S., "Application of Penalty Constraints for Multibody Dynamics of Large Space Structures," Paper AAS 92-157, Proceedings AAS/AIAA Spaceflight Mechanics Meeting, Colorado Springs, Co, Feb. 1992.